Copyright Warning & Restrictions

The copyright law of the United States (Title 17, United States Code) governs the making of photocopies or other reproductions of copyrighted material.

Under certain conditions specified in the law, libraries and archives are authorized to furnish a photocopy or other reproduction. One of these specified conditions is that the photocopy or reproduction is not to be "used for any purpose other than private study, scholarship, or research." If a, user makes a request for, or later uses, a photocopy or reproduction for purposes in excess of "fair use" that user may be liable for copyright infringement,

This institution reserves the right to refuse to accept a copying order if, in its judgment, fulfillment of the order would involve violation of copyright law.

Please Note: The author retains the copyright while the New Jersey Institute of Technology reserves the right to distribute this thesis or dissertation

Printing note: If you do not wish to print this page, then select "Pages from: first page # to: last page #" on the print dialog screen

ABSTRACT

FABRICATION AND EVALUATION OF A COLLAGEN-BASED FIBER-GEL THREE-DIMENSIONAL CONSTRUCT FOR PERIPHERAL NERVE REPAIR

by
Mevan Lakmal Siriwardane

Nerve regeneration following a peripheral nerve injury often relies on growth cone-mediated guidance and the presence of Schwann cells to support the regenerating axons and remyelinate portions of denervated nerve pathways. The emphasis of this work is to develop a synthetic nervous tissue construct that contains similar basal lamina or extracellular matrix to peripheral nerve in order to achieve a level of effectiveness in nerve repair and future peripheral nerve regeneration applications. To this end, three-dimensional nervous tissue constructs consisting of type I collagen are fabricated into a composite biomaterial scaffold to promote contact-guided growth of neuronal and glial cultures *in vitro*. The growth of adult tissue on these collagen-based materials is further evaluated. These constructs are assembled by wet spinning synthetic collagen fibers and loading them onto a soft collagen gel matrix composed of type I collagen.

Wet-spun collagen fibers serve as a rigid substrate to reinforce the gel while facilitating axon growth cone advancement along a polarized direction. In this study, the emphasis is to characterize the mechanical stability, thermal properties, and swelling response of the collagen fiber component of the construct. To improve these properties in the fiber component, chemical cross-linking with genipin and glutaraldehyde are evaluated. The result is a construct exhibiting mechanical integrity for facilitating adult Schwann cell orientation and the guidance and survival of adult dorsal root ganglion neurons in a co-culture 3-D system.

FABRICATION AND EVALUATION OF A COLLAGEN-BASED FIBER-GEL THREE-DIMENSIONAL CONSTRUCT FOR PERIPHERAL NERVE REPAIR

by
Mevan Lakmal Siriwardane

A Dissertation
Submitted to the Faculty of
New Jersey Institute of Technology
and University of Medicine and Dentistry of New Jersey
in Partial Fulfillment of the Requirements for the Degree of
Doctor of Philosophy in Biomedical Engineering

Joint Program in Biomedical Engineering

January 2013

.

APPROVAL PAGE

FABRICATION AND EVALUATION OF A COLLAGEN-BASED FIBER-GEL THREE-DIMENSIONAL CONSTRUCT FOR PERIPHERAL NERVE REPAIR

Mevan Lakmal Siriwardane

Dr. Bryan J. Pfister, Dissertation Advisor — Date
Associate Professor of Biomedical Engineering, NJIT

Dr. Steven W. Levison, Committee Member — Date
Director, Laboratory for Regenerative Neurobiology
Professor, Department of Neurology and Neurosciences
UMDNJ-New Jersey Medical School

Dr. Cheul H. Cho, Committee Member — Date
Assistant Professor of Biomedical Engineering, NJIT

Dr. George Collins, Committee Member — Date
Research Professor of Biomedical Engineering, NJIT

Dr. Raquel Perez-Castillejos, Committee Member — Date
Assistant Professor of Biomedical Engineering, NJIT

Dr. Chirag D. Gandhi, Committee Member — Date
Director, Endovascular Neurosurgery Fellowship Program
Assistant Professor of Neurological Surgery and Radiology
UMDNJ-New Jersey Medical School

BIOGRAPHICAL SKETCH

Author: Mevan Lakmal Siriwardane

Degree: Doctor of Philosophy

Date: January 2013

Undergraduate and Graduate Education:

- Doctor of Philosophy in Biomedical Engineering,
  New Jersey Institute of Technology, Newark, NJ, 2013
- Master of Science in Biomedical Engineering,
  New Jersey Institute of Technology, Newark, NJ, 2008
- Bachelor of Science in Biomedical Engineering,
  Louisiana Tech University, Ruston, LA, 2006

Major: Biomedical Engineering

Presentations and Publications:

Mevan L. Siriwardane, Kathleen E. DeRosa, George L. Collins and Bryan J. Pfister, "An in vitro 3-D model of collagen-based fiber constituents for peripheral nerve conduits," 38th Annual Northeast Bioengineering Conference, NEBEC 2012, Temple University, Philadelphia, PA, pp. 420-421, March 2012.

Mevan L. Siriwardane, Kathleen E. DeRosa and Bryan J. Pfister, "Collagen-based fiber-gel constructs engineered for Schwann cell guidance and adult axon growth," IEEE 37th Annual Northeast Bioengineering Conference, NEBEC 2011, Rensselaer Polytechnic Institute, Troy, NY, April 2011.

Mevan L. Siriwardane and Bryan J. Pfister, "Engineering Multi-functional Three-dimensional Nervous Tissue Constructs Based on Fiber-Gel Substrates," 2010 National Neurotrauma Symposium. Las Vegas, NV, June 2010.

I would like to dedicate this work to my beautiful wife, Kaarunya Satkunendrarajah, for her unconditional love and unwavering support throughout much of my graduate studies. Through her, I have learned to master my self-confidence, which is the backbone of success. It is with her loving support and guidance that I aspire to be successful in life.

ACKNOWLEDGMENT

This work would not have been possible without the support, patience, commitment and encouragement from my dissertation advisor, Dr. Bryan Pfister who provided me with numerous resources, intuition and opportunities as a graduate student. Despite his many other academic and professional commitments to the department, Dr. Pfister's creativity and energy has motivated and inspired me to continue doing fascinating research. Special thanks are given to Dr. Steven Levison and Dr. Chirag Gandhi for being on my committee and for providing clinical perspectives in neuroscience and neurological surgery, which were invaluable throughout my dissertation. I would also like to thank Dr. Cheul Cho, Dr. George Collins and Dr. Raquel Perez-Castillejos for serving on my committee and for providing feedback on my thesis. Kathleen DeRosa along with other students from Capstone Design spent significant time designing the automated wet spinning device, which has become an integral part of my dissertation. Special thanks to John Hoinowski for his vision, time, advice, and precious work put towards designing and building the wet spinning device. I want to thank my colleagues, Joseph Loverde, Dino Magou and Mat Long for their support as it has been a pleasure working alongside them in the lab for many years. Last, but not least, I would like to thank my beautiful wife, Kaarunya for her deep understanding, love, and patience during our first year of marriage. Many thanks also to my sister-in-law, Varna and my in-laws, Rajini and Sath Satkunendrarajah for their encouragement during hardships. My parents, Nilanthi and Upali and my lovely sister, Neesha receive my deepest gratitude for their many years of love and encouragement, which have provided the foundation for my success.

TABLE OF CONTENTS

TABLE OF CONTENTS
(Continued)

Chapter **Page**

TABLE OF CONTENTS
(Continued)

Chapter **Page**

TABLE OF CONTENTS
(Continued)

TABLE OF CONTENTS
(Continued)

Chapter **Page**

LIST OF TABLES

LIST OF FIGURES

LIST OF FIGURES
(Continued)

LIST OF SYMBOLS

μ	Micro (10^{-6} meters)
M	Mega (10^{6} meters)
G	Giga (10^{9} meters)
k	Spring constant
N	Newton
Pa	Pascal
DRG	Dorsal Root Ganglia
DIV	Days *in vitro*
% wt	Percent weight
% (v/v)	Percent volume by volume
% w/v	Percent weight by volume
®	Registered

CHAPTER 1

INTRODUCTION

1.1 Motivation

In recent years, there has been tremendous progress in understanding the interactions between biological tissue and materials. The advancements in the emerging field of tissue engineering have offered many therapeutic treatments and new methods in regenerative medicine. However, the progress of tissue engineering approaches in nerve regeneration has been slow and there is more to be learned about the mechanisms in which various natural and synthetic biomaterials interact with regenerating neural tissue. Despite the capacity of peripheral nerves to repair, functional outcomes after severe nerve trauma in humans are limited and often unsatisfactory [1, 2]. Outcomes vary widely depending on the extent/severity of the injuries and the distance and time required for axons to regenerate [2, 3]. Peripheral nerve injury (PNI) remains to be a serious health problem for society today. It affects nearly 2.8% of trauma patients, whom acquire life-long disability [4, 5]. Consequently, these injuries to both young and old generations of the population impose an enormous healthcare and economic burden on the society.

Approximately 360,000 people in the United States suffer from upper extremity paralytic syndromes yearly, which leads to extensive periods of restricted activity and bedridden disabilities [5]. In order to establish clinically effective strategies for nerve repair, axon guidance treatments for nerve tissue regeneration are in demand. Nerve conduits may provide a suitable alternative to overcome the limitations of nerve autologous grafts because its properties can be tailor-made with the use of biomaterial-

based approaches. It is desirable to create a nerve conduit for animal studies that naturally mimic the morphology and function of natural axon fascicles. Although collagen I (or collagen I) is a natural component present in most biological tissues, it does not play a significant role in peripheral nerve tissue. However, collagen I does have a role in early neuronal development as it is a favorable substrate for growth and guidance of developing axons in search of their targets. Therefore, collagen I was selected as the central component of the nerve conduit constituting the hydrogel and wet-spun fibers in this study. As a readily abundant material, collagen I was extracted from rat tail tendon was wet-spun into fibers to serve as an extra-cellular matrix (ECM) component of a guided nerve conduit for regenerating adult dorsal root ganglia axons.

1.2 Objectives

The primary emphasis of this study was to develop a collagen-based fiber-gel construct for supporting axon regeneration and Schwann cell guidance. The specific aims of the dissertation are defined as the following:

1) Fabrication and characterization of collagen I fibers
    a. Optimize parameters of current wet spinning apparatus for high yield production of controlled, uniform collagen fibers (<50 microns in diameter).
    b. Characterize diameter, uniformity, and mechanical properties.
    c. Establish cross-linking post-treatment methods to improve mechanical and swelling response of fibers.
2) Evaluation of Schwann cell guidance and migration on collagen I fibers
    a. Optimize methods for immobilizing extra-cellular matrix proteins onto fibers.

   b. Develop multi-filament or bundle of collagen fibers for Schwann cell guidance and DRG axon growth.

3) Co-culture primary adult rat dorsal root ganglion neurons and Schwann cells on 3-dimensional nerve tissue constructs
   a. Characterize axon outgrowth of primary adult DRGs cultured on 3-D fiber-gel constructs *in vitro*.
   b. Evaluate adult axon outgrowth response and growth morphology with Schwann cells in constructs.
   c. Develop 3-D nerve tissue constructs into a ready-made nerve conduit for future applications.

Overall, collagen-derived materials in a nerve conduit would offer the following benefits: revascularization, biodegradation, immuno-reactivity and guidance matrix for viable Schwann cells [6].

1.3 Background

Damage to the peripheral nervous system is shockingly more common and is primarily caused from trauma or complication of surgery. Nerve repair and regeneration presents unique clinical challenges, but significant contributions can be made through the proper application of biomaterial and/or biomedical engineering strategies. Traumatic injuries can occur due to stretch, crush, laceration (sharps or bone fragments) and blast exposure such as during wartime [2]. Nerve injuries occur 81% of the time in the upper extremities and 11% in the lower extremities, with a balance of occurrences in other

locations [7]. Injury to the peripheral nervous system (PNS) can range from severe to mild cases. The severe cases are characterized by major loss of function or intractable neuropathic pain. Mild cases result in minimal sensory and/or motor deficits affecting quality of life [2].

A thorough understanding of the physiology of the nervous system is crucial in addressing the challenges of bioengineering research in treating nerve tissue injuries. The application of biomaterials and engineering methodologies in nerve tissue repair requires a broad knowledge of the general organization and the cellular components of the nervous system, especially the anatomy of the peripheral nerves.

1.4 Organization of the Nervous System

The nervous system is classified into the central nervous system (CNS) and the peripheral nervous system (PNS). The CNS consists of the brain, spinal cord, optic, and olfactory and auditory systems. Many of the functions of the CNS include conducting and interpreting signals in addition to interfacing with the PNS via excitatory stimuli. The PNS consists of cranial nerves from the brain, the spinal nerves from the spinal cord, and the sensory nerve cell bodies (dorsal root ganglia) and their processes. Peripheral nerves innervate muscle tissue, transmitting both sensory and excitatory input to and from the spinal column. In this research, fetal and adult dorsal root ganglia from rat were chosen to investigate two- and three-dimensional axonal outgrowth using nerve conduit components made from collagen I-derived biomaterials.

In the nervous system there are two primary cell types: neurons and neuroglia. Neurons are the basic structural and functional elements of the nervous system and

consist of a cell body (soma) and its extensions (axons and dendrites). In this study, the axons and their outgrowth/regeneration behavior is the primary focus. Clusters of sensory nerve soma, known as ganglia, are located just outside the spinal column. As a sensory neuron, the dorsal root ganglia (DRG) is the primary cell model used in this research. While dendrites transmit electrical signals to the neuron cell body, the axon conducts impulses away and to other neighboring neurons with dendrite receptors. Glial cells, or neuroglia, are supporting cells that aid the function of neurons and are present in both PNS and CNS. Neuroglia includes Schwann cells in the PNS and astrocytes and oligodendrocytes in the CNS. The formation of glial scar tissue by the accumulation of astrocytes during SCI or other CNS injuries provides a hostile environment for the regenerating axons. Glial cells, unlike neurons, are more abundant and exhibit some capacity for cell division. Although neurons cannot divide by mitosis, they can regenerate a severed portion or sprout new neural branches under certain limited conditions. Unlike the CNS, neurons of the PNS have the capacity to regenerate their axons after injury and the Schwann cells within the denervated nerve pathways support the regenerating axons and support the remyelination of the larger nerves.

In the PNS, sheaths of living Schwann cells surround all axons. On the outer surface of this inner Schwann cell layer is the neurilemma, which is a basement membrane similar to that found in epithelial layers. Myelin serves to increase the propagation velocity of the nerve impulse, which becomes especially important for axons with extensive lengths (up to 1 m).

1.5 Anatomy of the Peripheral Nerve

In the context of designing nerve conduits for facilitating guided nerve regeneration, a firm understanding of peripheral nerve anatomy is essential. A peripheral nerve consists of motor and sensory axons bundled together by support tissue into an anatomically defined nerve trunk exhibiting a hierarchical level of structural organization shown in Figure 1.1. The perineurium, which is formed from many layers of flattened cells and collagen, surrounds groups of axons to form bundle-like fascicles. The epineurium is the outermost sheath of loose fibrocollagenous tissue, and it binds individual nerve fascicles into a nerve trunk. Peripheral nerves are well vascularized by capillaries within the support tissue of the nerve trunk or by vessels that penetrate the nerve from surrounding arteries and veins. A thin encapsulating layer called an endoneurium surrounds individual axons and their Schwann cell sheaths and is mainly composed of oriented collagen IV fibers. Within these endoneurial sheaths, the collagen fibers are present at varying degrees to form a wavy pattern in the epineurium, which protects the nerve from external stress [8, 9]. Collagen IV would be an ideal substrate for engineering fibrous scaffolds closely mimicking the micro-environment of peripheral nerve. However, collagen IV, unlike collagen I, is not relatively easy to purify and form into scaffolds. Collagen I as mentioned earlier is involved in early neuronal development serving as a favorable substrate for growth and guidance of developing axons. Since collagen I is readily abundant, easy to purify in the lab, and demonstrates favorable *in vivo* results comparable to nerve grafts [10-12], it was selected to fabricate nerve conduit materials consisting of collagen gels and wet-spun collagen fibers as the main structural component. The goal of this research is to engineer oriented collagen I fiber scaffolds,

which can serve as the extra-cellular matrix (ECM) architecture within peripheral nerve and maintain structural integrity under physiological conditions for a duration necessary for regenerating nerves after injury.

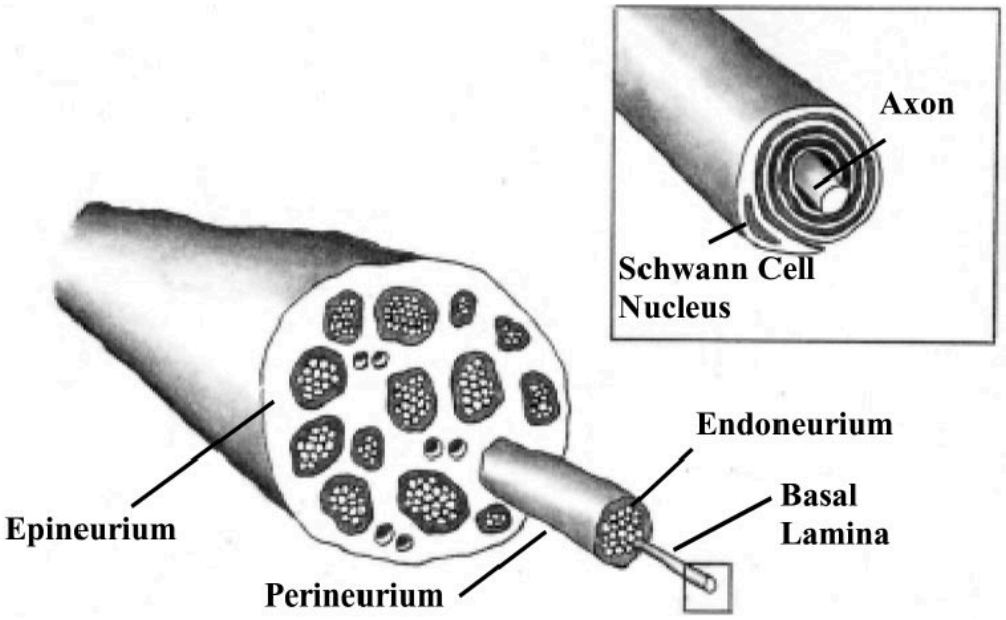

Figure 1.1 Anatomical structure of peripheral nerve. [13]

Another point of emphasis in this study is the fabrication of collagen-based scaffolds and the enhancement of their physiochemical properties to promote adult neuronal growth and Schwann cell response. Assessment of the physiochemical and mechanical properties of the collagen I fiber scaffolds is a key component in this research.

1.5.1 Role of Schwann Cells

As mentioned, Schwann cells are the glia of the PNS that help maintain the efficient functioning of the nerve fibers (myelinated and non-myelinated). In the PNS, peripheral axons are ensheathed by myelin, which helps to insulate the axon and also increase efficiency of signal transduction. Myelin significantly speeds up action potential conduction with an axon. For example, the conduction velocities of unmyelinated axons are limited to a range of 0.5 to 10 m/s [14]. In contrast, myelinated axons can conduct at velocities of up to 150 m/s [14]. The underlying reason for this marked increase in speed is due to the process of action potential generation, which occurs only at specific points along the axon, called nodes of Ranvier, where there is a gap in the myelin wrapping. The PNS also consists of non-myelinating Schwann cells which play a role in the maintenance of axons and nerve survival.

When there is induced trauma to a peripheral nerve, there is a host of cellular and molecular events occurring within the distal stump. Wallerian degeneration occurs in which all axons distal to the injury site degenerate. Axonal degeneration is evident by the disintegration of axoplasmic microtubules and neurofilaments due to a calcium-dependent proteolytic process. The series of events that occur during Wallerian degeneration are due to separation of the axon from its nourishment center, which is the nerve cell body as found within the spinal cord, dorsal root ganglia or autonomic ganglia [5, 15]. Within 24 hours, most of the axons along the distal stumps of severed nerves are disintegrated into granular and amorphous debris. After 48 hours, macrophages of the immune system immediately migrate to the sites of degenerating nerves to clean up the debris. Undifferentiated Schwann cells start proliferating within their basal lamina in

response to myelin debris and macrophage-secreted cytokines.

Following lesion-induced Wallerian degeneration, undifferentiated Schwann cells start to proliferate by mitosis, forming longitudinal strands of cells termed bands of Büngner. These proliferating cells also help degrade myelin within the injury site. These bands of Büngner remain within the basal lamina lined endoneurial tubes [5, 16]. Thus, the nerve lumen is naturally reengineered with hundreds of microchannels along the major axis of the nerve by the aligned orientation of Schwann cells. Furthermore, undifferentiated Schwann cells secrete a plethora of neurotropic and neurotrophic molecules, which provide indispensable pathways for physiochemically guided axonal regrowth [17-22]. Nerve growth factor (NGF), brain derived neurotrophic factor (BDNF), ciliary neurotrophic factor (CNTF) and neurotrophin 4/5 (NT-4/5) are produced by the Schwann cells during Wallerian degeneration and are thought to promote survival of regenerating neurons.

Previous studies provide extensive evidence that cellular and molecular changes in the distal nerve stump of damaged peripheral nerves are an important prerequisite for successful axon regrowth [23]. Although the mechanism involved in the formation of bands of Büngner remains poorly understood, bioengineered guidance conduits, which facilitate the formation of bands of Büngner by Schwann cells would have a long-term beneficial impact by accelerating and guiding axonal regeneration.

1.5.2 Extra-cellular Matrix of Peripheral Nerve

Since the early 20th century, the significance of the extra-cellular matrix (ECM) for nerve regeneration was well documented [24]. The ECM of natural regenerating peripheral nerves consists of a complex mixture of proteins and polysaccharides with the endoneurium playing a major role in regeneration. The major components of the endoneurium are laminin, collagen IV and fibronectin [25, 26]. The variety of ECM constituents within nerve suggests that the interaction between multiple ECM components is critical for healthy tissue.

As Schwann cells form bands of Büngner, they produce laminin, fibronectin, collagen (IV and VI) and proteoglycans, which together are major constituents of the endoneurial basal laminae or basement membrane [27-29]. The basement membrane provides a good substrate for the growth cone of regenerating axons. Furthermore, the bands of Büngner are essential to nerve regeneration because they are structures, which guide the regenerating axons to the periphery. In previous studies, neurite outgrowth has been guided *in vitro* by pathways of substrate-adsorbed laminin [30]. Schwann cells also produce cell adhesion molecules (CAM) such as integrins, NCAM, L1, TAG-1 and N-cadherins, which are used by regenerating axons as substrates for growth. Interestingly, many of these adhesion proteins were once actively expressed during neuro-embryogenesis. In previous studies, neurite outgrowth has been guided *in vitro* by pathways of substrate-adsorbed laminin [30]. Integrins present within the growth cone of regenerating nerves specifically bind to laminin and fibronectin via amino acid sequences arginine-glycine-aspartic acid (RGD), which is crucial for binding. In addition to the RGD peptide sequence, tyrosine-isoleucine-glycine-serine-arginine (YIGSR) and

isoleucine-lysine-valine-alanine-valine (IKVAV) are two other notable sequences present in laminin, which have been shown to be active in epithelial and neuron cell attachment [31] and in promoting neurite outgrowth [32], respectively. Collectively, regenerating axons interact with adhesion molecules and ECM proteins, which are critical for long-term growth.

Despite a better understanding of ECM constituents in the peripheral nerve, very little is known of the growth components and requirements for regenerating axons in adults. For various *in vitro* models of peripheral nervous systems, neurons from embryonic and neonatal mammals and birds have been extensively used in neurite outgrowth studies [12, 33-35]. Adult neurons have often been overlooked due to their limited growth potential. The use of adult DRG neurons provides a more realistic model for understanding underlying mechanisms associated with injury and repair since regeneration following peripheral nerve injury involves adult neurons, which exhibit slow and minimal growth compared to neurons from early developmental stages.

Previous studies suggest that neurons from adult animals may behave differently to certain stimulatory cues compared to immature neurons [36]. For example, adult sensory axons fail to grow on frozen sections of normal mature nerves likely due to inhibition by myelin-associated glycoprotein (MAG) [23, 37]. Adult DRG neurite extension is only optimal on sections of degenerating nerves. In contrast, neonatal DRG neurons are able to extend neurites on frozen sections of both normal and degenerating nerves with MAG being a stimulatory cue. An *in vitro* model consisting of tissue-engineered constructs to elucidate some of these growth mechanisms between immature and adult stage sensory neurons would be desirable. Hence, one of the goals of this study

is to investigate the growth response of adult DRG neurons and Schwann cell migration cultured on fiber-hydrogel constructs modified with various ECM proteins such as laminin, matrigel, poly-L-lysine and fibronectin.

1.5.3 Collagens in Regenerating Peripheral Nerves

The architectural and functional roles of collagens in connective tissues have been extensively studied and previously reported [8]. Despite being a vital component of extracellular matrices, the family of collagen proteins is rarely present within mature peripheral nerves. Within the mature nervous system, collagens are expressed in the layers of connective tissue that surround the CNS and PNS within the meninges, basement membranes and sensory end organs. Furthermore, collagens are a rarity in the vicinity of the neuronal soma. Collagens are present at varying levels within the perineurium, epineurium and endoneurium of the peripheral nerve. Importantly, collagens help maintain the mechanical integrity of the axon fascicle bundles present within nerve trunks. Collagens have been previously reported to play a determinant role in neural development by aiding in axonal guidance, synaptogenesis and Schwann cell differentiation [8, 38, 39]. For several decades, the function and importance of collagens have been largely overlooked until recently emerging studies have now convinced many to re-evaluate collagens as fundamental elements in the developing and diseased nervous system.

Collagen remains the most abundant protein in the human body with twenty-nine collagens numbered I to XXIX as reported in the literature [8]. Collagen I being the most common is the major fibrillar collagen that accounts for 25% of dry protein found in

mammals. This fibrous protein is an essential part of skin, bones, tendon, cartilage, ligaments and blood vessels. As an integral component of all connective tissues, collagen I is dispersed in the ECM in large quantities [40]. The different types of collagen can be categorized based on their function.

The first functional category within the collagen family is the fibrillar collagen, which consists of types I, II, III, V and XI. The signature feature common to these fibrillar collagen proteins is an uninterrupted triple helical region of about 1,000 amino acids in length [41]. Interestingly, collagen I is an adhesive substrate for many types of neurons. During growth and path-finding in the developing nervous system, collagen I is considered a favorable substrate for supporting the directed growth of axons during development since collagen contains RGD-sequences that can interact specifically with integrins of extending neurites [8, 42, 43]. Furthermore, collagen I serves as a protective role for neural tissue of the CNS by its presence in the meninges, which comprise the dura mater and the leptomeninges (arachnoid and pia mater) [44]. Beyond its involvement in development, the role of collagen I in the nervous system remains relatively unclear. Collagen II is expressed by immature Schwann cells in addition to both unmyelinated and myelinated mature Schwann cells [45]. In nerve injury, collagen III along with collagen I and V may potentially bind to inhibitory molecules such as chondroitin sulphate proteoglycan (CSPG) which are present in scar tissue formation [43]. Collagen V upon binding to glypican could potentially be involved in the terminal differentiation of Schwann cells, which determines if immature Schwann cells become unmyelinated or myelinated Schwann cells. In other words, collagen V is associated with

myelination [8]. Collagen XI is part of the cartilage matrix but also expressed in the frontal and occipital lobes of the brain during human development [46].

The second functional category of collagen proteins includes the non-fibrillar collagen IV, which is characterized by anti-parallel sheet-like structures that are the principal components of the basement membrane in the skin. In the nervous system, collagen IV is also the major component of the endoneurium or basement membrane of peripheral nerve and can be produced by Schwann cells as previously mentioned. The third functional category consists of collagens IX, XII, XIV and XVI, which are fibril-associated collagens in which the triple helical structures are interrupted and present in various lengths [47].

During Wallerian degeneration, the basement membrane starts to remodel and collagen fibrils deposit surrounding the proliferating Schwann cells. In fact, extensive remodeling of the endoneurial ECM and basal lamina tubes during Wallerian degeneration has been accepted as the driving mechanism providing the framework for re-growing axons [23, 48, 49]. Furthermore, previous studies have demonstrated that Schwann cells become surrounded by basement membrane and collagen fibrils following degeneration after a localized crush injury to rat dorsal roots [50]. The combination of Schwann cells, basement membrane and collagen fibrils results in the formation of Schwann tubes, which constitute the bands of Büngner as mentioned previously. Collagen fibrils observed following neurotrauma are created by the aggregation of monomeric collagen (tropocollagen) produced by fibroblasts into the extracellular space.

1.6 Collagen As a Biomaterial

Collagens have previously been used as biomaterials for guiding nerves in the regeneration processes following trauma in the PNS [51]. In this research, the focus is only on collagen I, which is used in both the fiber and matrix components of the nervous tissue construct. The ease of extractions and purification of collagen I makes it a readily used biomaterial. Also, collagen I is readily abundant and relatively easy to form into scaffold structures for a variety of tissue engineering applications. Hence, collagen I in the form of oriented fibrous scaffolds was an appropriate choice in the development of collagen-based nerve guidance constructs in this study.

1.6.1 Collagen Structure

Before using collagen I to engineer biomaterials into nerve guidance conduits, it is important to first understand its molecular structure, which directly influences its mechanical properties. As mentioned earlier, collagen I consists of triple helical molecules that are 1,000 amino acids in length and organized into a quarter-staggered configuration forming fibrils, which continue to self-assemble into longer and thicker fiber bundles with distinctive light and dark banding regions that is 67 nm in length.

A defining feature of collagen is its ability to self-assemble into fibers that play a significant role in maintaining the structure and mechanical integrity of any given tissue. Collagen is known to self-assemble through an enzymatic formation of intermolecular cross-links, which lead to a head to tail network within the fiber. The self-assembly mechanism is regulated *in vivo* by enzymes and chemical interactions between propeptides on protein molecules [52]. At a physiological pH of 7.4, collagen self-

assembly is initiated in which the assembled collagen fibers all possess identifiable quarter-staggered configuration with alternating light and dark bands when observed under high magnification. The regions where the collagen molecules fully overlap are discernable by dark banding regions. In contrast, the staggered ends of collagen molecules are defined by light banding regions. Within overlapping regions, collagen molecules are bound together by native cross-links that are formed as part of fiber formation and overall molecular stabilization. The bonds formed between these quarter-staggered molecules are covalent aldol cross-links formed between two lysine or hydroxylysine residues at the C-terminus of one collagen molecule with two similar residues at the N-terminus of an adjacent molecule [53]. These cross-links help stabilize the side-by-side packing of collagen molecules, which results in a strong fibril.

In addition to these native cross-links, there are also other chemical interactions that maintain the stability of collagen molecules. Hydrogen bonding between collagen molecules is facilitated by water that is also an essential component in the collagen self-assembly mechanism [54-56]. It is important to understand the importance and significance that water plays in influencing collagen stability and mechanics after self-assembly on both the micro- and macro-molecular level. The surface chemistry between water molecules and side chain groups of collagen help maintain the molecular conformation and mechanical properties seen in collagen [56]. Overall, various cross-links exist within the native collagen structure providing the mechanical strength, elasticity and wear resistance. Native cross-links within collagen include the following: intra-helical bonds (~1.5nm), inter-helical bonds (~4nm) and inter-microfibrillar bonds (~1.3-1.7nm). Intra-helical bonds are seen within the helical chain. Inter-helical bonds

link two or more helical chains together. In contrast, inter-microfibrillar bonds are present over a larger range and links neighboring side chains. In fixed biological tissues, the numbers of intra-helical and inter-helical bonds influences collagen's stability (denaturation temperature and resistance against enzymatic degradation). Inter-microfibrillar bonds, on the other hand, significantly affect the mechanical properties (tensile strength and strain at break) of collagen [57].

1.6.2 Collagen Self-assembly *in vitro*

Prior to fabricating synthetic collagen scaffolds for tissue engineering applications, an understanding of collagen self-assembly *in vitro* is very important. The *in vivo* collagen self-assembly mechanism can be partially manipulated under *in vitro* conditions. At lower pH levels, collagen starts to disassemble into smaller fibril subunits. In acid solutions, this physical transformation is termed "swelling". At a pH<4, positive charges develop on the collagen protein due to its complexing with surrounding acidic protons. As a result, collagen fibers repel each other and disaggregate into subunits. The attractive forces typically present between triple helices are eliminated, which yields a dispersion of insoluble collagen that is uniform, opalescent and optically isotropic [54, 58]. Collagen dispersions typically consist of long fibers with diameters in the range of 0.05-2.5 μm and length of 5-100 μm [59]. Interestingly, the process of disaggregation is reversible when the collagen dispersion is brought back to physiological pH with evident collagen fiber assembly when the acidity of the dispersion remains above pH 3 [60]. The pH dependent properties are interesting to note since the fiber and matrix components of the nerve tissue constructs in this study were derived from collagen dispersions.

1.6.3 Collagen Scaffold Fabrication

As synthetic polymers became available for medical purposes within recent decades, collagen remains one of the most widely used biomaterials. Collagen as a scaffold material is most desirable in tissue engineering since it is biocompatible, biodegradable and hemostyptic [61]. It is important to note that cross-linking can control the biodegradability of collagen for a variety of applications. Importantly, the surface of collagen is also known to promote ideal cell attachment, proliferation and differentiation of various cell types [62, 63]. Hence, collagen is often used to manufacture medical devices in the form of membranes, sponges, coating layers for implants and matrix material for a wide range of cell culture applications [63-65].

Scaffolds fabricated from biologically-derived materials exhibit improved clinical functionality assuming that the characteristic native features are preserved. Collagen is used extensively for tissue engineering applications because its signature biological and physiochemical properties are retained in *in vitro* preparations [66]. Most tissues rich in fibrous collagen such as skin and tendon are typically used to extract collagen. Some common animal sources for collagen extraction include bovine, porcine or avian. Interestingly, collagen extracted from rat tail tendons has been documented to take longer time to prepare with limited yield compared to the other animal sources just mentioned. However, the ease of the extraction and purification from rat tail tendon yields an improved batch-to-batch reproducibility in collagen concentration [67]. In this study, collagen I was extracted and purified from rat tail tendon by modifying existing protocols in the laboratory. In most extraction protocols, dilute acidic solvents are used to break

intermolecular cross-links of aldimine type. Here, dilute amounts of 0.1% acetic acid were used during the extraction of collagen I from rat tail tendon.

Among scaffold fabrication methods, electro-spinning has been extensively used in recent years to manufacture *in vitro* fibrous scaffolds for tissue engineering. In electro-spinning, fiber diameters typically range from a few microns to less than 100 nm. Electro-spun fibers ranging from nanometer to sub-micrometer scale aim to closely mimic the architecture of extra-cellular matrix components within native tissue. For example, electro-spun fibers are in the same scale as endogenous collagen fibrils, which have diameters ranging from 20 nm to 40 μm [52, 68, 69].

To date, pure collagen or collagen-synthetic polymer blends containing highly volatile fluoroalcohols such as 1,1,1,3,3,3-hexafluoro-2-propanol (HFP) or 2,2,2-trifluoroethanol (TFE) are commonly used for electro-spinning collagen scaffolds [66]. The high voltage required for polymer molecules to over come surface tension during electro-spinning may disrupt the native molecular cross-links present within naturally-derived proteins such as collagen. Also, electro-spinning collagen in fluoroalcohol solvents has been reported consistently to yield collagen nano-fibers, which do not swell in aqueous media but are readily soluble in water, tissue fluids or blood [70-72]. Electro-spun collagen fibers are most likely fragile and water soluble due to lack of native cross-links. Interestingly, gelatin is also water-soluble and is known to be a degradation product of water-insoluble collagen fibrils. The water solubility of electro-spun collagen scaffolds may suggest that there is extensive conformational change and denaturation of collagen into gelatin during the electro-spinning process [66].

Since electro-spinning of collagen yielded scaffolds lacking the native structure of collagen I, the technique was not considered suitable for this study. Alternative fabrication methods, which can manipulate collagen into oriented scaffolds with retained native biological and physiochemical properties is strongly desired. Currently, techniques for *in vitro* preparations of collagen scaffolds are relatively limited. Freeze drying or lyophilization is a dehydration process in which frozen water in a material sublimates directly from the solid phase to gas phase resulting in a dry porous material. Collagen sponges with varying degrees of porosity can be obtained from freeze drying and is favorable as scaffold materials for a variety of applications. Additionally, freeze-dried collagen retains its signature triple-helical and fibrillar structure. Although freeze drying is a promising approach for generating porous collagen scaffolds, orientation and fibrillar alignment are difficult to control.

In this study, wet spinning is introduced as a suitable fiber spinning technique for manufacturing oriented collagen monofilaments containing water-insoluble collagen fibrils. Unlike electro-spun collagen fibrous scaffolds, wet-spun collagen fibers are relatively stable scaffold materials, which do not dissolve instantaneously in water. Furthermore, the degree of swelling (water uptake) and degradation rate can be controlled by physical or chemical modification to increase collagen stability.

1.6.4 Physical Modification of Collagen Scaffolds

Dehydroxy-thermal (DHT) treatment and ultra-violet (UV) exposure are the most commonly used physical methods to cross-link collagen fibrous scaffolds. DHT cross-linking method is a well established technique in stabilizing collagenous tissues.

However, DHT is typically the less preferred cross-linking method due to lower cross-linking densities and the use of high temperatures to form cross-links. In DHT cross-linking, collagen fibers are typically heated under atmospheric pressure to a temperature above 105^{o}C, which leads to dehydration of collagen structure. The mechanism of DHT cross-linking involves a condensation reaction either by an ester or amide linkage with hydroxyl groups on the hydroxyproline residues found on the collagen triple-helix. The removal of water molecules results in the formation of amide bonds, which bring α-chains more closely towards each other thereby increasing the cross-links within the structure. As water molecules are removed, there is a visible change in the physical organization of collagen. In particular, the quarter-staggered organization of collagen molecules undergoes densification especially in the light banding region. Densification within the light banding region is due to the collapse of molecules during cross-linking because the water is being removed [73]. As the water molecules vacate regions, more sites are available for cross-link formation. Collectively, the degree of cross-linking is dependent on the duration of exposure and heat supplied during DHT treatment.

In terms of radiation treatment, UV exposure (254nm) offers another approach to physically cross-linking collagen fibrous scaffolds. In the UV method, the degree of cross-linking depends on the depth of penetration with exposure. The primary advantage of physical cross-linking is that the use of chemicals or reagents is not needed, which means minimal risk of toxicity. In general, physical cross-linking methods increase the mechanical strength of collagen fibers compared to chemical methods. However, physical modifications can induce denaturation of a portion of the collagen molecule, which may affect cell attachment, proliferation and differentiation [40, 74].

1.6.5 Chemical Modification of Collagen Scaffolds

The most commonly used cross-linking reagents for biological tissues are glutaraldehyde, formaldehyde, diisocynates and epoxy compounds [75, 76]. Glutaraldehyde (GA), an oily-colorless liquid at room temperature, is miscible in water. Furthermore, it is widely used in manufacturing industries for sterilizing medical/dental equipment in addition to water treatment and as chemical preservatives. GA is highly corrosive and vaporizes rapidly in the atmosphere. A glutaraldehyde molecule consists of two aldehyde groups as seen in Figure 1.2.

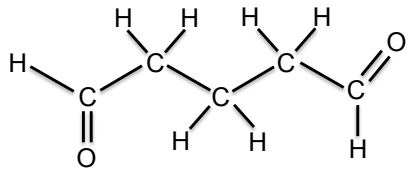

Figure 1.2 Glutaraldehyde molecule.

Glutaraldehyde (GA) is one of the most common chemical cross-linking reagents for collagen [77-81]. It is an effective cross-linker as it reacts very rapidly in retaining many of the viscoelastic properties of the collagen fibrillar network. The mechanism of GA reaction with collagen involves the formation of covalent bonds between collagen fibrils resulting from aldehyde-amino and aldol condensation reactions [81]. The result is a more tightly cross-linked network. In addition to intermolecular cross-links, GA can also lead to intramolecular cross-links formed between two α-chains by aldol condensation. Although GA remains widely used as a cross-linking reagent for collagen-

based biomaterials, the associated cytotoxicity concerns prevent its application for *in vivo* studies.

In recent years, genipin (Gp), a natural extract from the fruit of Gardenia Jasminoides, has been shown to be an effective cross-linker for cellular and acellular biological tissues. Furthermore, genipin has been used to cross-link various biomaterials including hydrogels and hydrogel composites [82]. Although Genipin has been previously used at concentrations of 0.625 to 1% to cross-link collagen gels, it has not been applied until recently for cross-linking collagen fiber scaffolds or electro-spun collagen mats [82-84]. Genipin presents many desirable properties as an alternative cross-linker because it is natural in origin and has no cytotoxic effect on biological tissues [83]. Its use as a cross-linking agent results in biomaterials with improved mechanical properties. Genipin is colorless in nature but forms a blue color stain when it reacts with amino acids [85]. The molecular structure of genipin is shown in Figure 1.3.

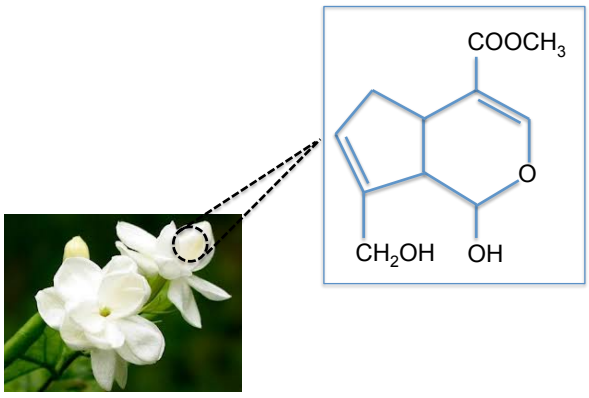

Figure 1.3 Structure of Genipin molecule extracted from Gardenia Jasminoides.

Specifically, the blue color pigment is a result of the end-product from the reaction of genipin with methylamine [85]. Genipin cross-linking is comparatively slower than glutaraldehyde. The cross-linking mechanism for genipin involves a

nucleophilic reaction from free amino groups of lysine or hydroxyline residues on collagen as seen in Figure 1.4. Tissue fixation with genipin may produce distinct cross-linking structures. Genipin is known to bridge peptide chains 1.6-2.5 nm apart, which can form inter-, intra-helical and inter-microfibrillar cross-links by polymerization [83].

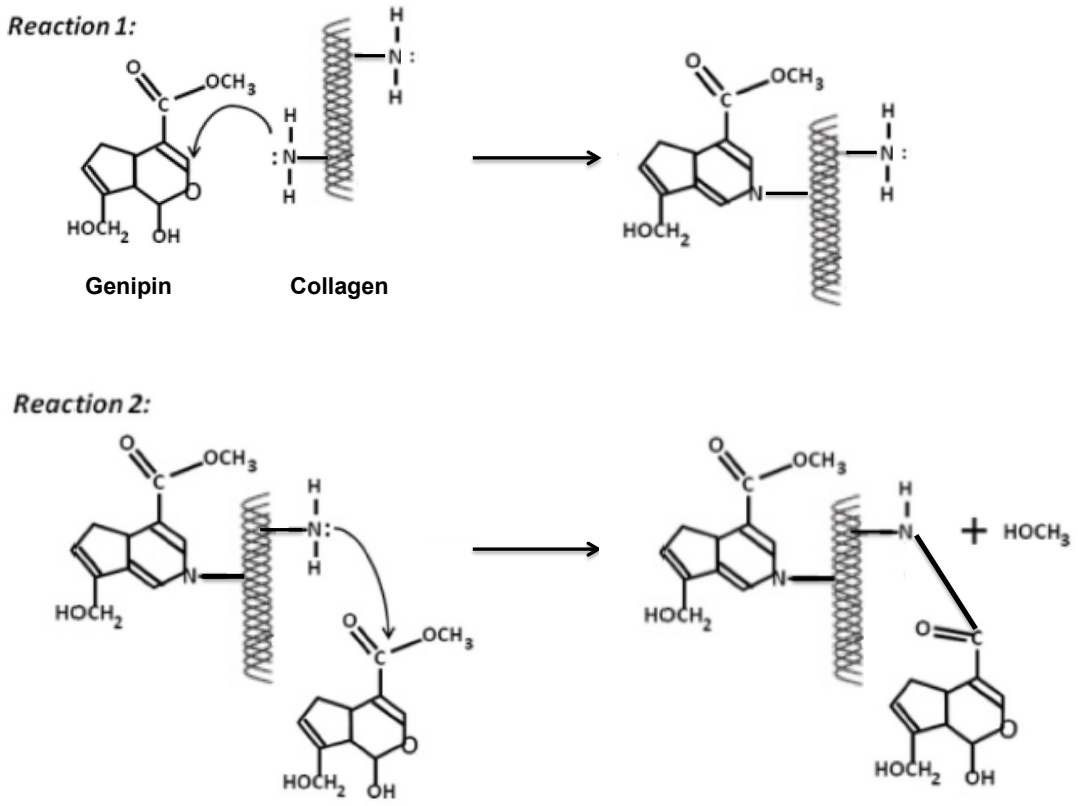

Figure 1.4 Cross-linking mechanism of genipin. Modified from [86].

1.7 Current Strategies and Concepts in Surgical Nerve Repair

The initial attempts at repairing nerve injuries were reported as early as the 17th century [87]. The development of various surgical options and their outcomes for the management of peripheral nerve injury gaps were later documented by the 19th century [88]. Some of the earlier surgical procedures included stretching or transposing the nerve, bone shortening, use of nerve grafts, or bridging of nerve ends via organic or synthetic materials serving as nerve conduits [88]. The management of larger peripheral nerve gaps was eventually classified into two general categories: (1) bridge operations (which included grafting, transposition and tubulization); and (2) manipulation of nerve (which is characterized by end-to-end apposition of the nerve stumps) [89]. Within the bridge operations category, there are three surgical reconstruction strategies: (1) direct repair, where the proximal and distal nerve ends are sutured back together, (2) nerve grafting, required to bridge a gap between nerve ends, and (3) nerve transfer, when the distal or proximal nerve segment is unusable or missing. When predicting the outcome of peripheral nerve repair, the factors that must be taken into consideration are the following: type, location, and extent of nerve injury; timing of surgery; type of repair technique; proper alignment of fascicles; surgical technique; and patient comorbidities [90].

1.7.1 Direct Repair

Direct repair is performed to suture proximal and distal nerve stumps back together. This technique is suitable when the two ends can be approximated with minimal tension [91]. A direct repair is preferred for reconnection of injured nerve ends where no gaps exist between the ends. The stumps are sutured together in what is called an end-to-end

neurorrhaphy, commonly known as end-to-end nerve repair [2]. When an end-to-end nerve repair is performed, an important microsurgical technique is to identify, isolate, and individually rejoin each perineurial-defined fascicle as seen in Figure 1.5.

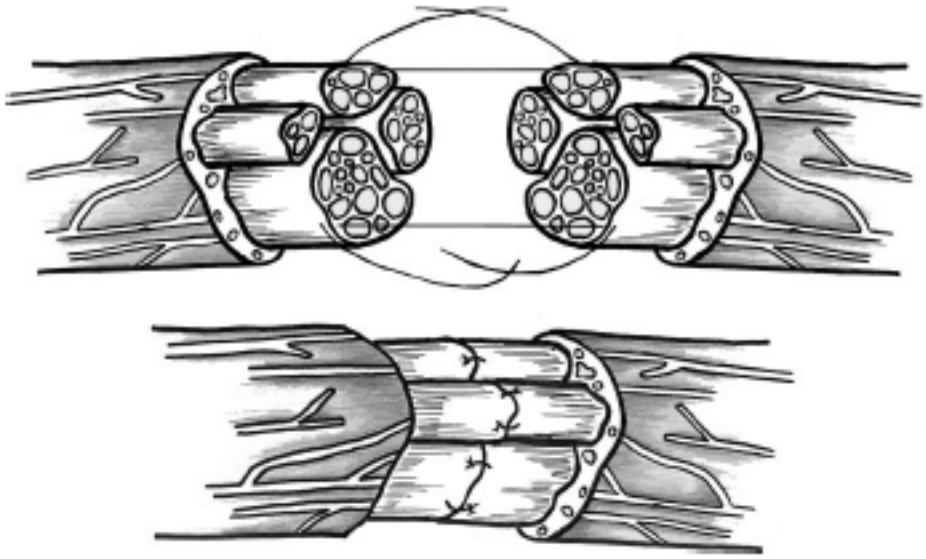

Figure 1.5 Direct repair by end-to-end neurorrhaphy. [13]

Direct repairs are most successful when the nerves are purely motor or purely sensory with minimal intraneural connective tissue [92, 93]. End-to-end nerve repair techniques include epineural repair, group-fascicular repair, and fascicular repair. Epineural repair is a commonly used technique that is ideal for treating sharp nerve injuries of proximal portion of nerves without nerve tissue loss and for partial injuries with good fascicle alignment [90]. As depicted in Figure 1.5, corresponding groups of fascicles are approximated with 2-3 sutures passing through the interfascicular epineurium. In order to ensure optimal nerve regeneration after direct repair, nerve

stumps or groups of fascicles must be precisely aligned without tension, and repaired with minimal tissue damage and minimal number of sutures [94-101]. The fewest number of sutures is ideal to minimize the severity of scar tissue. If there is no scar tissue at the suture line, proximal axons are more likely to extend unimpeded into a network of proliferating Schwann cells within the distal (degenerating) nerve stump, which promotes and directs regeneration [2]. Ultimately, the main goals of end-to-end epineural repair are to restore continuity of the nerve stumps without tension while obtaining proper fascicular alignment.

Although end-to-end neurorrhaphy can be successful, the challenges with this strategy include reproducing the original alignment of nerve fascicles without inducing tension. Furthermore, a direct repair is limited to outside the zone of injury, which means that the entire damaged nerve segment must be removed to prevent scar tissue formation. Unfortunately, surgical procedures to excise tissue can often leave a gap between nerve endings, which could induce longitudinal tension. The build-up of residual tension has been shown to attenuate or stop epineurial blood flow resulting in tissue necrosis and very poor outcomes.

Another approach for direct nerve repair is epineural sleeve neurorrhaphy, which utilizes an epineural cuff. In this technique, epineurium covering the distal stump is rolled back and a 2 mm nerve segment is resected. Then, the created epineural sleeve is pulled over the proximal nerve end and is sutured to the epineurium 2 mm proximal to the coaptation site with two sutures [90]. Since compression and tension is transferred from the repair site to the proximally located epineurium, epineural sleeve neurorrhapy improves the rate of functional recovery compared to end-to-end repair. In addition, the

epineural sleeve provides a biological chamber for the axoplasmic fluid leakage from transected nerve ends, which contributes to a neuropermissive environment for growing axons [90]. The epineural sleeve also provides guidance for regenerating nerve fibers, enables higher number of axons to reach target axons, and prevents a neuroma, which is deep neuropathic pain associated with loss of potential nerve function caused by the inability of regenerating nerves to reach the endoneurial environment of the distal stump due to hindrance from scar tissue [102]. However, the functional results of this technique must be further confirmed in clinical practice.

End-to-side repair is another technique of direct repair that is especially promising for repair of peripheral nerve injuries, where the proximal nerve stump is unavailable or a significant nerve gap exists. This approach is also known as *nerve transfer* and offers a major advantage since the injured nerve can recover function without compromising the function of the donor nerve. End-to-side repair involves the coaptation of the distal stump to the side of an injured donor nerve. In some cases, the donor nerve may be purposely neurectomized (surgical removal of nerve sections) allowing motor neurons to sprout more effectively. Although good sensory and motor recovery was reported is some cases, there are limited control groups and statistical analysis to confirm experimental validity [90]. Outcomes are still unpredictable and highly depend on the surgical technique itself.

1.7.2 Nerve Grafting

In the case of nerve gaps, in which nerve segments cannot be approximated and re-joined back together without tension, the current gold standard of repair is autologous nerve grafting shown in Figure 1.6. In this technique, graft segments are coaptated to the

corresponding groups of fascicles of proximal and distal nerve stumps. In comparison to direct repairs, nerve grafts revealed superior results [90, 103-105]. Furthermore, direct repairs induced nerve tension resulting in nerve ischemia. Nevertheless, the direct repair technique is still preferred if the nerve stumps can be coaptated under mild tension. Nerve grafting or tubulization techniques become particularly useful for large nerve gaps, which would require relatively large tension in order to perform direct coaptation. However, tubulization techniques are feasible only in short nerve gaps. For all other large nerve lesions exceeding 3 cm, nerve grafting is required [90].

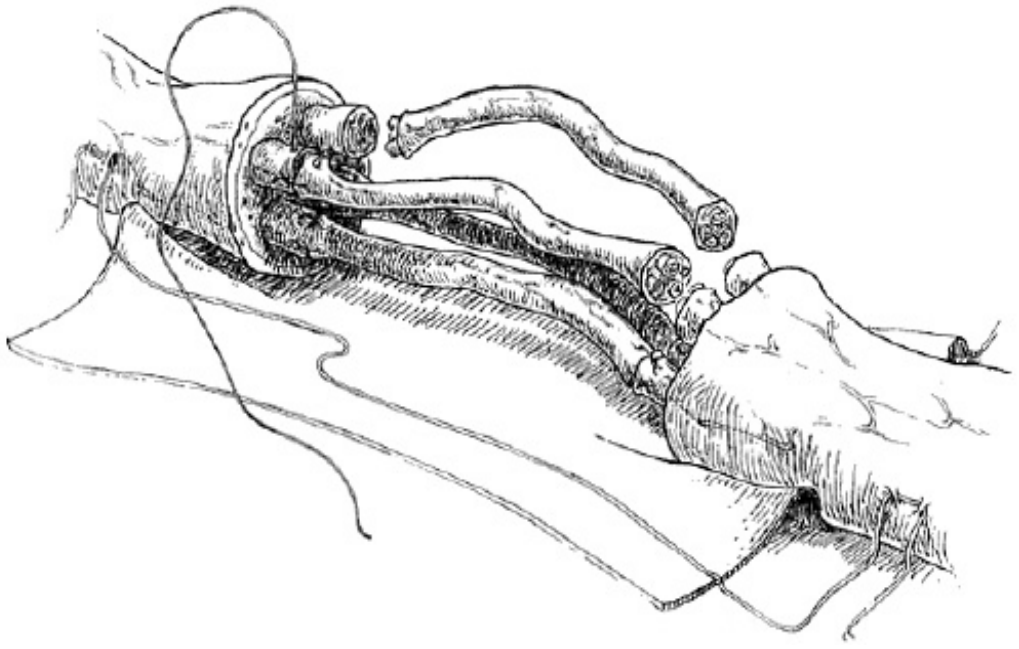

Figure 1.6 Nerve grafting using autologous nerve grafts or cable graft repair. [106]

Nerve autologous or autografts (nerve segments of autogeneic or self origin) were vastly studied during initial nerve grafting experiments dating back to 1870 [107]. Philipeaux and Vulpian first demonstrated proof-of-concept of nerve grafting by

transplanting 2 cm segments of lingual nerves into hypoglossal deficits in dogs. Better functional recovery outcomes along with experimental validity of the benefits of nerve grafting were later established in dogs, rabbits, and guinea pigs [88, 108]. Positive outcomes with nerve autografting were more consistently observed when Seddon repaired large peripheral nerve deficits in the extremities by using small diameter cutaneous nerve grafts in a "cable " fashion instead of using larger caliber grafts [5, 109]. With the advent of operating microscopes and improvements in microsurgical instrumentation and supplies, Millesi and his colleagues eventually improved upon clinical results and further popularized nerve autografting [110].

For repair of gaps longer than 5 mm, the gold standard for bridging the proximal and distal stumps is still the nerve autograft. To date, no tubular or other type of conduit has proved superior to the autologous nerve graft [5]. In the reconstruction of human median or ulnar nerve trunks, only the nerve autograft provides positive outcomes. Donor nerves typically used for autografts are small diameter (2-3 mm) cutaneous nerves harvested from either the arm or leg (ex. sural nerve) for repairing large gaps [5, 111]. Nerve grafts can be very effective because they contain Schwann cells and basal lamina endoneurial tubes that provide neurotrophic factors, including cell and endoneurial tube surface adhesion molecules [112].

Unfortunately, there are several disadvantages with nerve autografting. The use of autologous nerve grafts is limited since the donor nerve has to be excised from another part of the body. This requires multiple surgeries and may lead to loss of function at the donor site and/or donor site morbidity. The signs of morbidity at the donor site typically arise in the form of scar and neuroma pain [113]. Furthermore, limited availability of

donor tissue presents another obstacle if the autograft material is of insufficient length and diameter to optimize the repair. Results obtained using nerve autografts remain variable, ranging from extremely poor to very good. Also, graft phenotype (sensory versus motor) is critical because most motor axons regenerate only within motor nerve grafts, not sensory nerve grafts. Motor neurons have been previously reported to regenerate preferentially down motor nerves when given a choice between motor and sensory nerve pathways [114-117]. Additionally, experimental studies in rodents have suggested that motor nerve grafts support improved nerve regeneration compared to sensory nerve grafts. The potential factors that may influence the success of motor nerve grafts over sensory nerve grafts may rely on differences in the nerve architecture, neurotrophic support, or biochemical markers [114-116, 118-122]. Therefore, specificity of the nerve graft is another factor that should be considered. Motor nerve grafts may also be preferred over sensory due to their larger endoneurial tube diameter, resulting in greater axon numbers [2]. Conversely, sensory nerves are the preferred source for autografts since the primary complication is only localized numbness compared to motor deficits seen with motor nerve grafts.

Although nerve autografts have remained the gold standard for peripheral nerve gap repair for over 50 years, donor site morbidity and limited amount of available donor grafts remain to be major concerns with this technique. In cases where the reconstruction of gaps require lengths of donor graft exceeding available nerve autografts, the only clinical option is the application of allograft material from cadaver donors [90]. Unlike autografts, allografts are obtained from cadaveric donors within the same species. Nerve allografts provide guidance and viable donor Schwann cells, which support and enable

growing host axons to pass from the proximal to distal stump in order to reinnervate target organs. The main advantage of nerve allografts is the lack of donor site morbidity and the unlimited length of nerve tissue available for transplantation. Furthermore, the injured nerve in recipient can be replaced with the same nerve type from the donor.

Despite the low immunogenic potential of nerve allografts compared to skin, muscle, or bone, immunosuppressive treatment is still required to prevent rejection of the graft. Interestingly, the immunogenicity of nerve allografts tends to decrease over time as the process of exchanging Schwann cells from donor origin to host cells proceeds [90, 123, 124]. Without immunosuppression following transplantation, the blood-nerve barrier of donor nerves is broken down and the graft is revascularized leading to infiltration of immune cells. Then, macrophages begin to actively phagocytose both the intact and damaged myelin. CD4 and CD8 T-cells are activated in the periphery and infiltrate the graft and target the donor origin Schwann cells. The donor Schwann cells within the graft increase their major histocompatibility (MHC) class II alloantigens, which serve as antigen presenting cells (APCs). Activated T-helper cells and APCs release cytokines including tumor necrosis factor-α (TNF-α), interleukin-1 and -2 (IL-1, -2), and interferon-γ (IFN-γ), which initiate the cascade of different mechanisms leading to allograft rejection [90]. The final outcome is that the graft is rejected, becoming fibrotic and nonfunctional [90, 125-127]. Therefore, strategies to prevent allograft rejection include the following: MHC matching, allograft pretreatment, and host immunosuppression. Among the current immunosuppression treatments in nerve allografting procedures, the use of cyclosporine A (CsA) only recently became the hallmark of immunosuppressive protocols. Interestingly, some experimental studies

report that outcomes following nerve allografting in CsA-immunosuppressed recipients are comparable with autograft repair [128, 129]. Furthermore, successful nerve allotransplantation including clinical outcomes and details on immunosuppressive therapy has been promising. Although significant sensory recovery including light touch, temperature, and pain sensation were observed in patients with allografts, recovery of motor function remained scant with recovery only limited to patients with upper extremity nerve lesions [130].

Non-nerve tissues have also been explored as alternatives to suture repair of nerve for bridging very short nerve gaps. Conduits from many different biological tissues have been used with varying success. For example, arteries, veins, muscle and other materials have been extensively tested [131-134]. Unfortunately, there are numerous disadvantages with the use of blood vessel, muscle, and other biological tissues for bridging nerve defects. Severe tissue reaction, early fibrosis, scar infiltration, and lack of control over the conduit's mechanical properties are significant problems [135]. As a result, these limitations have led to the consideration of bioengineered conduits made from novel synthetic materials.

1.7.3 Conduit Repair

Although autografts remain to be the clinically accepted approach to treating nerve gap repair, donor site morbidity, secondary surgery, and prolonged surgery durations are still significant concerns. These many disadvantages spawn the development of bioengineered conduit/nerve guides. A conduit as an entubulation model provides an environment conducive for outgrowing axons, growth of Schwann cells, and neurotrophic

stimulation by the distal stump, which are critical factors for optimal return of nerve function [136]. In recent years, various natural and synthetic materials have been tested in experimental and clinical conditions.

Synthetic guidance conduits exhibit numerous opportunities for repair of peripheral nerve defects because their physical and chemical properties (i.e., strength, diameter, porosity, degradation rate) can be precisely manipulated to optimize performance for *in vivo* studies. Interestingly, earlier attempts at regeneration through 10 mm long chambers had comparable results to nerve autografts in rats [137]. Furthermore, promising results were also seen with using plasticized polyester tubes to successfully reconstitute the nerve trunk of a rat sciatic nerve [138]. The polyester family, which includes polylactic acid, polyglycolic acid and poly(lactic-co-glycolic) acid has been an early set of materials for testing due to their availability, ease of processing, and FDA approval [139]. One of the first degradable synthetic polymers evaluated as a conduit material was polyglactin (Vicryl mesh), which demonstrated no significant irritation or toxicity to regenerating nerves despite unusual nerve morphology compared to normal nerve [140]. Overall, the use of synthetic biodegradable conduits has shown promising results in nerve regeneration applications. Some of these promising biomaterials include poly(phosphoester), poly(lactic-co-glycolic) acid, poly(organophosphazene), poly(L-lactide-co-μ-caprolactone), poly(DL-lactide-co-glycolide) and poly(3-hydroxybutarate) [141-145].

Despite promising findings with these synthetic polymers, they are not able to facilitate long-term growth over long gaps due to collapse, scar infiltration, and early resorption [135]. Furthermore, biodegradable synthetic materials have shown some

release of cytotoxic degradation products, which may introduce additional problems associated with resorption such as macrophage invasion, fibrosis, and disorganized axonal growth [94, 135]. In order to design a successful bioengineered conduit, several key properties that should be considered are the following: easily fabricated with desired diameter, implanted with relative ease, and easy sterilization. Additionally, an ideal conduit must be flexible but still able to maintain structural and mechanical integrity *in vivo*. Some other parameters in the design that should also be considered are tube dimensions, permeability, luminal surface topography, and inherent electrical charge within conduit [5, 139]. Ultimately, the goal of an ideal bioengineering conduit is to consistently perform better than an autograft.

In recent years, the design of nerve guidance conduits has focused more on improving the single lumen of the conduit to bridge larger nerve gaps. Numerous combinatorial approaches have been incorporated into the design such as collagen and laminin-containing gels, Schwann cells, and growth factors [146]. Although the addition of hydrogels into the lumen of conduits is a major improvement for nerve regeneration, there still needs to be an oriented micro-architecture in place for supporting long-term guidance of regenerating axons through long nerve gaps. The incorporation of filaments or oriented scaffolds into the lumen of the conduit may potentially provide important physical cues to appropriately steer axons towards the distal nerve stump for reconstitution of nerve processes. Hence, the primary challenge is selecting appropriate biomaterials, which support contact guidance of regenerating axons, do not exhibit cytotoxicity effects, and can be naturally remodeled after regenerative processes have been completed. The main emphasis of this dissertation is towards developing collagen

I-derived fiber and hydrogel constructs to evaluate contact-guided axon growth of embryonic and adult sensory neurons, and Schwann cell migration and orientation to optimize a proof-of-concept model for a novel bioengineered nerve conduit.

CHAPTER 2

DEVELOPMENT AND CHARACTERIZATION OF AUTOMATED WET SPINNING DEVICE FOR COLLAGEN FIBER FABRICATION

In this study, the emphasis is on the evaluation of synthetic collagen fibrous scaffolds manufactured from a wet spinning technique. These collagen scaffolds are firm collagen monofilaments synthesized by a custom-built, miniaturized wet spinning device. Concentrations of collagen dispersions for wet spinning were tested and optimized based on fiber uniformity, tensile strength, thermal stability, and ease of fabrication. The physiochemical properties of collagen fibers were tested by analyzing swelling response, denaturation and glass transition temperature of non-crosslinked and crosslinked samples. The mechanical strength of the fibers was analyzed using instron.

2.1 Introduction

Engineering methods to construct biological tissue substitutes are important for finding new approaches to repair diseased or damaged tissues [147-152]. A commonality in repair strategies is an engineered biomaterial scaffold that provides a physical and biochemical template for tissue regeneration. While cell growth can be greatly affected by physical properties such as porosity, surface roughness and elasticity [150, 153-155], directed tissue formation is equally important to the development of tissue architecture. Innovative methods for guided tissue growth must also include a well-defined architecture in which the native cells will respond favorably.

Scaffolds exhibiting fibrous structures are of unique interest for many tissue engineering strategies that require unidirectional alignment of growing cells [156]. Current techniques for fabricating micro to nano-fiber scaffolds are salt or particulate leaching [157-160], rapid prototyping [161, 162], self-assembled hydrogels [163-169], electro-spinning [66, 170-173] and phase separation [174]. In addition, several conventional fiber spinning techniques in the textile industry such as dry spinning, melt spinning, and wet spinning have also been utilized for orienting polymeric materials into fibrous scaffolds for biomedical applications [175-181]. Synthetic polymers are readily used for fiber spinning and scaffold fabrication due to the ease of manipulation and reproducibility under various processing conditions. Conversely, natural polymers are often preferred since they more closely mimic the physiochemical properties of the extra-cellular matrix (ECM) and avoid complications such as inflammation or material toxicity [182]. Conventional fiber spinning techniques, however, are typically not suitable for processing biological polymers into fibers; e.g. the high temperatures of melt spinning or the use of harsh solvents. Among the scaffold fabrication techniques, biopolymers processed under wet spinning conditions are less prone to denaturation and loss of native molecular orientation.

Wet spinning is often used to create single fibers from biological polymers such as chitosan, hyaluronic acid, silk, alginate and collagen [178, 183-186]. It is generally a manual process of injecting a polymer solution through a needle (spinneret) into a coagulant bath for pH-dependent precipitation [176-178, 180, 187-189]. As the precipitate is extruded into the coagulation bath, shear forces can orient the chain

molecules into a thin filament [189]. The fiber is then collected from the coagulation bath and dried.

2.2 Materials and Methods

Here, an automated wet spinning device was custom built to improve reproducibility of fiber fabrication and yield of continuous collagen fibers up to half a meter in length. The design enables user-defined adjustment of the important processing parameters in wet spinning: needle gauge size of the spinneret, extrusion rate of the collagen dispersion, pH of the coagulation bath, speed of the fiber collection, and the drying time. In this study, the effects of collagen dispersion concentration on fiber size, uniformity, mechanical strength and swelling response were investigated. In addition, crosslinking reagents were evaluated as a post-processing step to increase the mechanical stability and control the swelling response of collagen fibers.

2.2.1 Preparation of Collagen Dispersions

Collagen I was extracted and purified from tendons dissected from Sprague-Dawley rat tails (8-9 weeks old) following a previously established protocol [190]. The extracted tendons were digested in sterile 0.7% acetic acid (1g / 150ml) for 5-7 days at 4^{o}C with mechanical agitation (stir bar). The tendon solution was transferred to 50 ml centrifuge tubes and spun at 3500rpm for 30 min. The collagen supernatant was retained while discarding the pellet of tendon debris. Collagen supernatant was spun again at 2500rpm for 10-15 min to further separate remaining tendon debris. The supernatant was dialyzed in a cellulose membrane tube (MWCO: 12,000-14,000) overnight at 4^{o}C in dialysis

buffer (0.5M Na_2HPO4, 0.5M NaH_2PO4, pH 7.4). After dialysis, the semi-solid gel of collagen was transferred to 50 mL centrifuge tubes and spun at 3500 RPM for 30 min to further concentrate the collagen. The collagen pellet was spread onto dishes and lyophilized at -80°C to 20°C for 48 hours to gradually remove water content resulting in a dry porous sponge as seen in Figure 2.1.

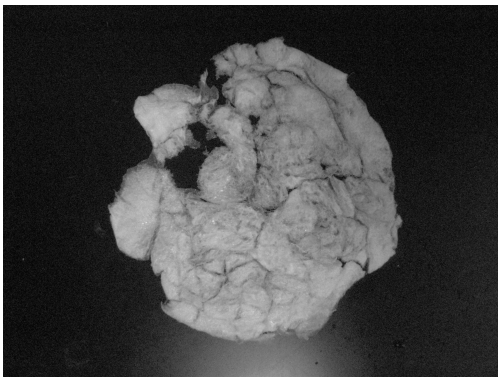

Figure 2.1 Lyophilized collagen sponge.

Freeze-dried collagen was weighed and used to prepare 0.75, 1.0, 2.0 and 3.4 percent weight (% wt) collagen dispersions in 0.2% glacial acetic acid. Collagen within the dispersion is not completely soluble. A collagen dispersion contains small fiber portions of insoluble collagen, some of which disassemble into smaller fibril subunits in the presence of acidic solutions below pH 3. This physical transformation of disassembly is regarded as swelling, which results in dispersions appearing uniform and opalescent as shown in Figure 2.2.

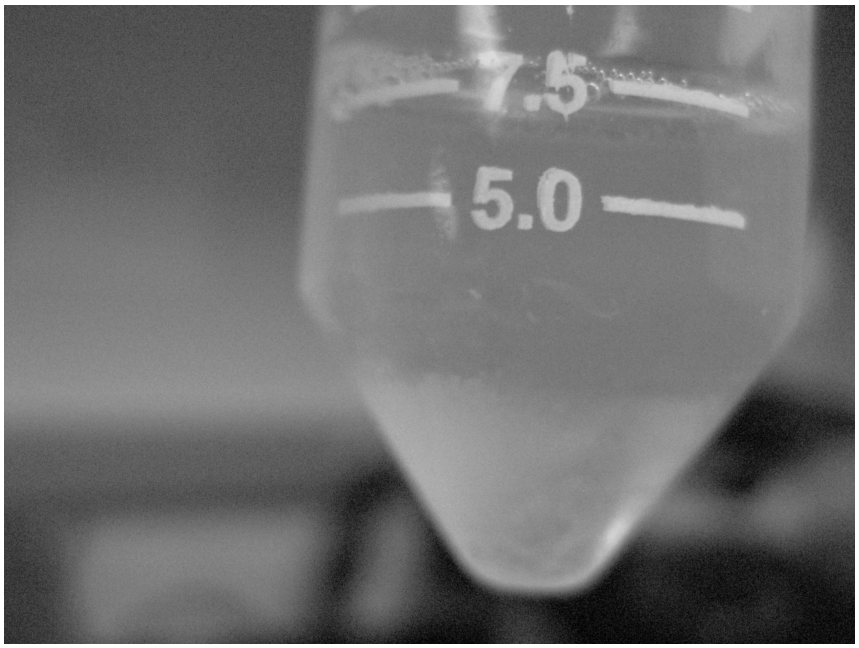

Figure 2.2 Collagen dispersion at approximately 2.5 mg/ml.

The concentration (in mg/ml) of the collagen within the dispersions was determined by modifying the bicinchoninic acid (BCA) Protein Assay (Pierce, Thermo Scientific). Since collagen in a dispersion is not completely solubilized, the BCA reactivity is inhibited, underestimates the actual concentration of collagen, and cannot be compared to the supplied albumin protein standards [191]. To create useful standards, rat tail collagen with known concentration was purchased from BD Biosciences and diluted in 0.02M acetic acid to 2.0 mg/ml, 1.0mg/ml and 0.75mg/ml. The samples of collagen dispersions were diluted ten-fold to within the 0.75 – 2.0 mg/ml concentration range of the protein standards. 25 μL of standards and samples were loaded into the wells of a 96-well plate.

To assist in solubilizing and unfolding of collagen, 0.2% w/v sodium dodecyl sulfate (SDS) was added to the BCA reagent. This amount of SDS induced a negligible

non-specific reactivity of the BCA. 200 μL of the BCA reagent/SDS solution was added to each well and the plate was placed on an orbital shaker for up to 270 min at 25^{o}C to facilitate BCA reactivity. An Emax precision microplate reader spectrophotometer (Molecular Devices, Sunnyvale, CA) was used to measure absorbance of the protein standards and the unknowns. A standard curve of the absorbance vs. concentration of the protein standards was used to extrapolate and confirm the concentrations of the dispersions for wet spinning.

2.2.2 Wet Spinning

Collagen dispersions were extruded into a room temperature coagulation bath of ammonium hydroxide (Acros Organics, Fair Lawn, NJ) and acetone (HPLC grade, Fisher Scientific) at a 1:50 volume ratio. The pH and bath level were periodically monitored within the chamber using pH litmus paper and adjusted with ammonium hydroxide if pH fell below 9. The coagulation bath works by dehydration; forcing water from the dispersion and precipitating collagen into solid monofilament strands. Fibers were then manually transferred to a drying rack in which they were air-dried under the tension of their own weight at room temperature for a minimum of 48 h.

2.2.3 Automated Collagen Wet Spinning Device

The wet spinning device consisted of a syringe pump, a custom made coagulation bath chamber, fiber collection belt and a geared variable speed DC motor for controlling the rate of fiber collection as shown in Figure 2.3. A 10-ml syringe (BD Biosciences) containing the collagen dispersions of 0.75, 1, 2 or 3.4 wt% was loaded into a syringe

pump system (Fisher Scientific Model No. 78-01001) (Dupont, Wilmington, DE) operated at a rate of 12.4 ml/hr. The syringe pump was connected via 0.38 mm (inner diameter) Viton® tubing to the spinneret - a blunt end, type 304 stainless steel 22-gauge needle (inner diameter = 406 μm, McMaster-Carr, Elmhurst, IL). A clamp was built to hold the spinneret submerged about 2 inches into the coagulation bath with slight contact on the surface of the collection belt.

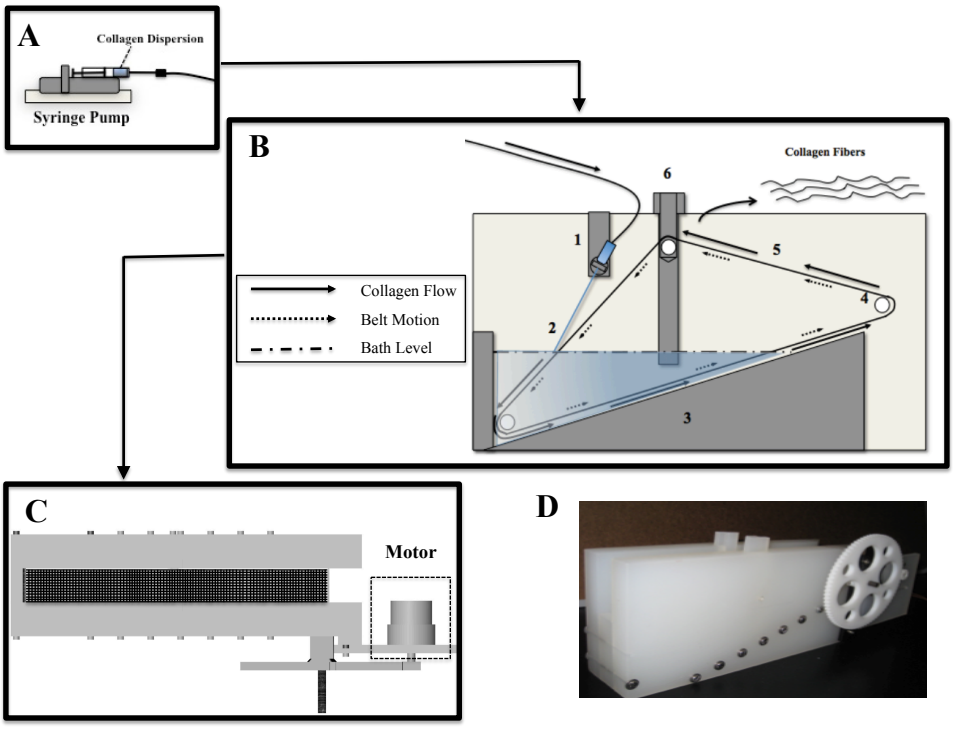

Figure 2.3 Schematic of the wet spinning system. (A) Syringe pump controls the extrusion rate of collagen dispersion into the device. (B) Wet spinning device with inside view depicting the flow and deposition of collagen; (1) spinneret clamp, (2) spinneret tip, (3) middle connector, (4) rod connected to gears/motor, (5) collection belt and (6) tension adjustment for belt. (C) Pro/E top view of device showing the location of the motor. The motion of the belt is driven by the gear-motor system. D) Actual side view of device.

The coagulation chamber was formed from three parts of ½ inch thick polypropylene: 2 rectangular sides of the chamber and a middle section. A set of 18

stainless steel machine screws and washers (McMaster-Carr, Elmhurst, IL) were used to fasten the three-part chamber and provide a leak-proof tight seal to contain the coagulation bath. The middle section (or connector) had an incline ramp of 20^{o} designed to limit the amount of coagulation bath to no more than 150 mL per wet spinning session.

A polytetrafluoroethylene (PTFE) mesh was used as the fiber collection belt (0.018-inch (457 μm) mesh size, McMaster-Carr, Elmhurst, IL). The PTFE mesh was cut to a length of 11 inches and width of 0.9375 inches and sewn together using polypropylene sutures (Ethicon, Somerville, NJ). Three rotating delrin rods supported the collection belt within the inner chamber; one rod was directly connected to a gear located on the shaft of the motor to drive the belt and a second rod was used to adjust the tension of the belt, Figure 2.3B. The third rod was used to guide the movement of the belt.

The collection belt was driven by a 12V DC 60 RPM, 3200 g-cm torque motor (Jameco Electronics, Belmont, CA). Collection of collagen filaments was optimized at a belt speed of 6 RPM. To gear down the motor speed, two gears with 5 inch and 0.5 inch diameters (gear ratio of 10:1) were designed using Pro Engineer Wildfire 4 (PTC, Needham, MA) software and printed on a rapid prototype, 3-Dimensional printer (SST 1200es, Dimension, Inc., Eden Prairie), Figure 2.3 C&D.

2.2.4 Fiber Uniformity Analysis

To determine fiber diameter and uniformity, dried fibers were cut into 1cm lengths. A low magnification 4x objective on a Nikon Eclipse TE2000-S inverted microscope was used to take images of the fiber, which were merged together to create a photo montage

of the entire 1 cm fiber using Adobe Photoshop. Fiber diameter was measured randomly at 10 points along the fiber using Image J software (NIH). Diameter measurements for each fiber group (0.75, 1, 2, 3.4 % wt and crosslink-treated fiber groups) were used to calculate the mean fiber diameter and standard deviation to analyze fiber uniformity.

2.2.5 Cross-linking

In a post-processing step, 0.75% wt collagen fibers were cut into 3 cm segments and cross-linked with genipin or glutaraldehyde to increase mechanical strength and reduce the swelling response. Fibers were immersed in solutions 1.0% genipin (Wako Pure Chemical Industries, Ltd., Japan) in 40% (v/v) ethanol or 1.0% (v/v) of glutaraldehyde in water at 25^{o}C for 24h. The cross-linking reagents were aspirated from the dishes and then rinsed for 10 min in ddH2O, 2 min in PBS and 2 min in 70% ethanol. This rinsing procedure with ddH2O and PBS was repeated three times to ensure that residual cross-linking reagents are thoroughly removed. Fibers were then air dried inside a sterile tissue culture hood for 24 h.

2.2.6 Mechanical Testing

An Instron 3342 Universal testing machine (Instron, UK) was used to generate uniaxial force-extension curves for 0.75, 1.0, 2.0 and 3.4 wt% collagen fibers and for cross-linked fiber groups. Air-dried fibers (n=10) from each of the fiber groups (0.75% wt, 1.0%wt, 2.0% wt, 0.75% wt genipin crosslinked and 0.75% wt gluteraldehyde crosslinked) were cut into 3 cm segments and mounted with tape to grip the ends of the fibers to prevent slippage while ensuring that the fibers were not damaged at the contact points of the

clamp. The fibers had an average diameter range of 46-193 μm depending on the dispersion concentration. ASTM standard D3822-01 was followed in this study since it involved tensile property measurements of natural and synthetic single textile fibers. According to this method, the minimum gauge length for effective testing of specimens is 10 mm. Here, the gauge length for each sample was set to 2 cm. Results obtained from fibers that broke at contact points or from fibers that slipped from the clamps were rejected. The extension was applied at 5mm/min. The strain was determined by the increase in fiber length divided by the original length.

Fibers were tested under an extension rate of 5 mm/min and a gauge length of 2 cm for each sample. Force – extension curves were used to directly determine the spring constant k using the equation:

$$F = kx,$$

where F is the force applied to the fiber, x is the amount of fiber extension under the applied force, and k is the spring constant. The stiffness of the fibers can be quantified by observing changes in the slope of the curve k. The fiber stiffness in terms of the tensile or Young's modulus was also calculated using the equation

$$\sigma = E\varepsilon$$

The stress σ was calculated by dividing the applied force by the averaged fiber diameter measurements. The strain ε was calculated by dividing extension by the fiber gauge length. The tensile modulus E was calculated from the slope of the stress-strain curve within initial 5% strain.

2.2.7 Fiber Swelling Response

The extent of water absorption was evaluated between non-crosslinked and crosslinked 0.75% fibers with 1.0% genipin and 1.0% glutaraldehyde. Fibers (n=10) were incubated in PBS (pH 7.4) at 37^{o}C and fiber diameters were measured at 30 min, 60 min, 24 h and 6 weeks using ImageJ software. Average fiber diameters were determined from measurements at 10 locations along the fiber. To minimize variation in measurements at each time point, diameters were measured at the same location along the fiber.

2.2.8 Differential Scanning Calorimetry (DSC)

The thermal properties of wet-spun collagen fibers were quantified using thermo-analytical methods. Differential scanning calorimetry (DSC) provides information on structural changes in collagen fibers when subjected to a heat-cool-heat cycle. Specifically, DSC was used to determine thermal stability of collagen fibers. Thermal analysis including the denaturation and glass transition temperature of the collagen fibers was determined using the Q100 differential scanning calorimetry (TA Instruments New Castle, DE). The non-crosslinked fibers were used as the control for the study. Fibers were cut into small pieces and weighed. Approximately, 5mg of sample was hermetically sealed in aluminum DSC pans. The reference holder consisted of an empty DSC pan, which was sealed and crimped. Heating was applied by heat-cool-heat with a heating rate of 10 ^{o}C/min over a range of 10-250 ^{o}C. A cooling rate of 10 ^{o}C/min for the cooling cycle was applied until the sample is cooled to 10 ^{o}C and the heat operation mode is restarted. The heat-cool-heat method was used to determine, thermal denaturation

temperature, endothermic transition, and glass transition. The results were used to validate glutaraldehyde and genipin crosslinking.

2.2.9 Cell Culture and Immunocytochemistry

Dried collagen fibers were cut into 1 cm segments, rinsed for 10 min in ddH2O, 2 min in 70% ethanol and air dried inside a sterile tissue culture hood. The ends of fibers were glued down with 2 mg/ml collagen to the wells of a 6-well polystyrene tissue culture treated plate and allowed to air dry overnight prior to cell plating. Dorsal root ganglia (DRG) were isolated from embryonic day sixteen (E-16) fetuses from timed-pregnant Sprague-Dawley rats (Charles River, Wilmington, MA). DRG explants were isolated in L-15 medium and dissociated using trypsin (0.25%) for 1 hour at 37°C. Neurobasal medium + 5% FBS was then added, and the tissue was triturated followed by centrifugation at 1000 rpm for 5 minutes. The supernatant was aspirated and the cells were re-suspended at $5x10^6$ cells/mL in Neurobasal medium supplemented with 2% B-27, 500 μM L-glutamine, 1% Penicillin/Streptomycin, 1% FBS, 2 mg/mL glucose (Sigma, St. Louis, MO), 10 ng/mL 2.5S nerve growth factor (BD), 10 mM 5-Fluoro-2'-deoxyuridine (FdU) (Sigma), and 10 mM uridine (Sigma). A 5 μL of the DRG cell suspension was plated at the ends of the fibers (non-crosslinked 0.75% wt, 1.0% genipin, and 1.0% glutaraldehyde fiber groups). Cells were constrained to the end of the fiber by the placement of the cell suspension as a bubble size droplet. The cultures were incubated (37°C and 5% CO_2) for 2 hours to allow neurons to attach before 2 mL of media was added. The culture media was changed every 2-3 days *in vitro* (DIV) by replacement with fresh media pre-warmed to 37°C.

The neuronal adhesion and neurite outgrowth response were assessed via immunohistochemistry for neurofilaments within axons. The cultures were fixed in 4.0% paraformaldehyde (Fisher, Fairlawn, NJ) for 1 h, rinsed in PBS and permeabilized using 0.1% Triton X-100 (Kodak, Rochester, NY) + 4% goat serum (Invitrogen) for 1 h. Neurofilament antibody (NF-200, Sigma-Aldrich, St. Louis, MO) was added (in 0.1% Triton X-100, 4% goat serum in PBS) for 18-24^{o}C for 1 h at 1:400. Secondary fluorophore-conjugated antibody (Alexa 488-conjugated IgG, Molecular Probes) was added in PBS at 18-24^{o}C for 2 h.

2.3 Results

The characterization of the wet spinning device, evaluation of physiochemical and mechanical properties of the collagen fiber end-product, and the neuronal cell response to cross-linking treatments are detailed here. The following sections present comprehensive characterization results and provide established protocols for the fabrication of the collagen fibers using the device.

2.3.1 Characterization of Wet Spinning Device

After the design of the automated wet spinning device, a series of mechanical and physiochemical characterization methods were used to evaluate the end-product collagen fibers. The characterization of fibers helped identify the necessary parameters that needed to be optimized to manufacture reproducible, uniform collagen fiber scaffolds for neural tissue engineering applications.

2.3.2 Collagen Dispersions and Quantification of Collagen Extracts

Collagen dispersions induced minimal colorimetric change within initial 30 minutes following the BCA protein assay. This is likely due to dispersions consisting primarily of insoluble components of collagen that hinder the colorimetric reaction. Hence, any assay results from the standard protocol could not be compared to the BSA protein standards for quantification. Here, the BCA protein assay was modified to help solubilize collagen to improve the colorimetric reaction by adding 0.2% w/v SDS to the BCA reagent. Additionally, physical agitation of the 96-well plate with an orbital shaker was observed to expedite the reaction.

To test this protocol, colorimetric absorbance measurements were compared between the BSA kit standards and standards made from a commercially available collagen at a known concentration. Hence, collagen I derived from rat tail tendon purchased from Becton Dickinson (BD) Biosciences was utilized as standards. Regression analysis was used to compare the absorbance versus concentration curves for the BSA standards and collagen standards as shown in Figure 2.4 A.

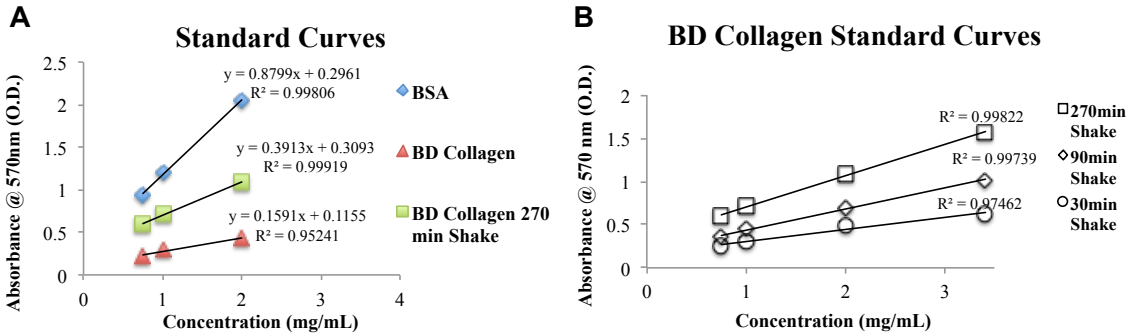

Figure 2.4 Quantification of collagen by modifying BCA protein assay. (A) Comparison of standard curves from bovine serum albumin (BSA), Becton Dickinson (BD) rat tail collagen I standards and BD standards following 270 min of shaking. (B) The effects of

0.2% w/v SDS and shaking intervals of 30, 90 and 270 min on absorbance values of BD collagen.

The results also show that using 0.2% w/v SDS and shaking the samples up to 270 minutes enhanced the colorimetric reaction, Figure 2.4 B. No significant changes in absorbance values were detected beyond 270 minutes. Since the collagen standards closely matched the BSA standards, they were more suitable for interpolating the concentration of the unknown collagen dispersion samples.

2.3.3 Automated Wet Spinning Device

Fibers from 0.75% wt collagen dispersions were wet-spun either manually or automatically using our device to generate samples. Fibers were dried for 24 h and cut into 1 cm segments. Each 1 cm segment of fiber was equally divided into 1 mm intervals using a grid layout on NIH ImageJ software. A measurement was taken at random within each of these intervals for a total of 10 measurements per fiber. The mean fiber diameters of wet spun collagen fibers produced from the automated wet spinning device were 46.5 ± 10.9 μm and fibers produced manually were 57 ± 31.1 μm, respectively. Importantly, wet spun fibers produced from the automated device were more uniform than manually produced fibers as indicated by the reduced standard deviations. Fibers generated from the device were also longer and continuous providing higher yields for each wet spinning process.

The ability of this device to extrude dispersions through the syringe pump system and form fibers was compared for 0.5, 0.75, 1.0, 2.0 and 3.4% wt dispersions. Dispersions of 0.5% wt produced brittle two-dimensional films while 0.75% wt

dispersions generated consist strands, which had a well defined fiber morphology. Fibers from 0.75 and 1.0 % wt dispersions were readily extruded into the coagulation bath, whereas the viscosity of 2.0 and 3.4% wt dispersions made it difficult to load into the syringe, flow through the Viton® tubing and extrude out of the spinneret. Therefore 2.0 and 3.4% wt dispersions were gently heated to 40°C to reduce viscosity, which facilitated loading and spinning. The diameters and uniformity of fibers produced from 0.75 and 1.0% wt were 46.5 ± 10.9 µm and 55.9 ± 14.9 µm, respectively. The fibers from 0.75% wt were smaller than fibers produced from 1.0% wt but were not significantly different, $p>0.05$ as shown in Figure 2.5. Further increases in collagen dispersion concentration led to increased fiber diameters and larger variability. 2.0 and 3.4% wt collagen dispersions produced fibers with mean diameters of 105.02 ± 24 µm and 193.4 ± 38.9 µm, respectively.

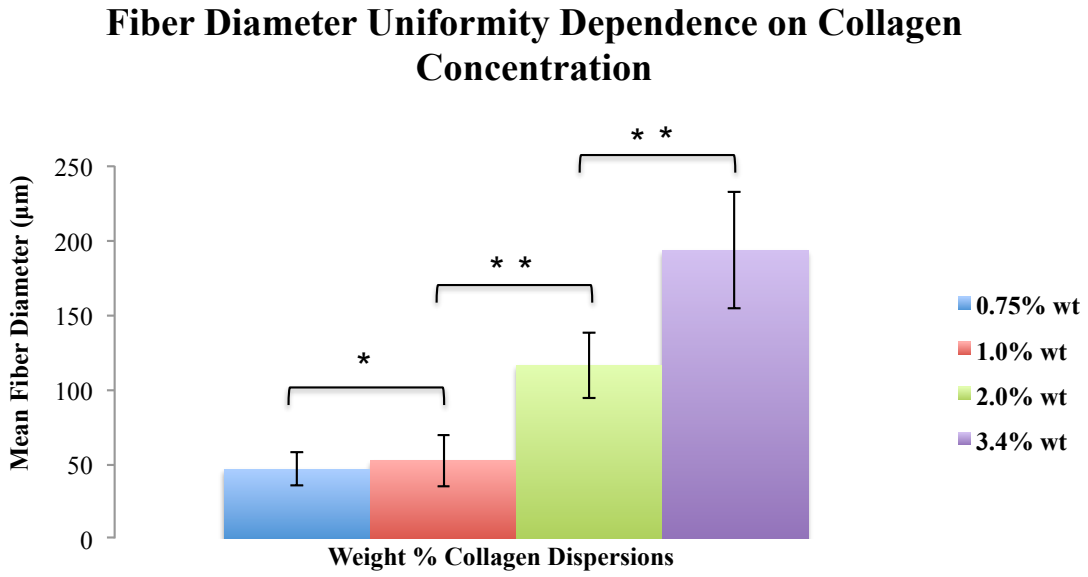

Figure 2.5 Fiber diameter and uniformity in relation to collagen dispersion concentration. (* denotes $p>0.05$ or statistically insignificant, ** denotes $p<0.05$ or statistically

significant difference)

2.3.4 Mechanical Analysis

The effects of collagen dispersion concentration and crosslinking treatment on fiber strength were analyzed. Instron tensile test data in the form of force-extension curves were used to determine the degree of stiffness *k* based on the slope of the curve. Force-extension curves independent of mean cross-sectional areas were evaluated for all the dispersions to determine fiber stiffness. Additionally, the mean cross-sectional area of the fibers was used to obtain approximate stress-strain curves.

For non-crosslinked fiber samples, the force-extension curves revealed that the fiber stiffness decreased as the concentration of dispersion increased as seen in Figure 2.6 A.

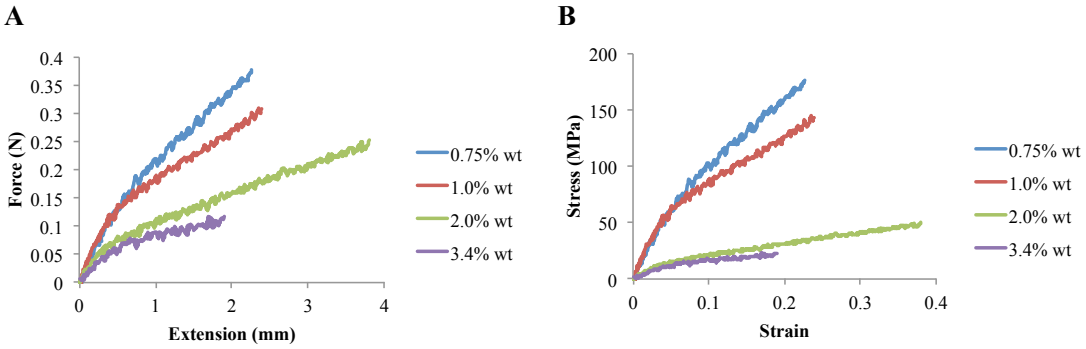

Figure 2.6 (A) Force-extension curves and (B) stress-strain curves for different wet-spun fibers.

The 0.75% wt and 1.0% wt dispersions measured within the initial 5% strain had tensile moduli of 1265 ± 171 MPa and 800 ± 143 MPa, respectively, Table 2.1. The 2.0% and 3.4% wt dispersions had much lower moduli of 286 ± 58 MPa and 236 ± 98

MPa, respectively. Using mean diameter measurements for determining stress could result in inaccurate stress values as the measured moduli would occur in areas of high stress. This finding correlated with the relationship between elastic modulus and increasing collagen concentration. Higher elastic moduli were seen in fibers produced from lower concentrations since the fiber diameters were smaller as shown in Figure 2.6 B. The results suggest that as the concentration of dispersion increases from 2.0 and 3.4% wt, the fibers become less stiff with smaller deformation. The weak mechanical properties of fibers from 3.4% wt dispersion as observed in the stress-strain curve are characterized by the limited deformation and low ultimate tensile strength upon failure as seen in Figure 2.6 B.

The improvement of cross-linking fibers on mechanical properties was investigated. Fibers wet-spun from 0.75% wt dispersions were cross-linked in a treatment of 1.0% glutaraldehyde (GA) and 1.0% genipin (Gp) and tested under tensile analysis. Cross-linking was a post treatment where dried fibers were rehydrated with a cross-linking solution and then dried for a minimum of 24 hours prior to mechanical testing. Since the procedure could affect fiber mechanical properties, a sham group was prepared by soaking 0.75% wt wet-spun fibers in dH_2O only and dried in parallel with fiber cross-linking treatments.

Table 2.1 Effects of Concentration and Crosslinking on the Tensile Properties of Wet-spun Collagen Fibers.

%wt Collagen Dispersion	Tensile Modulus	UTS	% Elongation
Dry 0.75	1265 ± 171 MPa	262 ± 62 MPa	18.4 ± 4.9
Dry 1.0	800 ± 143 MPa	240 ± 25 MPa	36.7 ± 8.0
Dry 2.0	286 ± 58 MPa	57 ± 15 MPa	43.6 ± 9.1
Dry 3.4	236 ± 98 MPa	25 ± 2 MPa	11.2 ± 2.0
0.75 Non-crosslinked in Water	707 ± 68 MPa	59 ± 18 MPa	10.9 ± 1.6
0.75 Crosslinked 1.0% Genipin	2394 ± 148 MPa	222 ± 74 MPa	16.4 ± 1.3
0.75% Crosslinked 1.0% Glutaraldehyde	2821 ± 168 MPa	136 ± 2.6 MPa	10.8 ± 1.9

For cross-linked fiber samples, the stress-strain curves revealed that the tensile modulus increased following 1.0% GA and 1.0% Gp treatments compared to the sham and dry fiber groups shown in Figure 2.7. Collagen fibers treated with 1.0% GA and 1.0% Gp had greatly increased tensile moduli of 2821 ± 168 MPa and 2394 ± 148 MPa, respectively, Table 2.1. Interestingly, the procedure of rehydrating and drying collagen fibers lowered tensile strength from a mean tensile modulus of 1265 ± 171 MPa to 707 ± 68 MPa.

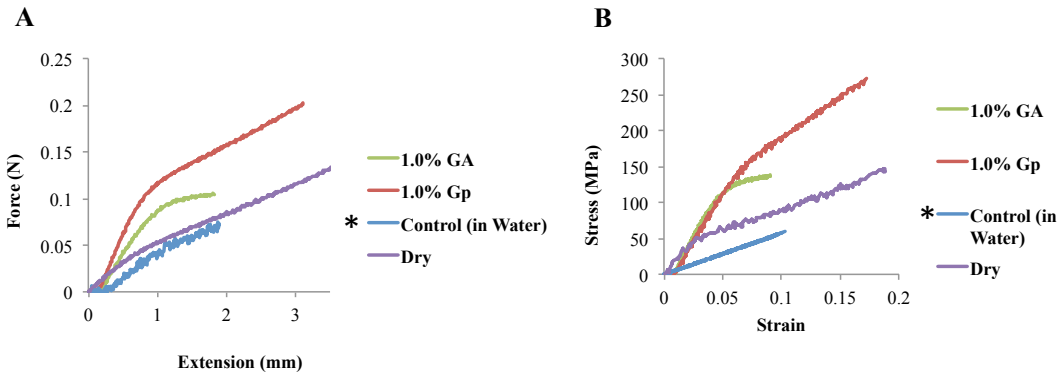

Figure 2.7 (A) Force-extension curves and (B) stress-strain curves for different cross-linking treatments of 0.75% wt wet-spun collagen fibers. * denotes control group or sham group in water to compare with cross-linking treatments in water.

2.3.5 Swelling Response

Collagen fibers like other natural polymers are known to undergo water absorption under physiological conditions. The degree of swelling was quantified based on fiber diameter before (dry) and after incubation in PBS for 30 min, 60 min, 24 h and 6 weeks at 37^{o}C. Non-crosslinked 0.75% wt fibers swelled to slightly more than twice its diameter within 30 min of incubation as observed in Figure 2.8. With the presence of crosslinkers 1.0% glutaraldehyde and 1.0% genipin, the degree of swelling in terms of diameter was reduced from 2X the diameter to 1.5X and 1.3X the diameter, respectively.

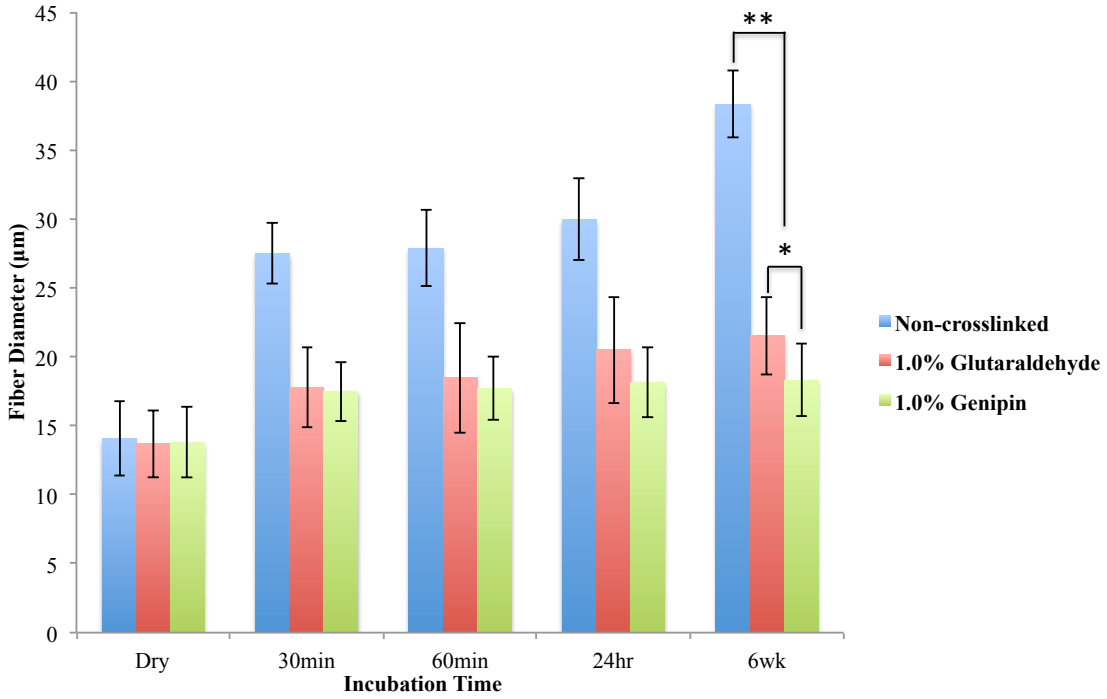

Figure 2.8 Swelling behavior for non-crosslinked and cross-linked 0.75% wt collagen fibers in PBS. (*denotes $p>0.05$ or statistically insignificant, ** denotes $p<0.05$ or statistically significant difference)

The swelling response trend in the fibers with and without cross-linkers suggest that cross-linking may limit water adsorption in collagen fibers. Furthermore, the use of 1.0% genipin was equally effective as 1.0% glutaraldehyde in lowering the swelling response of the collagen fibers.

2.3.6 Differential Scanning Calorimetry

Thermal analysis using differential scanning calorimetry (DSC) was used to characterize the thermal transitions of collagen in fibers spun from each dispersion including both crosslinked and non-crosslinked samples. During the first heat step of the heat-flow-heat

test, a broad endotherm in the graph is due to water being driven off from the collagen fibers as seen in a thermogram of non-crosslinked 0.75% wt collagen fibers, Figure 2.9.

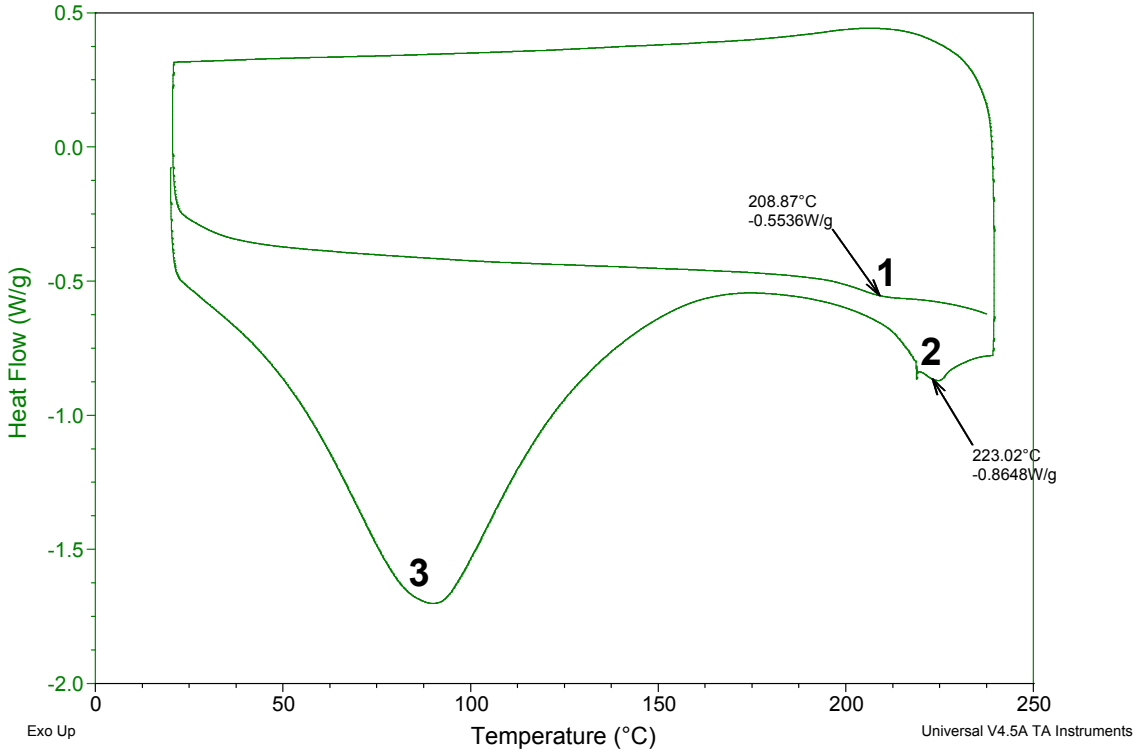

Figure 2.9 Typical thermogram for 0.75% wt non-crosslinked collagen fibers. (1) Glass transition temperature, (2) Denaturation temperature, (3) Broad peak representing water loss from sample.

By increasing the temperature, the denaturation temperature is reached when all the native hydrogen bonds that link the α chains of the collagen triple helix together are finally broken. A steady increase in temperature results in the irreversible uncoiling of the collagen triple helix and denaturation into gelatin. A small endothermic peak marks denaturation at 180-230° C. The collagen fibers were then cooled back down to 10° C during which the glass transition temperature is observed at 185-210° C. The glass transition temperature occurs when the mobility of particles increases within the structure

resulting in the material changing from solid rigid phase to a plastic, rubbery phase. As the concentration of the collagen dispersions increased, both T_d and T_g decreased as seen in Table 2.2. 0.75% and 1.0% wt dispersions had denaturation temperatures of 223.02 ± 1.5 ^oC and 213.41 ± 2.0 ^oC, respectively. The glass transition temperatures of 0.75% and 1.0% wt were 208.87 ± 1.5 ^oC and 201.93 ± 0.5 ^oC, respectively, which were closely similar. There was a significant reduction in denaturation temperatures for 2.0% and 3.4% wt with values of 187.24 ± 0.5 ^oC and 186.35 ± 0.5 ^oC, respectively. Likewise, the glass transition temperatures for 2.0% and 3.4% wt dispersions were also lower with values of 185.11 ± 0.1 ^oC and 182.96 ± 0.5 ^oC, respectively.

Table 2.2 Comparison of Thermal Properties for Wet-spun Collagen Fibers

Weight %	Denaturation Temperature (T_d)	Glass Transition Temperature (T_g)
0.75	223.02 ± 1.5 C	208.87 ± 1.5 C
1	213.41 ± 2.0 C	201.93 ± 0.5 C
2	187.24 ± 0.5 C	185.11 ± 0.1 C
3.4	186.35 ± 0.5 C	182.96 ± 0.5 C
0.75, Cross-linked 0.1% GA	232.93 ± 0.5 C	206.63 ± 2.0 C
2.0, Cross-linked 0.1% GA	231.83 ± 2.0 C	203.26 ± 0.5 C
0.75, Cross-linked 1.0% GA	238.53 ± 2.0 C	213.58 ± 1.5 C
0.75, Cross-linked 1.0% Gp	218.75 ± 1.5 C	211.65 ± 2.0 C

Furthermore, the denaturation temperatures for 0.75% and 2.0% wt dispersions increased to 232.93 ± 0.5 C and 231.83 ± 2.0 C, respectively, when cross-linked with 0.1% glutaraldehyde. For 1.0% glutaraldehyde cross-linker, the denaturation and glass transition temperatures of 0.75% wt collagen increased to 238.53 ± 2.0 C and 213.58 ± 1.5 C, respectively. Also, fibers cross-linked with 1.0% genipin demonstrated an increase in denaturation and glass transition temperatures of non-crosslinked fibers with

values of 218.75 ± 0.5 C and 211.65 ± 2.0 C, respectively. The increase in denaturation temperature validates the effectiveness of cross-linking in this study.

2.3.7 Cell Response on Wet-spun Collagen Fibers

The cytotoxicity of the crosslinked wet-spun collagen fibers produced from 0.75% wt dispersions were evaluated. Dissociated dorsal root ganglia neurons were plated on the ends of cross-linked fibers treated with 1.0% genipin and 1.0% glutaraldehyde. At 10 days *in vitro* (DIV), the cultures were assessed for neuronal adhesion to the fibers by staining with neurofilament to investigate the morphology of neurite outgrowth on the fibers. Also, Calcein AM (green) and propidium iodide (red) were used as LIVE/DEAD staining reagents to assess cell viability. Glutaraldehyde cross-linked fibers resulted in widespread cell death compared to robust neuronal viability on the genipin cross-linked fibers as seen in Figure 2.10 C and D, respectively. These results support genipin as a viable alternative neuro-compatible cross-linker in future neural tissue engineering applications.

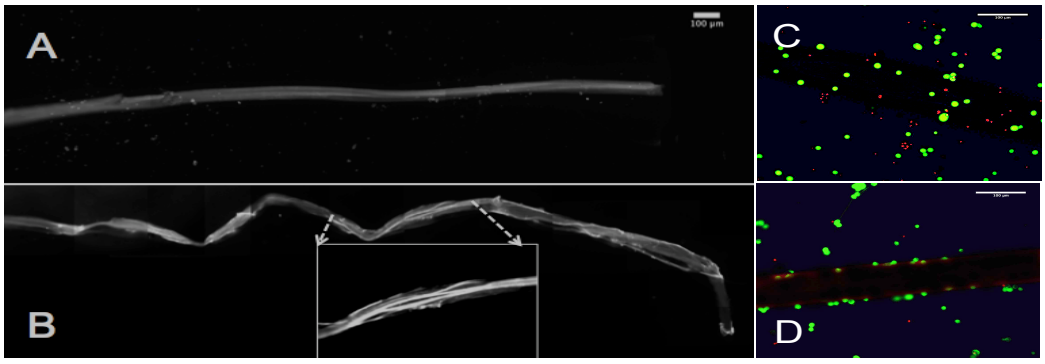

Figure 2.10 Growth response of dissociated embryonic DRGs at day 10 on 0.75% wt wet-spun collagen fibers treated with cross-linking reagents. A) Cell death and cellular debris on 1.0% glutaraldehyde-treated fibers. B) Axon growth seen on 1.0% genipin-treated fibers. Fluorescent staining with Neurofilament-200, Sigma. C) Nuclei of dead cells (red) on 1.0% glutaraldehyde-treated fibers. D) Minimal cell death on 1.0% genipin-treated fibers. Scale bar = 100 μm.

2.4 Discussion

2.4.1 Wet Spinning Device and Technique Development

A wet spinning device was engineered for the controlled fabrication of synthetic collagen fibers. The motivation for creating this device was the ability to produce uniform collagen fibers with consistent diameters and mechanical properties from batch to batch. To determine optimal wet spinning parameters, collagen fibers were characterized by tensile behavior, size, diameter uniformity, and thermal phase transitions. Fibers developed from the device had greatly improved diameter uniformity, consistent elastic moduli and thermal response compared to the commonly used manual extrusion technique.

Wet spun fibers are controlled through the adjustment of four parameters: collagen dispersion concentration, dispersion extrusion rate, spinneret size, and speed of the collection belt. Small spinneret gauge sizes were required to produce small diameter fibers. Spinnerets with gauges above 22 were too narrow and dispersions above 2.0% wt resulted in obstruction due to its high viscosity and insoluble collagen particulates. A needle gauge of 22 was the ideal spinneret size for the fibers produced and tested in this study. It is important to note that higher yields or longer lengths of fibers were obtained when the amount of air bubbles in the dispersions were minimized. The presence of bubbles during extrusion typically obstructs the continuous flow of dispersions into the bath.

It was discovered that uniform fibers were produced when the speed of the collection belt matched the extrusion rate. The speed of the motor (60 RPM) was too fast to collect fibers. Therefore, a 10:1 gear ratio was used to slow down the speed to 6 RPM where 0.75-3.4% wt dispersions consistently formed fibers on the collection belt at an extrusion rate of 12.4 ml/hr. It is also important to note that the spinneret must be in slight contact with the surface of the moving collection belt to reproduce continuous and uniform collagen fibers.

An important advantage of the design is that the device minimizes the quantity of chemical reagents required for each production cycle and its small size enables portability and transport into sterile working environments (i.e. tissue culture hoods). Importantly, the self-contained chamber supports various coagulation baths and can even be used to house cross-linking reagents for future cross-linking treatments. These features make the device ideal for any bench top research setting.

2.4.2 Properties of Wet-spun Collagen Fibers

Uniform fiber properties were mostly affected by the use of a syringe pump for controlling flow rate and a collection belt. Using a collagen dispersion concentration of 0.75% wt flow rates above 12.4 ml/hr resulted in precipitated collagen with irregular, poorly defined fiber morphology. Flow rates below 2.0 ml/hr resulted in thin, flat 2-D films of precipitated collagen. As flow rates were steadily decreased from 12.4 ml/hr to 2.0 ml/hr, fibers were produced with decreasingly smaller diameters ranging from 46.5 ± 10.9 μm to 23.2 ± 10.9 μm, respectively. Accordingly, for applications requiring smaller diameter fibers, the flow rate can be reduced.

In this study the emphasis was on evaluating the effects of collagen concentration on mechanical and physiochemical properties of the fibers, keeping the remaining device parameters constant. At high concentrations (3.5% - 5% wt), collagen dispersions contained large insoluble collagen particulates. These particulates would clog and disrupt the extrusion. 3.4% wt was the maximum concentration that resulted in a dispersion visually clear of particles and would not clog the spinnerets tested. For concentrations above 2% wt, the high viscosity of the dispersions made it difficult to extrude through the syringe, tubing and spinneret. Here, a method of heating was utilized to reduce the viscosity of the dispersions by placing them into a 40^{o}C water bath for 10 min prior to wet spinning. Heating allowed the 2 and 3.4% wt dispersions to be extruded through the tubing and into the coagulation bath. It was observed that the 0.75% wt dispersions consistently formed the most well defined fibers.

DSC was used to assess the thermal stability of non-crosslinked and cross-linked collagen fibers. There was a particular concern with the fibers made from the heated dispersions. The DSC thermographs of the collagen fibers made from 2.0 and 3.4% wt dispersions revealed a reduction in T_g. This suggests that the collagen may have become denatured during the heating process.

With heat, the water content within collagen fibers is heated, the triple helix melts and progressively dissociates into three randomly coiled peptide α-chains characteristic of gelatin. In agreement with other thermal analysis studies in the literature, it was observed that thermal denaturation of collagen depends on water content and the degree of cross-linking [192-195]. Thermal data revealed that interstitial water content should be taken into account at higher concentrated collagen dispersions. Specifically, the presence

of interstitial water increases between fibrils packed within the thick fibers as collagen concentrations are increased. Water can obviously have a negative correlation on the dry mechanics of the fibers at higher collagen concentrations. According to the thermochemical properties among the dispersions, the 0.75% wt fibers exhibited the most thermal stability as evident by the higher helix-coil transition temperature.

The hypothesis was that increasing collagen dispersion concentration would create fibers of larger sizes and higher strengths. Indeed, higher dispersion concentrations resulted in larger diameter fibers, but with less control of diameter uniformity. Similarly, other studies have shown that fiber diameter depends on the collagen concentration [196, 197]. At higher concentrations, viscosity and turbulent flow during extrusion is believed to lead to the formation of large and irregular diameters, refs.

The concentration of the dispersions also influenced the mechanical properties of the fibers. It was observed that the tensile modulus and UTS of the fibers decreased as the collagen concentration in the dispersions increased. For higher collagen concentrations, it is possible that the viscosity of the dispersion inhibits the movement of collagen fibrils to orient against the shear forces exerted during extrusion [198].

If there is a lack of fibril orientation, tensile stress would be unevenly distributed with regions of weak points where failure may occur. In thicker fibers, fibrillar packing is low because there is less orientation of fibrils. Therefore, increasing collagen concentrations and/or collagen fiber diameters exhibit lower tensile modulus due to potential inter-fibrillar slippage. In contrast, low concentration dispersions (0.75-1.0% wt) produced thin, small diameter fibers, which resulted in tighter fibrillar packing and orientation. The tensile strength increases as the cross-sectional area decreases due to

less possibility of defects within thinner segments of fibers [198, 199]. Fibers with higher fibril alignment have small diameter, which results in lower force at break and higher tensile strength as previously reported. As fiber diameter decreases, there is an increase in longitudinal alignment and fibrillar packing density, which leads to stronger interactions within or between individual collagen fibrils [198, 200-203]. Consequently, 0.75% wt dispersions yielded fibers with higher modulus and tensile properties. Since there is minimal inter-fibrillar slippage in smaller diameter fibers, the tensile strength of low concentrated dispersions (i.e., 0.75% wt) is significantly higher.

2.4.3 Fiber Cross-linking

Cross-linking the collagen fibrils within the fibers should increase the tensile properties and limit the swelling or water uptake into the fibers. These properties may be important to long-term performance in tissue engineering applications. In this study, genipin was evaluated as an alternative biocompatible cross-linker using glutaraldehyde as a positive control. Collagen fibers cross-linked with genipin exhibited nearly two-fold increase in tensile modulus compared to dry non-cross-linked fibers. Both cross-linkers were effective in enhancing the tensile properties of the fibers. Since the genipin-treated fibers displayed comparable tensile properties to glutaraldehyde-treated fibers, there is future potential for the use of genipin-treated collagen scaffolds in nerve guidance conduit materials.

The effects of crosslinking were also considered on fiber swelling or water uptake response of collagen fibers. With cross-linkers, water absorption was significantly reduced since there are limited spaces for water to enter due to the degree of cross-links

present within collagen. Within 30 minutes, the effects of the cross-linkers were already noticed due to a reduction in swelling compared to non-crosslinked fibers. By six weeks, the non-crosslinked fibers exhibited diameters that were nearly 3 times the original, dry size. In contrast, glutaraldehyde and genipin reduced swelling to 1.4 and 1.2 times the original diameter, respectively.

During the preparation of crosslinked fibers, it was discovered that the soaking process of cross-linking could itself change the properties of the fiber. As a sham control, non-crosslinked fibers were immersed in water for 24 hours and compared to the cross-linked fiber groups. Interestingly, the sham control of swelling and re-drying the fibers resulted in a reduction in their mechanical properties. These results suggest that cross-linking significantly enhances the physiochemical and mechanical properties of the collagen fibers. Importantly, the efficacy of cross-linking with genipin was validated to be comparable to glutaraldehyde.

2.4.4 Neuronal Biocompatibility of Fibers

Although glutaraldehyde cross-linking greatly improved the mechanical strength of the collagen fibers, the potential toxic effect has been a vital drawback for this commonly used chemical reagent for biological tissues. A few studies have previously demonstrated that genipin has the potential to be used as a substitute cross-linking agent [57, 84-86, 204], however, its cyto-compatibility with neuronal tissue was uncertain. Here, it was observed that DRG neurons on genipin-treated fibers had a viability of > 95% at 10 days *in vitro*. In contrast, the glutaraldehyde-treated fibers displayed < 5% viability during the same time point in culture. These cytotoxicity findings seem to correlate with previously

reported studies in the literature [204-206]. Thus, the enhancements in mechanical stability and controlled rate of swelling in addition to favorable viability of neuronal cultures validates the future use of genipin for neural tissue engineering applications.

In terms of future studies, the focus is now on experimenting with more cross-linking and surface modification methods to immobilize extra-cellular matrix proteins on the surface for enhanced long-term axon outgrowth and Schwann cell migration response to the wet-spun collagen fibers. While these new additions to the study will improve the application of wet-spun collagen fibers in tissue engineering, this miniaturized wet spinning device has expanded upon currently used wet spinning apparatuses in industry by providing compactness, cost-effectiveness in use of reagents and portability into sterile working environments.

CHAPTER 3

ENGINEERING IN VITRO COLLAGEN-BASED NERVE TISSUE CONSTRUCTS

Previous published reports indicate that biomaterial-based grafts in the form of synthetic tubes, channels, three-dimensional (3D) gels, scaffolds, or substrates have shown considerable promise in directing regenerating axons *in vitro* and *in vivo*. However, many of these biomaterial strategies continue to fall short of the autologous nerve grafts, which remain to be the current gold standard in repairing severe nerve lesions (<20mm). In general, neurite extension on 2D surfaces remains to be far better compared to neuronal cultures embedded in 3D substrates. Therefore, producing aligned fiber scaffolds distributed within a 3D space is essential for recreating an ideal regenerating environment for growing axons. In this study, 3D nerve tissue constructs were engineered consisting of a compliant collagen gel matrix and a fiber component for promoting "contact-guided" axon growth. Preferential axon outgrowth was investigated on synthetic and natural polymer fibers by utilizing small diameter (<100 μm) fibers of poly-L-lactic acid (PLLA) and collagen I, respectively. Collagen I extracted from rat tail tendon was processed into fiber strands using the controlled wet spinning device. Gel constructs containing fibers induced greater axon outgrowth distances with significantly more directionality along the aligned fibers. Interestingly, wet-spun collagen I from rat tail tendon displayed a highly aligned outgrowth pattern from embryonic and adult DRG axons suggesting potential use for peripheral nerve repair.

3.1 Introduction

In recent years, tissue engineering has played a key role in redefining strategies in the field of nerve repair. In both *in vitro* and *in vivo* studies of axonal regeneration, gels, sponges, and tubes are types of scaffolds vigorously evaluated in nerve tissue guidance conduits. Gels and sponges are advantageous in reconstruction of both peripheral and spinal cord injuries because they can be used for filling posttraumatic cavities and serving as carriers for cells and therapeutic agents [207-211]. Soft gels have become a promising approach in providing a more realistic 3D environment conducive to axon regeneration for *in vitro* and *in vivo* studies [212-214]. Furthermore, numerous studies have also focused on facilitating neurite outgrowth using hydrogel scaffolds modified using covalent-linked ECM-derived proteins and RGD-peptide sequences [215]. Gels alone, however, do not adequately provide a clear direct path for oriented guidance of regenerating axons through a lesion. To date, no standard material or fabrication technique has been widely established as the optimum for promoting directional outgrowth. Thus, an alternative scaffold design strategy is necessary for facilitating directed axon guidance and growth in 3D.

Mechanical cues presented by 2D rigid substrates induce far greater neurite extension than cells in 3D cultures [216]. Axon growth preference for rigid substrates may have been explained many years ago by Lamoureux, Heidemann, and several others who discovered that growth rates of neurites were strongly correlated to applied tension, in which a pulling phenomenon was observed during elongation of growth cone [217, 218]. Although growing axons favor the 2D substrates, high demand for developing 3D substrates/gels/scaffolds to provide a more ““biomimetic”” environment still remains.

Earlier work conducted by Gomez and Letourneau demonstrated that when presented a choice, growth cones follow the preferred of 2 substrates, exhibiting a contact guidance response [219]. Previous work in the area of developing 3D constructs has led to a strong belief that ideal constructs may involve incorporating "2D-like" substrates/surfaces in 3D space.

Here, methodology was established to promote survival, adhesion, and preferential neurite outgrowth of primary dorsal root ganglion (DRG) neurons on 3D fiber-gel constructs. Unlike some other strategies where axons are constrained to grow within tubes or channels, growth cones were given a choice to extend within soft, confluent collagen gels or to grow along a single fiber presented in close proximity to the axons in 3D space. In this study, the fiber components evaluated were biodegradable synthetic poly-L-lactic acid (PLLA) and natural collagen fibers with micron-size diameters (<100μm). Collagen fibers from collagen I of rat tail tendon were fabricated using a wet spinning technique as previously described. Rat tail tendon was the preferred source of collagen I based on previous studies in the lab, which suggested that neurite outgrowth is less restricted on two-dimensional substrates coated with rat tail collagen compared to collagen I from bovine tendon. Mean outgrowth of axons on rat tail collagen was significantly different from extensions on bovine tendon collagen molecular layers on 2-D petri dishes. Furthermore, collagen I from rat tail tendon was isolated with more ease and reconstituted more homogenously compared to bovine tendon. Hence, collagen fibers were synthesized from rat tail tendon isolates for all subsequent experiments. The role of surface modified extra-cellular matrix proteins on PLLA and

collagen fibers were evaluated for their effects on neurite outgrowth response in embryonic and adult DRG neurons.

3.2 Materials and Methods

In this particular study, the focus was on developing collagen-based fiber-gel constructs for mediating axon growth by contact guidance. Here, the growing axons were presented a choice between two components of this construct: (1) fiber component in the form of PLLA or wet-spun collagen fiber and (2) gel component consisting of collagen gel matrix or hydrogel. The hypothesis is that axons will elicit preferential contact guidance towards the fiber instead of the gel due to stiffer mechanical properties for extension and elongation of growth cones. The efficacy of these material components will ultimately determine if they are suitable for engineering nerve guidance conduits.

3.2.1 Preparation of Fiber Components for Fiber-Gel Constructs

PLLA fibers (80 μm in diameter) used in this study were obtained from Dr. Zohar Ophir, Medical Device Concept Laboratory, New Jersey Institute of Technology. The surface of the PLLA fibers was also modified by physical adsorption of collagen I at 2.0mg/ml as a comparison with wet-spun collagen fibers. Collagen I used for gel matrices and for wet spinning fibers was obtained via extraction [220] from rat tail tendons obtained from euthanized Sprague-Dawley rats (200-250g).

3.2.2 Wet Spinning

Collagen I in lyophilized form following extraction was reconstituted in glacial acetic acid to obtain a 0.75 wt % collagen dispersion at pH 4, which was loaded into a 10 cc plastic syringe. The syringe was mounted onto a syringe pump (Harvard Apparatus) with Viton tubing connecting the syringe to a blunt-tipped, 22-gauge needle with an inner diameter of 0.4 mm (McMaster-Carr). The tip of the spinneret was immersed into a coagulation bath containing HPLC-grade acetone and ammonium hydroxide at pH 9. The syringe was adjusted to a constant flow rate of 0.21 mL/min. Fibers were deposited on a teflon mesh conveyor belt connected to the shaft of a DC motor operating at a rotational speed of 6 rpm. Once firm, the collagen fiber strands were collected manually and cut into 1 cm long segments for assembly of the fiber-gel constructs.

3.2.3 Hydrogel Preparation

Collagen I gels from rat tail tendon were prepared at approximately 0.8mg/mL concentration using the following mixture: 10 µL of 1N NaOH, 180 µL of tissue culture grade H_2O, 800 µL of collagen I (~4.0 mg/mL) derived from rat tail tendon, and 100 µL of 10X MEM (Sigma), 59.58 g/L HEPES (Sigma), and 22.0 g/L $NaHCO_3$ (Sigma). Approximately, 400 µL of 0.8mg/mL collagen gel was filled into 24-well tissue culture plate and left to incubate up to 1 hr. Single PLLA and collagen filaments were then loaded onto the surface of gel layer prior to cell plating. DRG explants were plated on the end of the fiber and given up to 3 hrs to adhere prior to adding 100 µL of additional collagen gel to complete the assembly of fiber-gel neural constructs as shown in Figure

3.1. After the top layer of collagen gel was incubated up to 1 hr, 500 µL of media was gently added to the top of each fiber-gel construct.

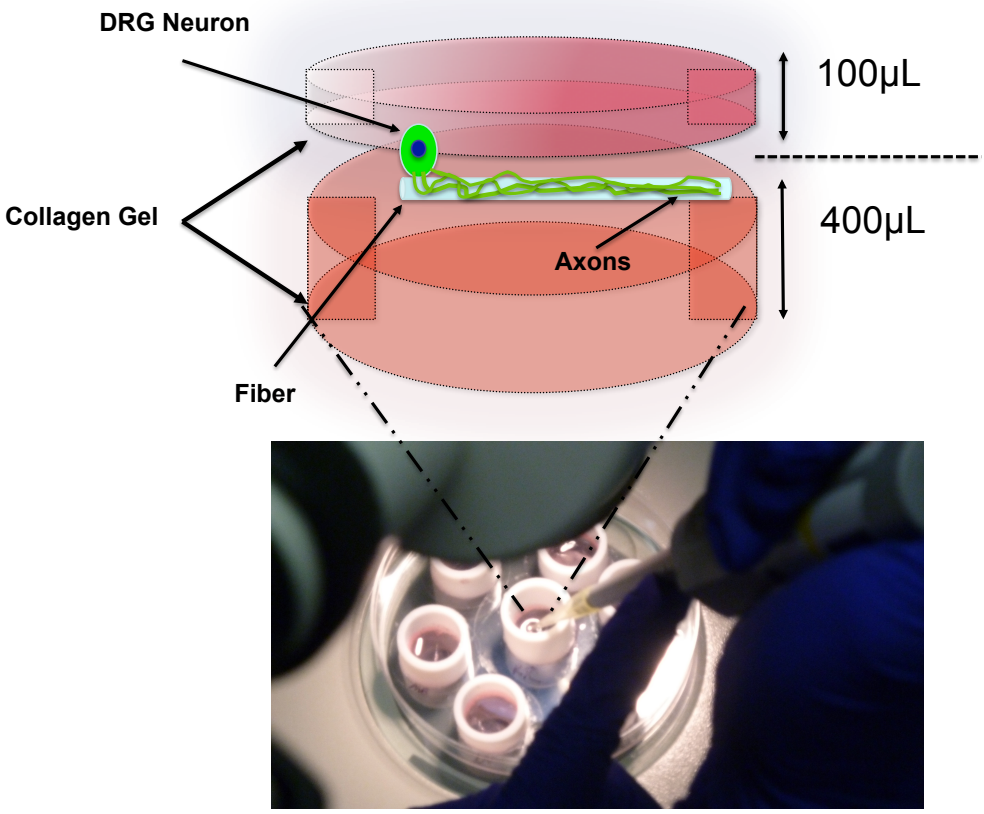

Figure 3.1 Schematic illustration of the assembly of fiber-gel neural constructs.

3.2.4 Surface Modification of Fibers

In this study, the influence of ECM-derived proteins on the surface of fibers was evaluated. The surfaces of PLLA and collagen fibers were modified by laminin (LN), poly-L-lysine (PLL), and matrigel (MG) each at 50µg/mL for 1 hour and rinsed three times with PBS for 5 minutes each. The surface modification was performed by physical adsorption only. Surface-treated fibers were incubated for 2 hours in a 37^{o}C incubator

with 5% CO_2 prior to cell plating. These fiber-treated groups were evaluated with adult DRG neuronal cultures after 10 days in culture.

3.2.5 Cell Culture

E16 rat DRG explants were isolated from fetuses of Sprague Dawley rat strain in accordance with procedures approved by the Institutional Animal Care and Use Committee (IACUC) at Rutgers State University-Newark and New Jersey Institute of Technology. DRG explants harvested from 4 to 5 pups were isolated in L-15 medium (See Appendix A). An average of 20-25 DRG explants are obtained from the spine of one pup as seen in Figure 3.2.

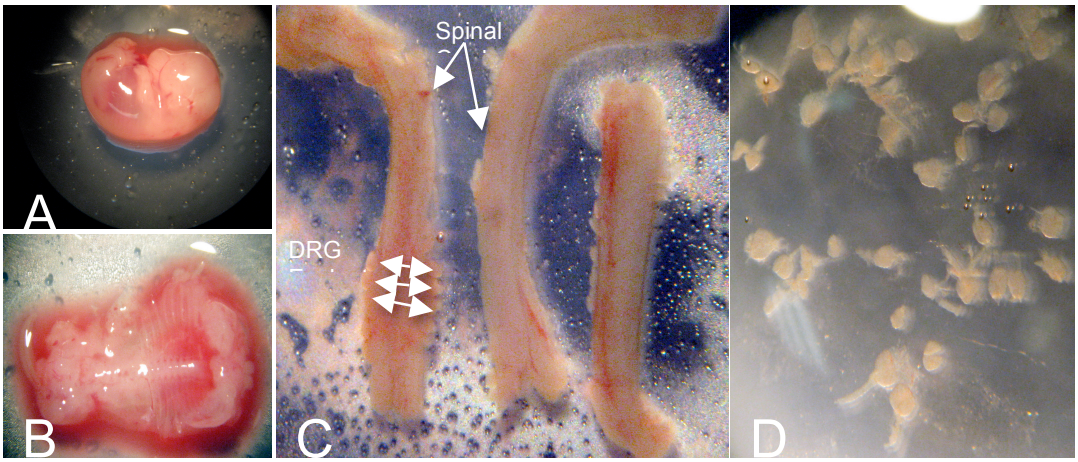

Figure 3.2 Embryonic Dorsal Root Ganglia (DRG) Dissection. (A) E16 rat fetus, (B) View of dissected fetus showing vertebrae, (C) Dissected fetal spinal cords with DRGs, and (D) Closer view of isolated DRG explants prior to plating.

A single explant was immediately plated onto the end of a single fiber supported in 400μL of collagen gel. DRG cultures were maintained in complete growth medium consisting of Neuralbasal medium (Invitrogen, Carlsbad, CA) supplemented with B-27 (Invitrogen), 1% FBS (Hyclone, Logan, UT), 1 mM L-Glutamine (Invitrogen), 2.5 g/L glucose, and 10 ng/mL 2.5S nerve growth factor (Becton Dickinson, Bedford, MA). All were treated with mitotic inhibitors (20μM 5-Fluoro-2-deoxyuridine [Sigma], and 20μM uridine [Sigma]). After 2 days, the medium was exchanged with complete medium plus mitotic inhibitors (20 μM 5-fluoro-2-deoxyuridine [Sigma], and 20μM uridine [Sigma]) for up to 14 days.

Similarly, neuronal cultures were also prepared from dissociated adult DRG explants from previously euthanized female rats. The dissection of adult DRGs is seen in Figure 3.3.

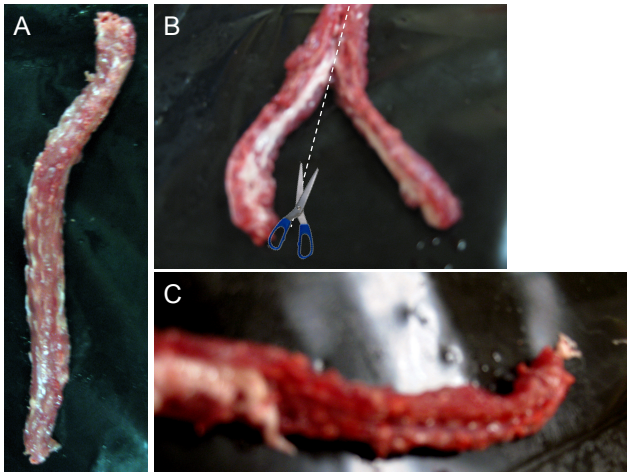

Figure 3.3 Adult Dorsal Root Ganglia (DRG) Dissection. (A) Vertebral Column of Adult Rat, (B) View of symmetrically cut vertebral column, (C) Spinal cord pulled away to expose DRGs.

Adult DRGs were dissociated using 0.25% collagenase (Worthington) for 1 hour followed by 0.25% trypsin for an additional 1 hour at 37°C. Neurobasal medium + 5%

FBS was then added to inactivate the trypsin, and the tissue was triturated followed by centrifugation at 1000 rpm for 5 minutes. Cells were then re-suspended in 1 mL of fresh media and passed through a 2-layer bovine serum albumin (BSA) density gradient (5% and 10%) to separate DRG neurons from Schwann cells and myelin. The gradient was then centrifuged at 1000 rpm for 5 minutes and the resulting pellet was re-suspended in 200 μL fresh media. The cell suspension was then plated at 2.5 x 10^3 cells immediately adjacent to the ends or directly above the fiber groups (PLLA, collagen-PLLA, collagen fibers) by using 5 μL size droplets. The cultures were placed in a humidified tissue culture incubator (37°C and 5% CO_2) for 3 hours at which point 500 μL of additional media was added to each culture. The culture media was changed every 2-3 days *in vitro* (DIV) by replacement with fresh media pre-warmed to 37°C. For specifics on the tissue harvest, please refer to Appendix B.

3.2.6 Quantification of Neurite Outgrowth

Embryonic DRG explants were grown for up to 14 days on the following experimental groups: PLLA fiber/collagen gel, collagen-coated PLLA fiber/collagen gel, and collagen fiber/collagen gel. Neurite lengths were determined using merged images of DRG explants stained with Calcein AM. Photos were merged using Photoshop (Adobe). On 1, 8, 10, and 14 days, neurite lengths from embryonic DRG explants were measured from the outer perimeter edge of the ganglia to the furthest tip using Image J software (NIH). The number of explants measured was 5 for each fiber-gel group at each time point. Furthermore, the length was measured parallel to the fiber axis. In this study, 2-D control groups of DRG explants grown on tissue culture-treated polystyrene coated with 2.0

mg/ml collagen were used for comparison with 3-D cultures. A 3-D control consisting of gel without fiber was also compared to all experimental groups containing fibers.

Adult DRG explants were grown for up to 10 days on the following experimental groups: PLLA fiber/collagen gel, collagen-coated PLLA fiber/collagen gel, and collagen fiber/collagen gel. Similarly, neurite lengths were measured using merged images of dissociated adult DRG neurons using Image J software at 2, 5, and 10 days *in vitro*.

Neurite lengths of adult DRGs grown on LN, PLL and MG-treated fibers were measured at 10 days *in vitro*. Control groups of unmodified PLLA and collagen fibers were also evaluated.

3.2.7 Mechanical Testing of Fiber Components

Stress-strain curves for PLLA and collagen fibers (0.75% wt collagen dispersion) were generated under uniaxial tension using an Instron 3342 Universal testing machine (Instron, UK). Fibers were cut into 3 cm segments using a fine razor blade and stored at room temperature until needed for tensile analysis. Each fiber sample was placed between the clamps of the instrument in order to mount. The Instron operated at an extension rate of 5 mm/min and a gauge length fixed at 2 cm for each sample. The secant modulus was defined by dividing the average stress by the average strain in the linear region within 5% strain of the stress/strain curve for each fiber.

All tensile studies were performed at room temperature using dry fiber samples. Air-dried fibers (n=10) from each of the fiber groups were mounted with tape to grip the ends of the fibers to prevent slippage while ensuring that the fibers were not damaged at the contact points of the clamp. Results obtained from fibers that broke at contact points

or from fibers that slipped from the clamps were rejected. The strain was determined by the change in fiber length divided by the original length.

3.3 Results

3.3.1 Development of Collagen-Based Fiber-Gel Nerve Tissue Constructs

The ability to fabricate continuous synthetic collagen fibers with a miniaturized wet spinning device presented various opportunities in the development of collagen fibrous scaffolds for nerve guidance constructs. Here, the hypothesis was that fibers or monofilaments loaded within a 3-D hydrogel would provide facilitated axon outgrowth of embryonic and adult sensory neurons *in vitro*. Following the assembly of fiber-hydrogel constructs, the growth response of DRG axons was evaluated by immunocytochemistry and other staining methods to determine if contact guidance influences directed growth. In other words, the goal was to evaluate if regenerating axons show preferential growth when presented two substrates: (1) soft hydrogel matrix and (2) stiff fiber component.

Furthermore, this study addressed whether mechanical or biochemical cues presented on the fibers preferentially influence neurite outgrowth. The findings helped identify factors that could be optimized in collagen fiber scaffolds to make them more suitable for neural tissue engineering applications. Thus, the following sections present overall results on the growth response of neuronal cultures on the fiber-hydrogel composite materials while providing an early assessment for use in future designs of nerve guidance conduits.

3.3.2 Growth Response of Embryonic DRGs on Fiber-Gel Constructs

Neurite measurements were performed on composite images of DRG explants stained with Calcein AM (Invitrogen) at 1, 8, 10, and 14 days *in vitro* (DIV). Neurite lengths were measured from the surface of the DRG explant to their farthest tips using the tracer tool in Image J (NIH). The neuronal cultures were allowed to grow up to 14 DIV to assess long-term viability in the fiber/gel constructs. Importantly, a 2-D control group was used for comparison with 3-D growth and consisted of DRG explants grown on tissue culture treated polystyrene dishes containing a 2.0 mg/ml molecular layer of collagen on the surface.

By 14 DIV, the neurite outgrowth distance for 2-D control, 3-D control (gel only), PLLA fiber/collagen gel, col-PLLA fiber/collagen gel and collagen fiber/collagen gel were the following: 3.9 ± 0.7 mm, 2.8 ± 0.4 mm, 4.6 ± 0.3 mm, 6.8 ± 0.9 mm, and 6.4 ± 0.7 mm, respectively. In addition, the growth rates for 2-D control, 3-D control (gel only), PLLA fiber/collagen gel, col-PLLA fiber/collagen gel and collagen fiber/collagen gel were calculated by the slope of neurite outgrowth distance over days to be the following: 273 μm/day, 202 μm/day, 338 μm/day, 486 μm/day and 449 μm/day, respectively. Growth rates and mean outgrowth distances of DRGs growing on PLLA fibers suggest that the presence of fibers in a collagen gel significantly improves neurite growth response in a 3-D gel matrix compared to the control group.

Furthermore, the presence of collagen-coated PLLA and collagen fibers in a gel significantly improved axon growth distance compared to constructs with gel only, Figure 3.4. A statistical comparison at day 14 revealed that there was no significant difference in the mean growth distances between collagen-PLLA and collagen fibers, $p >$

0.05. In contrast, neurite lengths on collagen-PLLA and collagen fibers were significantly different in comparison to the rest of the experimental groups.

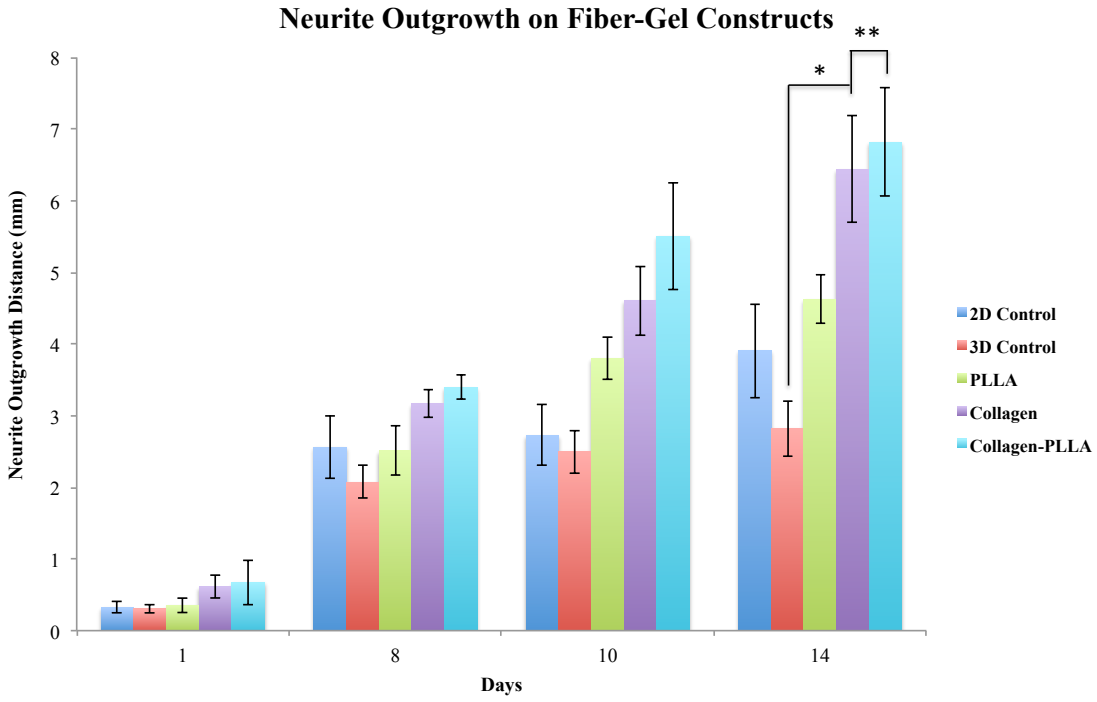

Figure 3.4 Embryonic E-16 DRG Neurite Extension on Fiber-Gel Constructs. ** denotes $p>0.05$ or statistically insignificant, * denotes $p<0.05$ or statistically significant difference.

It is important to note that neurite growth distances on collagen-PLLA and collagen fibers were substantially larger than growth distances seen on 2-D collagen substrates. These findings suggest that the growth rate limitations of axons within 3-D gel systems can be overcome by the use of fiber substrates to facilitate contact guidance for neurite extension within soft hydrogels.

3.3.3 Neurite Outgrowth Morphology on Fiber-Gel Constructs

Images were acquired at 4X magnification and merged to create montages of axon growth using Photoshop (Adobe). In fiber-gel constructs containing unmodified PLLA fibers, neurites displayed contact guidance along the length of the fiber, however, wide branching and random oriented growth within the gel were still observed. Collagen-PLLA fibers, which were PLLA fibers modified with a thin molecular layer of collagen, revealed significant alignment of neurites along the fiber and minimal branching as observed in Figure 3.5. Collagen fibers wet-spun from collagen I (rat tail tendon) exhibited a similar outgrowth pattern of neurites as seen with the collagen-PLLA fiber/gel constructs. A control group consisting of collagen gel without any fiber substrate validated that contact-guided growth was induced by the presence of a fiber in the gel regardless of the fiber type. As expected, the neurite morphology of the control group was a uniform radial outgrowth pattern.

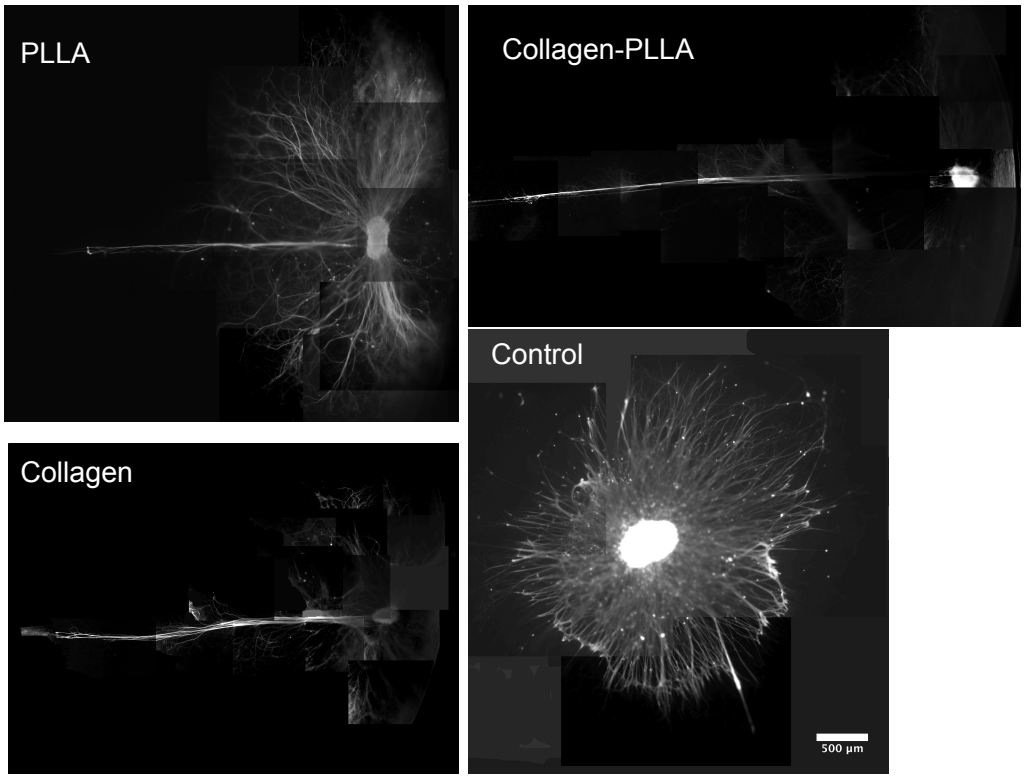

Figure 3.5 Embryonic E-16 DRG neurite outgrowth morphology on fiber-gel constructs at 10 DIV. Control group is construct without fiber component. Neurons stained with Calcein AM. Scale bar = 500 µm.

3.3.4 Growth Response of Adult DRGs on Fiber-Gel Constructs

A neurite outgrowth study was also performed for dissociated adult sensory neurons harvest from DRGs on the fiber-gel constructs as previously described. The same fiber-gel constructs as mentioned in the embryonic growth study were similarly evaluated with the adult DRG neurons. By 10 DIV, the neurite outgrowth distance for 3-D control (gel only), PLLA fiber/collagen gel, col-PLLA fiber/collagen gel and collagen fiber/collagen gel were the following: 0.62 ± 0.1 mm, 1.1 ± 0.1 mm, 1.6 ± 0.2 mm, and 1.5 ± 0.1 mm, respectively. In addition, the adult growth rates for 3-D control (gel only), PLLA fiber/collagen gel, col-PLLA fiber/collagen gel and collagen fiber/collagen gel were the following: 59 µm/day, 111 µm/day, 142 µm/day and 139 µm/day, respectively. As

compared to embryonic growth studies, the presence of collagen-coated PLLA and collagen fibers in a gel also significantly improved adult neurite outgrowth distance compared to constructs with gel only, Figure 3.6 A.

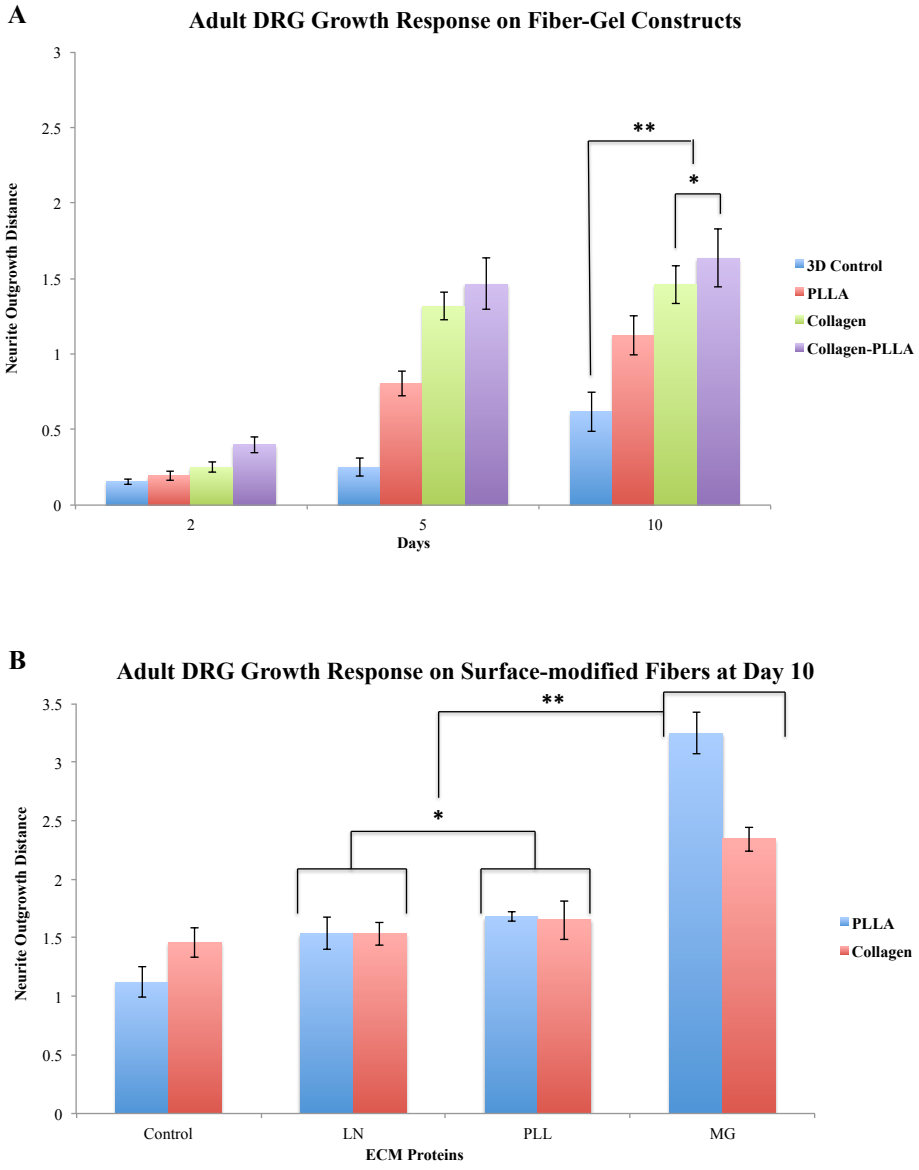

Figure 3.6 Neurite lengths of adult DRGs grown on fiber-gel constructs, where control is a 3D gel without fiber (A). Effect of ECM-modified PLLA and collagen fibers on the neurite outgrowth of adult DRGs, LN=laminin, PLL=poly-L-lysine, MG=matrigel, where control is unmodified fibers (B). * denotes $p>0.05$ or statistically insignificant, ** denotes $p<0.05$ or statistically significant difference.

As expected, the values for neurite lengths and growth rates were much smaller in the adult DRGs due to limited growth potential as seen by all experimental groups. When PLLA and collagen fibers were surface modified via adsorption of ECM proteins, matrigel (MG) significantly improved adult neurite outgrowth distance on both PLLA and collagen fiber-gel constructs at 10 DIV compared to untreated, laminin (LN) and poly-L-lysine (PLL) groups, Figure 3.6 B. In PLLA fiber-gel groups, laminin and poly-L-lysine treatments yield neurite growth distances that were larger from the untreated control group. However, the growth distances between laminin and poly-L-lysine treatments were statistically insignificant, $p>0.05$. In collagen fiber-gel groups, only matrigel treatment exhibited a statistical significant difference and improvement in growth distance compared to untreated, laminin and poly-L-lysine groups. Similarly, the growth distances between laminin and poly-L-lysine treated collagen fiber-gel constructs were statistically insignificant.

The outgrowth morphology of the adult sensory neurons was also assessed for PLLA, col-PLLA, and collagen fiber-gel constructs. In PLLA fiber-gel constructs, neurites grew at random with wide branching and limited axons growing preferentially along the fibers, Figure 3.7 A. However, collagen-PLLA fiber-gel constructs displayed alignment of neurites along the fiber and minimal branching as observed in Figure 3.7 B. Wet-spun collagen fibers showed a similar outgrowth pattern of neurites as seen with the collagen-PLLA fiber/gel constructs, Figure 3.7 C-D. Overall, the adult neuronal outgrowth response was similar to the embryonic DRG neurite interaction on the same experimental groups.

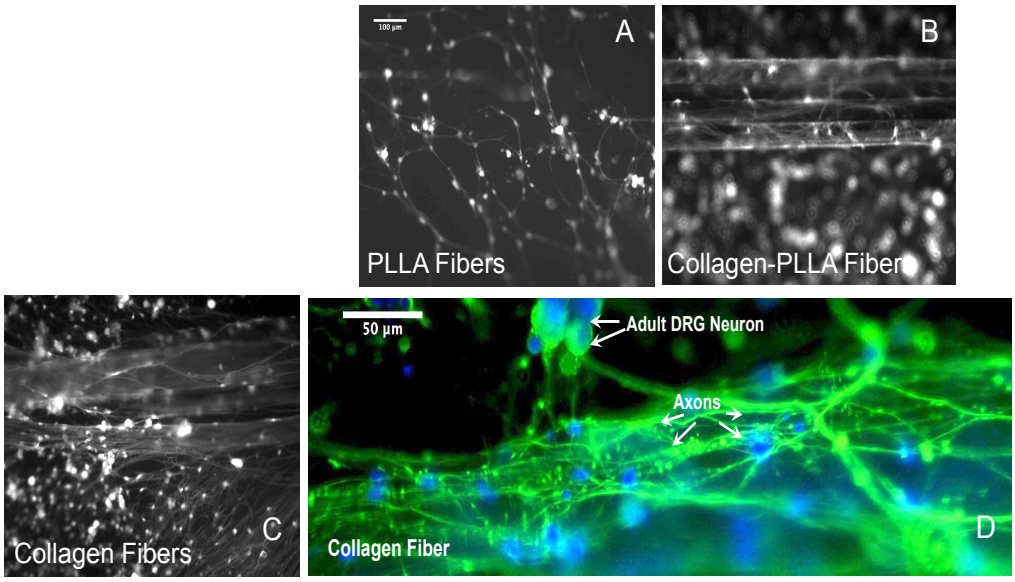

Figure 3.7 Axon outgrowth morphology of adult DRG neurons on PLLA fibers (A), Collagen-PLLA fibers (B), Wet-spun Collagen fibers (C), 10 DIV, 100 µm scale bar. NF 200 (green) and DAPI nuclear stain (blue) of adult DRG axonal processes elongating and orienting along single collagen fiber at 10 DIV (D).

3.3.5 Growth Response of Adult Schwann Cells on Fiber-Gel Constructs

The growth response and behavior of adult Schwann cells towards the fiber-gel constructs were investigated *in vitro*. Adult Schwann cells were cultured on collagen fiber bundles either non-treated or treated with 1.0% genipin cross-linker. Here, the adhesion and viability of the Schwann cells on the fibers were assessed. The treatment of collagen fibers with ECM protein constituents was also evaluated based on Schwann cell migration. A comparison of adult Schwann cell migration on PLLA and wet-spun collagen fibers was assessed using fiber-gel constructs. Both fiber groups were treated with laminin (LN), poly-L-lysine (PLL), and matrigel (MG) at 50 µg/ml concentration. PLLA and collagen fiber-gel constructs demonstrated significant improvement in

Schwann cell migration distance when treated with ECM constituents compared to control groups after 7 days *in vitro* (DIV), Figure 3.8. Interestingly, PLLA fibers with the ECM treatments exhibited a more profound enhancement of migration distance compared to collagen fibers with the same treatment.

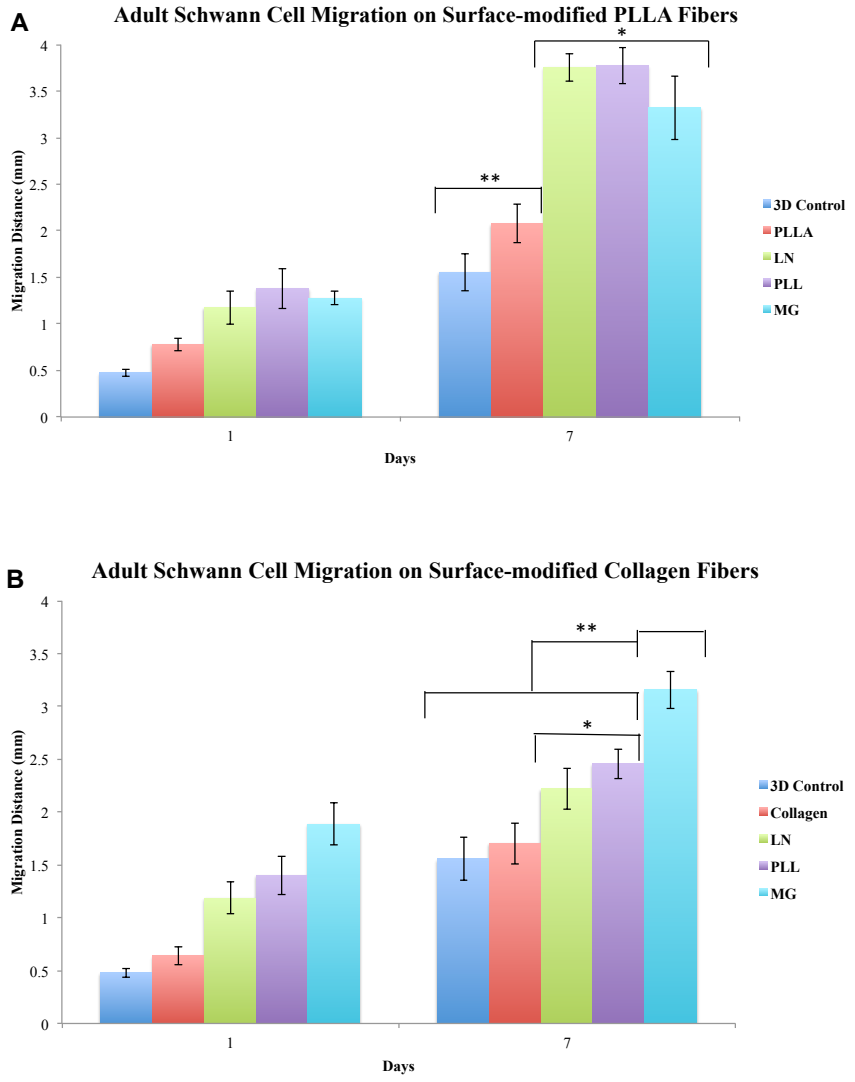

Figure 3.8 Migration distances of adult Schwann cells grown on surface-modified PLLA fiber-hydrogel constructs. (A). Migration distances of adult Schwann cells grown on surface-modified collagen fiber-hydrogel constructs (B). Control group is a gel without fiber. * denotes $p>0.05$ or statistically insignificant, ** denotes $p<0.05$ or statistically significant difference.

Furthermore, the effect of matrigel was more notable on collagen than PLLA fibers. In PLLA fiber-gel constructs, there was no statistical difference among laminin, poly-L-lysine, and matrigel treatments. Overall, the presence of a fiber enhanced migration compared to the control group, which was gel without fiber. On the surface-modified collagen fibers, adult Schwann cells displayed a polarized growth morphology *in vitro* when plated on the fiber-gel constructs as seen in Figure 3.9. In the laminin-treated group, Schwann cells appeared densely packed and organized on the surface of the fiber. Schwann cells on fibronectin and matrigel-treated fibers exhibited long processes compared to other treated groups.

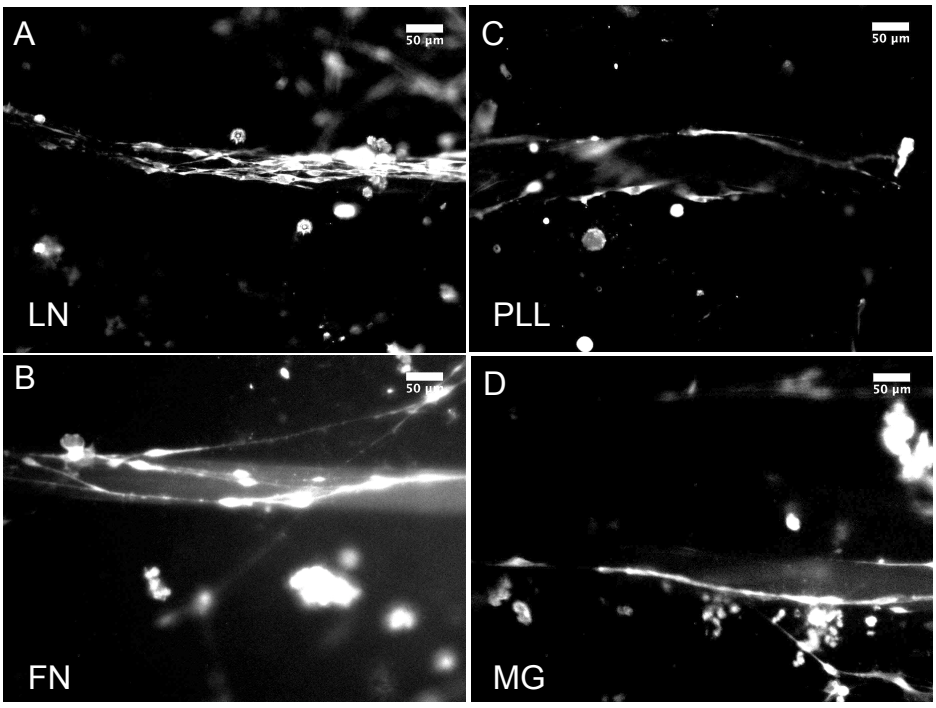

Figure 3.9 Surface morphology of adult Schwann cells grown on surface-modified collagen fiber-hydrogel constructs. (A) LN: Laminin-treated collagen fibers, (B) FN: Fibronectin-treat collagen fibers, (C) PLL: Poly-L-Lysine-treated collagen fibers, and (D) MG: Matrigel-treated collagen fibers. Scale bar = 50 µm.

3.3.6 Tensile Analysis of Fiber Components

The tensile strength and percentage extension of PLLA and collagen fibers were determined from Instron. The tensile modulus and ultimate tensile stress (UTS) at failure were much higher for PLLA fibers compared to the 0.75% wt wet-spun collagen fibers, Table 3.1. PLLA fibers (Elastic modulus =12.4 ± 0.83 GPa, UTS=2.2 ± 0.11 GPa) were mechanically stiffer to non-crosslinked collagen fibers (Elastic modulus =1.95 ± 0.59 GPa, UTS=0.24 ± 0.09 GPa). The rationale for comparing the tensile properties between PLLA and collagen fibers was to evaluate the growth response of embryonic and adult DRG axons in relation to substrate stiffness as a model for contact-guided axon growth.

Table 3.1 Tensile Properties of PLLA and Wet-spun Collagen Fibers

Fiber Group	Tensile Modulus	UTS	% Elongation
PLLA	12.4 ± 0.83 GPa	2.2 ± 0.11 GPa	36.2 ± 4.5
Collagen	1.95 ± 0.59 GPa	0.24 ± 0.09 GPa	15.5 ± 2.9

The higher stiffness in PLLA fibers did not have a significant effect on the outgrowth response since the neurite lengths were shorter compared to growth on col-PLLA fiber/collagen gel and collagen fiber/collagen gel constructs. Hence, the molecular layer of collagen on the PLLA fibers had a more profound effect on growth response than the mechanical cues of unmodified PLLA fibers.

3.4 Discussion

3.4.1 Nerve Tissue Fiber-Gel Constructs

The focus of this study involves a neural tissue engineering application with the long-term objective to develop a nerve guidance conduit for peripheral nerve regeneration. The first step was to engineer a substrate consisting of biodegradable collagen and growth-promoting small diameter fibers in an oriented manner to guide axonal regeneration. The substrate was engineered in the form of a fiber-gel construct, which is a composite of single fibers embedded within a soft hydrogel matrix. The manufacturing of the constructs was accomplished by using wet spinning to produce the collagen fiber components. Furthermore, collagen hydrogel self-assembly played a vital role in making the gel matrix component for both PLLA and collagen fiber-gel constructs. The biological effects of the fiber-gel constructs were studied using primary cultures of embryonic DRG explants and dissociated adult DRG neurons. The data showed that single fibers from both PLLA and collagen could serve as suitable substrates for adhesion and contact guided axonal outgrowth. While both fiber types had a positive influence on neurite outgrowth, these effects were significantly stronger for the wet-spun collagen fibers.

3.4.2 Neurite Extension on Fiber-Gel Constructs

Growth rates and mean outgrowth distances of DRGs growing on PLLA fibers suggest that the presence of fibers in a collagen gel significantly improves neurite growth response in a 3-D gel matrix compared to the control group. Furthermore, the presence

of collagen-coated PLLA and collagen fibers in a gel significantly improved axon growth distance compared to constructs with gel only. A statistical comparison at day 14 revealed that there was no significant difference in the mean growth distances between collagen-PLLA and collagen fibers, $p > 0.05$. In contrast, neurite lengths on collagen-PLLA and collagen fibers were significantly different in comparison to the rest of the experimental groups. It is important to note that neurite growth distances on collagen-PLLA and collagen fibers were substantially larger than growth distances seen on 2-D collagen substrates. These findings suggest that the growth rate limitations of axons within 3-D gel systems can be overcome by the use of fiber substrates to facilitate contact guidance for neurite extension within soft hydrogels.

As expected, the values for neurite lengths and growth rates were much smaller in the adult DRGs due to limited growth potential as seen by all experimental groups. This finding correlates well with other previously reported studies, which suggest that adult DRG neurons are less sensitive to substrate curvature of fiber scaffolds compared to postnatal and embryonic stage DRG neurons [221]. Therefore, the lack of sensitivity of adult DRG neurons to fiber curvature may result in smaller neurite outgrowth distances as seen in this study. Additionally, adult neurons of the CNS have been reported to have differing cAMP levels as compared to earlier stage neuronal cultures *in vitro* and *in vivo* [222]. Hence, the limited growth potential of adult DRG neurons may be attributed to low concentrations of cAMP compared to embryonic DRGs. Despite the slow outgrowth rates from the adult DRGs, the trend in growth response on the constructs for adult DRG neurites was similar to what was observed with embryonic DRG explants. In both embryonic and adult DRG outgrowth studies, neurite lengths on collagen-PLLA fiber-gel

constructs and collagen fiber-gel constructs surpassed the outgrowth distances seen on unmodified PLLA fiber-gel constructs and the control group. This finding suggests that embryonic and adult DRG neurons responded similarly to the presence of collagen on the surface of the fiber-gel constructs. In contrast, unmodified PLLA fibers lacked any ECM constituents and therefore, did not exhibit preferential growth along the fiber in the constructs.

3.4.3 Effects of ECM Constituents on Neurite Outgrowth

An extensive review of the literature suggests the importance of physical and chemical cues for eliciting and guiding axonal outgrowth. In regenerating nerve tracts, physical cues are often presented in the longitudinal arrays of axon fascicles. Meanwhile, chemical cues are presented by adhesive matrix proteins associated with Schwann cells and the basal lamina [35, 223, 224]. In this study, physical cues are present in the fiber component of the constructs. To determine the effects of adhesive ECM constituents as chemical cues, neurite outgrowth on laminin, poly-L-lysine, and matrigel were evaluated using adult sensory neurons. These ECM proteins when combined with a fiber substrate may closely resemble filamentous substrates present during CNS and PNS development in addition to being present in damaged nerve tracts.

Interestingly, matrigel significantly improved adult neurite outgrowth distance on both PLLA and collagen fiber-gel constructs at 10 DIV compared to untreated, laminin (LN) and poly-L-lysine (PLL) groups. This finding implies that adult DRG neurites display a growth preference towards the cocktail of proteoglycans, collagen IV and laminin present in matrigel. In PLLA fiber-gel groups, laminin and poly-L-lysine

significantly improved neurite growth distances that compared to the untreated control group. Laminin is known to promote neurite outgrowth and plays a role in repair of both the CNS and PNS [225-228]. Thus, it is no surprise that coating the PLLA fibers with laminin significantly enhanced neurite outgrowth in adult sensory neurons. However, the growth distances between laminin and poly-L-lysine treatments were statistically insignificant. This observation implies that both laminin and poly-L-lysine enhances neurite outgrowth in relation to unmodified PLLA fibers. In collagen fiber-gel groups, only matrigel treatment displayed a significant improvement in growth distance compared to untreated, laminin and poly-L-lysine groups. Similarly, the growth distances between laminin and poly-L-lysine treated collagen fiber-gel constructs were not significantly different.

CHAPTER 4

DESIGN OF NERVE GUIDANCE CONDUIT: A PROOF-OF-CONCEPT STUDY

Despite the capacity for peripheral nerve repair, functional outcomes after nerve injuries are often unsatisfactory and insufficient in bridging extensive nerve lesions greater than 2 cm [2]. Hence, a nerve guidance conduit that promotes sustained axonal growth of adult dorsal root ganglion (DRG) neurons while facilitating Schwann cell migration would be clinically desirable. Adult DRG neurons were chosen to provide a clinically relevant approach to evaluating the efficacy of engineered collagen-based fiber-hydrogel conduits *in vitro*.

The collagen fibers were fabricated using an automated wet spinning device followed by chemically cross-linking with genipin to form a dense bundle of fibers. Fiber bundle was then manually loaded into a hollow conduit formed by electro-spun polycaprolactone (PCL) mats. Collagen hydrogel was loaded into the lumen of the conduit to fill the empty volume surrounding the fiber bundle while securing the fibers in place and ensuring that the construct remains intact. Surface modification of collagen fibers with extra-cellular (ECM) constituents was also evaluated to enhance Schwann cell migration. Adult rat DRG neurons survived at least 28 days in culture and grew preferentially along the longitudinal axis of collagen fibers. Schwann cell migration and orientation along the collagen fiber bundles were observed growing in tandem with axonal processes from DRGs. The findings in this study signify an early step towards the

development of semisynthetic, tailor-made collagen-based scaffolds for the treatment of neuronal injury.

4.1 Introduction

In spite of considerable regeneration potential of the adult peripheral nervous system (PNS), axon regeneration is limited to growth rates of 1 and 3 mm/day in humans and animals, respectively [229-232]. These growths rates become a major limitation and challenge for regenerating nerves following a traumatic injury where lesions are longer than 1-3 mm. To date, numerous therapeutic strategies for functional restoration of damaged nerves are widely studied. Autologous transplantations remain to be the most common, clinically established treatment for repair of lesions up to 7 cm. For lesions greater than 2 cm, however, autograft material may be of insufficient length to consummate the repair [5, 233]. The severe disadvantages with nerve autografting include morbidity and painful neuromas in the donor site in addition to potential infections [5, 17, 234, 235]. A secondary injury is necessary to repair the primary one, which may create further complications.

Bioengineered synthetic nerve guides were introduced as a promising alternative to overcome the limitations of autologous transplants. An immediate benefit of artificial conduits is the elimination of a secondary injury. Furthermore, bioengineered synthetic conduits have the ability to support neurotropic and neurotrophic communication between proximal and distal ends of the nerve, block inhibitory factors, and provide physical guidance for axonal regrowth [236]. Unlike autografts, bioengineered nerve guides do not induce donor site morbidity and loss of sensation at donor site. Guidance

conduits can be engineered to assist in directing axons from the proximal to the distal stump without any interference of meandering due to imperfectly aligned degenerating fascicles of the closely apposed distal stump [237]. Thus, the goals of this present study were to engineer collagen-based materials into a conduit, assess the collagen-based material components' effect on neurite outgrowth enhancement and Schwann cell migration *in vitro*, and demonstrate the feasibility of surgical manipulation.

To date, relatively few studies have been done to evaluate the growth response of adult neurons on biomaterials *in vitro* [238-240]. Due to slow and limited growth potential of adult neurons, numerous *in vitro* models of the peripheral nervous system have extensively used immature neurons from embryonic and neonatal mammals and birds. As a result, the growth mechanisms of adult sensory and motor neurons have been overlooked. In this study, sensory neurons from adult rat dorsal root ganglia (DRG) were cultured on collagen-based components of a nerve guidance conduit to provide a more realistic model for understanding underlying growth mechanisms of adult neural tissue.

4.2 Materials and Methods

Here, the experimental methods include the following: systematic development of the conduit, adult DRG and Schwann cell growth response on internal conduit components, and surgical manipulation of conduit. In particular, the assessment of long-term growth response and viability of adult DRGs and Schwann cells on the fiber-hydrogel components were important. The validation of structural integrity of the conduit for handling and surgical implantation was another critical aspect of this study.

4.2.1 Materials and Equipment

Purified suspensions of adult rat sensory neurons were isolated from 2 to 3 month old Sprague Dawley rat dorsal root ganglia as described in Appendix B. Collagen I was extracted and purified from rat tail tendons as detailed in Appendix C. Collagen fibers and hydrogel components of the inner conduit were both manufactured from collagen I. Fetal bovine serum (FBS), 7S nerve growth factor (NGF), penicillin-streptomycin, and L-glutamine were purchased from Invitrogen Corporation (Carlsbad, CA) for neuronal growth media.

Collagen fibers, which served as the fiber component of the conduit interior, were fabricated as continuous monofilaments using a custom-built wet spinning device. The device and wet spinning process were previously introduced in Chapter 2.

4.2.2 Fabrication of Nerve Guidance Conduits

Nerve conduits were fabricated by electro-spinning 15% wt polycaprolactone (PCL) in methylene chloride ($MeCl_2$) at a flow rate of 2 ml/hr and voltage of 12.5 kV. Fabrication process is shown in Figure 4.1. For this study, electro-spun PCL mats were obtained from Dr. George Collins. PCL was previously reported to be used in the fabrication of multi-channel nerve guidance conduits and has shown favorable compatibility with neural tissue [241, 242]. It is important to note that electro-spinning can also be used to fabricate outer sheaths from other FDA approved materials such as poly-L-lactic acid (PLLA), polyglycolic acid (PGA) and poly(lactic-co-glycolic) acid (PLGA) [5]. In this study, electro-spun PCL mats were selected simply because they were already available and served as a proof-of-concept.

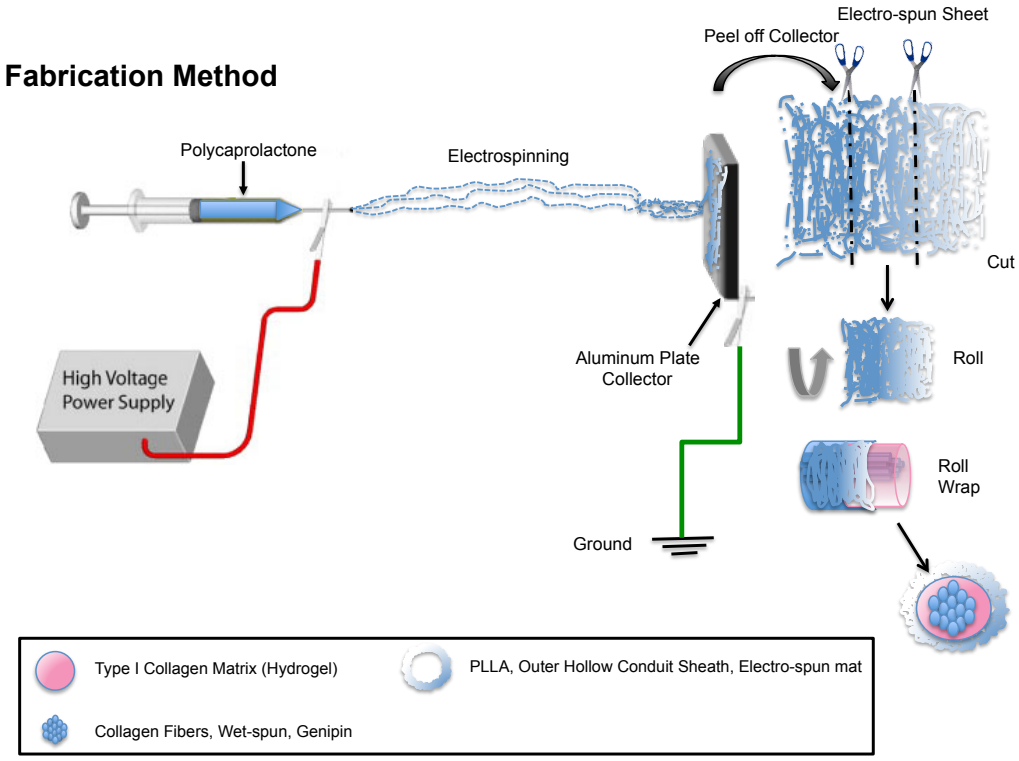

Figure 4.1 Electro-spinning of outer sheath and conduit assembly

The electro-spun PCL random-oriented mats were collected and cut into 1.5 cm x 1.0 cm sheets to form the conduits. The PCL sheets were wrapped around a 12 mm segment of Tygon tubing (1.15 mm outer diameter) to form a hollow tube for the design of the conduit as shown in Figure 4.2. The resulting final dimensions of the NCs were 1.5 cm in length, 1.75 mm inner diameter (lumen) and 2.25 mm outer diameter.

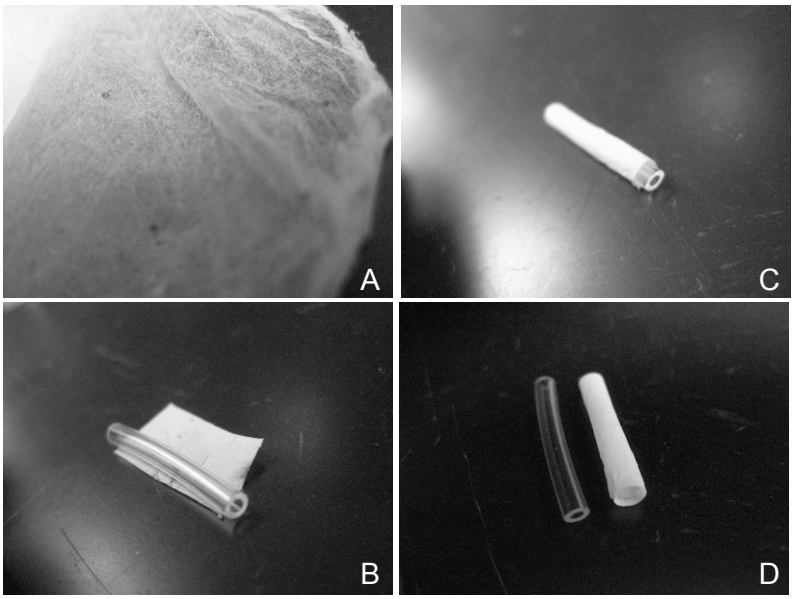

Figure 4.2 Manufacturing of outer sheath for conduit. (A) Electro-spun PCL mat. (B) 1.5 cm x 1 cm section of mat and 1.2 cm length of Tygon tubing. (C) Electro-spun mat wrapped around tubing. (D) Hollow outer sheath created by slipping off mat from tube with fine forceps.

The inside lumen of the NCs was filled with collagen-based hydrogel and a collagen multi-filament bundle. Hydrogels from collagen I (rat tail tendon) at a 0.8 mg/ml final concentration were fabricated by mixing the following constituents on ice: 57% dH2O, 32% of (2.5 mg/ml collagen stock), 10% 10X Minimum Essential Medium (10X MEM, Lonza, Walkersville, MD) and 0.8% 1.0M NaCl. Collagen fibers of 40-50 micron diameter were fabricated by wet spinning and their ends were taped side by side to manually align multiple fibers in a dish. Multi-filaments were then cross-linked by 1.0% genipin for 24 hr to create a bundle of fibers as shown in Figure 4.3. Each bundle of fibers was then cut to 1cm length segments.

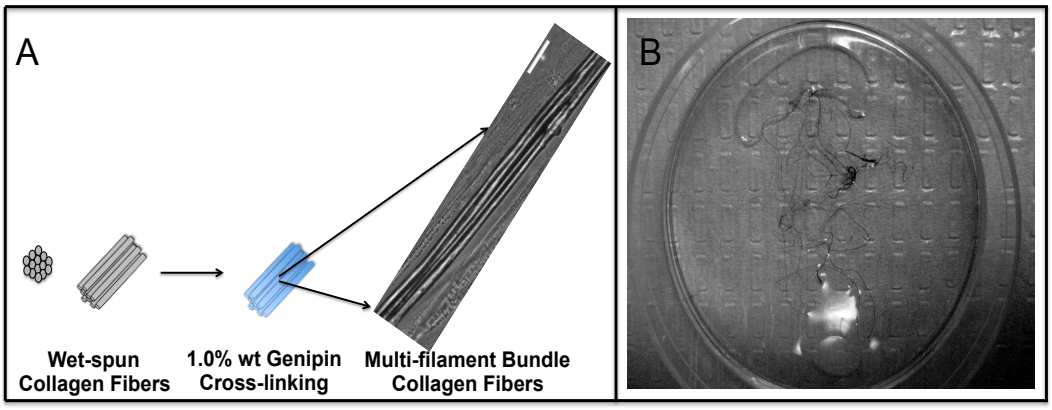

Figure 4.3 (A) Post-treatment genipin crosslinking of wet-spun collagen fibers and the stabilization into a multi-filament bundle for the fiber component of the nerve conduit and (B) Image depicting dark blue pigment coloration of fibers after genipin cross-linking. Scale bar=100μm.

4.3 Results

4.3.1 Fabrication of Collagen-Based Nerve Guidance Conduits: Proof-of-Concept

The success in demonstrating contact-guided axon outgrowth on fiber-gel constructs established the groundwork for developing a practical conduit design. In this study, protocols and methods were developed to generate fiber bundles containing multiple collagen filaments. The hypothesis was that collagen fiber bundles loaded within a 3-D hydrogel would support axon outgrowth of adult sensory neurons and sustain the viability and migration of Schwann cells *in vitro*. Here, the feasibility of assembling collagen-based fiber-hydrogel conduits was validated and the ease of surgical manipulation of assembled conduits were assessed. The goal in this study was to ensure that the novel collagen fiber-hydrogel conduits were mechanically stable for transplantation in a rat sciatic nerve injury model.

4.3.2 Fabrication of Outer Conduit Sheath

Nerve guidance conduits were fabricated by the assembly of multiple components: (1) a dense outer sheath, (2) collagen hydrogel matrix filler, and (3) a bundle of collagen multi-filaments. The outer sheath of the conduits was successfully electro-spun using 15% wt polycaprolactone (PCL) in methylene chloride ($MeCl_2$). The fiber density of the electro-spun mat was controlled by the duration of electro-spinning. The electro-spun mats were easy to manipulate with a pair of fine forceps and appeared to have an electrostatic attraction to itself. Mats were cut into small cross-sections, wrapped around the Tygon tubing, and slipped off to obtain a hollow sheath. In terms of structural integrity, the electro-spun PCL mats were sufficient in strength to support 9-0 nylon sutures. It is important to note that the hollow outer conduit sheath is prone to collapse without the presence of a filler material within the lumen. Hence, a collagen hydrogel was incorporated as a filler matrix to provide a 3-D space for growing axons and to make the conduit more stable.

4.3.3 Loading of Multi-filament Collagen Fiber Bundle

Collagen fiber bundles were constructed by 1.0% genipin cross-linking for 24 hr as seen in Figure 4.4. The duration of cross-linking was determined based on the enhanced mechanical results for collagen fibers undergoing genipin cross-linking as previously mentioned. The fiber bundle was then manipulated with a pair of fine forceps and carefully inserted into the lumen of the conduits.

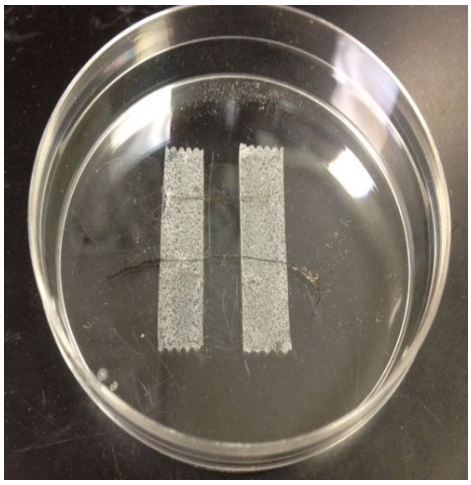

Figure 4.4 Assembly of multi-filament collagen fiber bundles via genipin cross-linking. 10-20 collagen filaments are laid down parallel in a bundle and held in place by two bands of scotch tape. Multi-filament bundles are immersed in 1.0% genipin for 24 hr.

4.3.4 Assessment of Collagen Hydrogel Matrix

As mentioned earlier, a collagen hydrogel component was used as the filler for the assembly of the nerve guidance conduit. In previous studies, we evaluated various collagen hydrogel concentrations in relation to stiffness. Previous data in the lab has revealed that low concentrations of collagen gel are ideal for neurite outgrowth since the inter-fiber spaces are larger for axons to burrow and navigate through during growth cone extension compared to higher concentrated gels. Data collected from previous master's thesis research in the lab indicate that neurite outgrowth of embryonic DRGs was optimal in collagen gels with 0.8 mg/ml concentration. These findings agree with other previously reported studies [12]. Hence, 0.8 mg/ml collagen gels were allowed to self-assemble within the lumen of the conduit outer sheath by incubation at 37^{o}C as seen in Figure 4.5. The collagen mixture was given at least 30 minutes to self-assembly into semi-solid hydrogels with a pink appearance. The constituency of the hydrogels was sufficiently stable within the conduit to manipulate without collapsing.

Collagen hydrogels were successfully loaded into the lumen of conduits containing collagen fiber bundles. The collagen mixture filled the empty voids of the volume surrounding the fiber bundle. A volume of 40 μL was determined to be sufficient for filling the lumen of conduits measuring 1.5 cm in length, 1.75 mm inner diameter and 2.25 mm outer diameter.

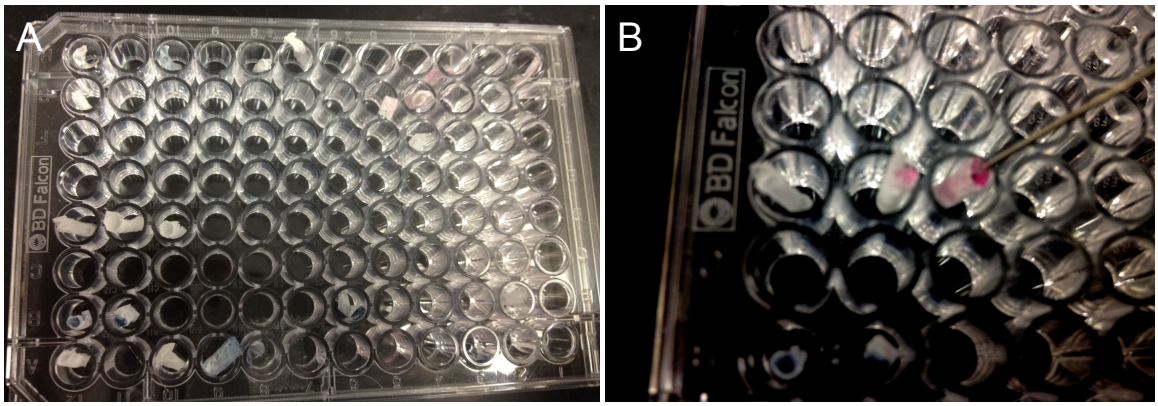

Figure 4.5 Assembly of nerve conduits. 96-well plate used as an assembly platform (A). Loading of collagen hydrogel in pink using a 20-gauge syringe needle (B).

4.3.5 Assessment of Conduit Fabrication

The fabrication of the conduits was evaluated based on the loading of the fiber bundle and the collagen hydrogel into the lumen of the conduit. An important parameter to assess during assembly was to ensure that the fiber bundle spanned the entire length of the conduit. Furthermore, the firmness of the fibers upon contact with the hydrogel was also critical to evaluate. The firmness is related to the degree of swelling or water resorption which can be minimized by cross-linking as described previously. In order to demonstrate that the fiber bundle traversed the entire conduit after fabrication, the outer sheath of the conduit was cut and unraveled to expose the hydrogel and fiber bundle in the interior of the conduit as seen in Figure 4.6.

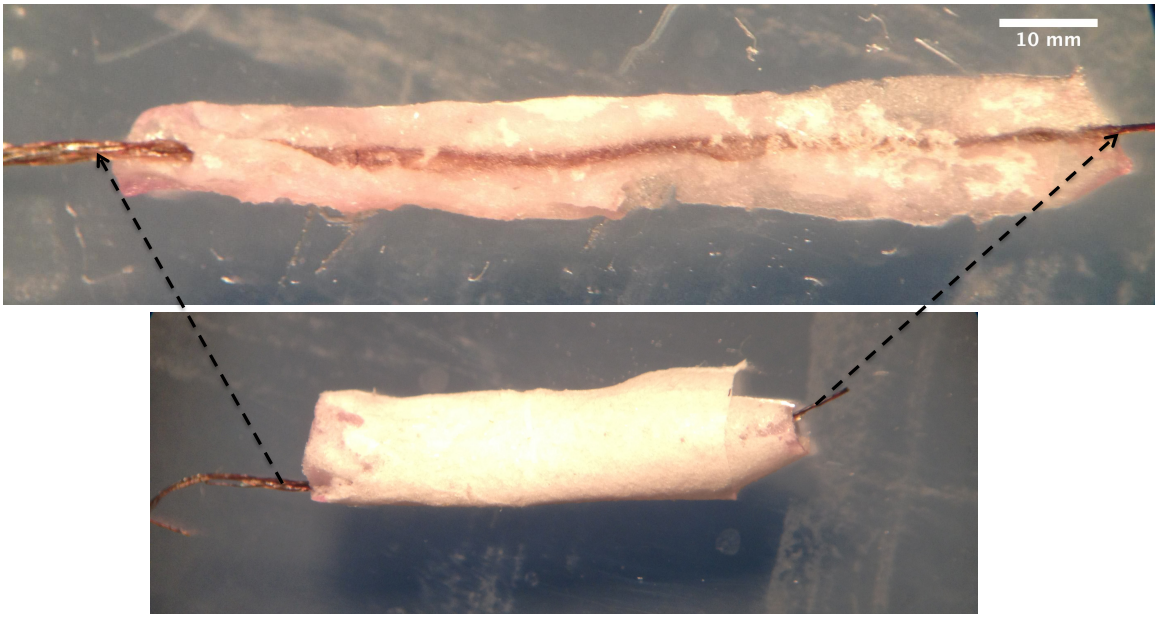

Figure 4.6 An assembled conduit is cut and unraveled to evaluate interior. The collagen fiber bundle traversed the entire length of the conduit as seen in the unraveled, exposed conduit.

4.3.6 Surgical Manipulation of Conduit

In order to assess the ease of surgical manipulation with the conduit, an adult rat cadaver was used to determine the structural integrity of the conduit during implantation into a 1 cm transected rat sciatic nerve. In order to isolate the sciatic nerve, a skin incision originating from the knee was made to the hip for exposure of underlying muscles. The muscles were retracted to reveal the sciatic nerve. The ends of the conduit were secured with 9-0 nylon sutures (ETHILON™). The conduit remained stable during implantation as seen in Figure 4.7. The proximal and distal end segments of the transected sciatic nerve were sutured into the ends of the conduit.

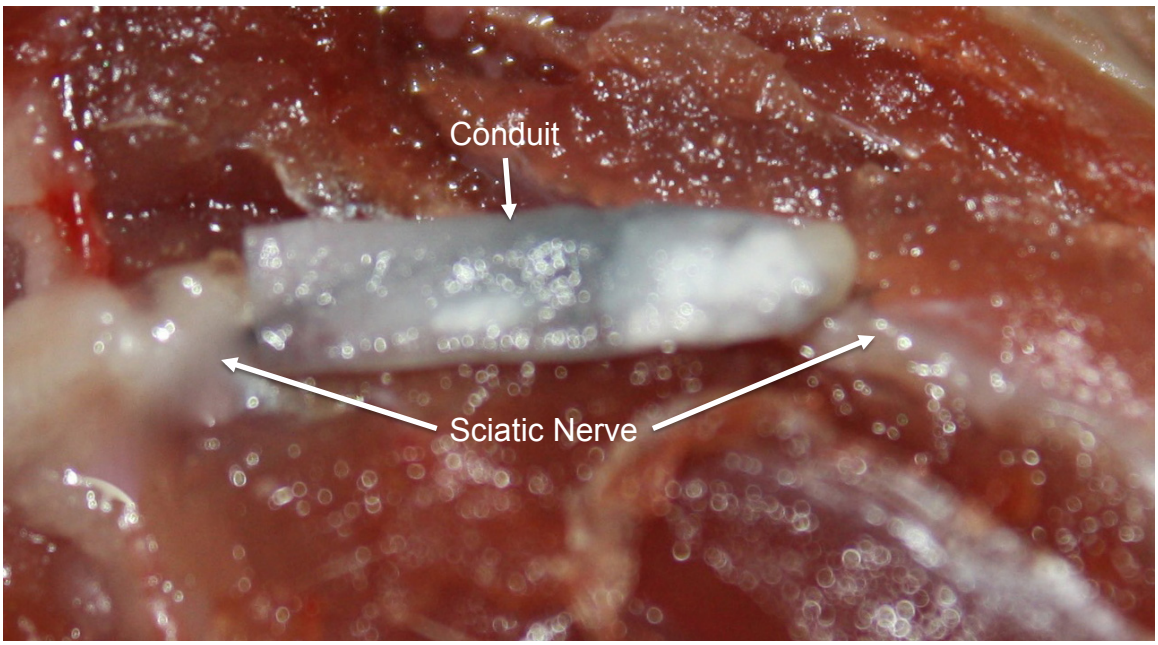

Figure 4.7 Transplanted conduit within a 1 cm transected rat sciatic nerve. The conduit remained structurally stable during surgical manipulation.

4.3.7 Adult DRG Growth Morphology on Conduit Components

The growth response and morphology of adult sensory neurons in the presence of internal conduit collagen-based components were investigated *in vitro*. Adult DRG explants were dissociated into single neurons and cultured on collagen fiber bundles treated with the following ECM constituents: laminin, fibronectin, poly-L-lysine and matrigel. Here, the growth morphology of the adult DRGs on the fibers were assessed in relation to the type of ECM constituent on the surface of the fiber. DRG axons were immuno-labeled with NF-200 in green and the cell body nuclei were stained with DAPI in blue as seen in Figure 4.8. After 14 days *in vitro*, axons grew preferentially along the fibers in all surface-treated groups.

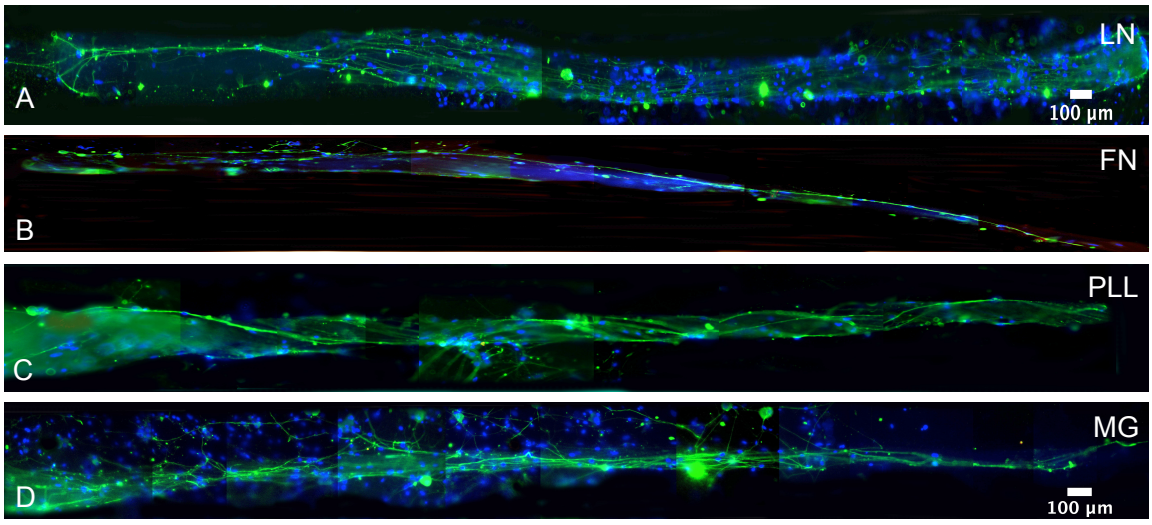

Figure 4.8 Adult DRG axonal outgrowth on collagen fiber-gel constructs treated with ECM constituents. A) LN: Laminin, B) FN: Fibronectin, C) PLL: Poly-L-lysine and D) MG: Matrigel. NF-200 Neuro-filament (Green) and Nuclear DAPI stain (Blue). Day 14 *in vitro*. Scale bar = 100 µm.

4.3.8 Cyto-compatibility on Genipin Cross-linked Collagen Fibers

The neurocompatibility of genipin crosslinked wet-spun collagen fibers produced from 0.75% wt dispersions was evaluated using glia cultures. Adult Schwann cells were plated on the ends of cross-linked fibers treated with 1.0% genipin. At 21 days *in vitro* (DIV), the cultures were assessed for neuronal adhesion to the fibers and stained for nuclear DAPI stain to investigate adhesion on the fibers as shown in Figure 4.9. Genipin cross-linked fibers were treated with laminin, fibronectin and matrigel prior to seeding of adult Schwann cells. The presence of stained nuclei along the fiber length in all treatments suggests that genipin cross-linking is favorable to Schwann cell growth.

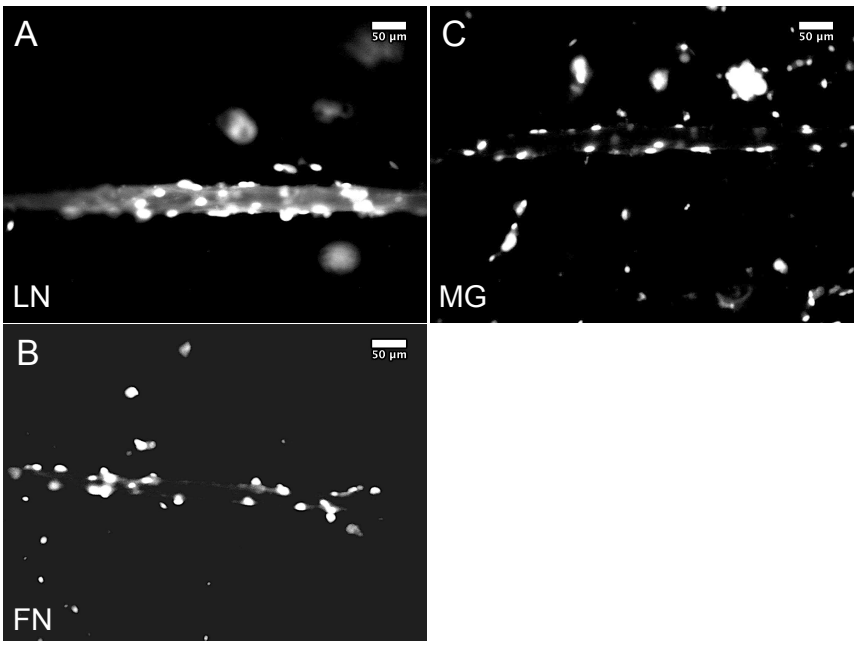

Figure 4.9 Adult Schwann cell adhesion and compatibility on Genipin cross-linked collagen fiber-gel constructs. A) LN: Laminin, B) FN: Fibronectin, C) MG: Matrigel. Nuclear DAPI stain. Day 21 *in vitro*. Scale bar = 50 µm.

4.4 Discussion

4.4.1 Fabrication of Collagen-Based Nerve Guidance Conduits: Proof-of-Concept

The proof-of-concept studies mentioned previously represent the initial evaluation of nerve guidance conduits engineered from collagen-based fiber-hydrogels. The series of aforementioned studies validate the conduit's ability to induce and support neurite outgrowth of adult DRG cultures. Furthermore, this assessment provides meaningful insight on design areas that need to be optimized for successful outcomes following transplantation of conduit into sciatic nerve injured rat models.

4.4.2 Assembly of Collagen-Based Nerve Guidance Conduits

To determine the feasibility of fabricating the collagen-based conduits, the respective individual components needed to be assessed. The components used for assembly of conduits consisted of the following materials: (1) a dense outer sheath made of 15% wt PCL, (2) collagen hydrogel matrix filler, and (3) a bundle of collagen multi-filaments cross-linked with 1.0% genipin. The outer sheath of the conduits was successfully fabricated by electro-spinning. After evaluating various electro-spinning parameters, it was determined that the degree of fiber density of electro-spun mats can be controlled by the duration of electro-spinning. Furthermore, the fibers composing the mats can be tailored-made to have a variety of sub-micron diameter ranges based on the applied voltage, size of the spinneret, and distance between spinneret and collector.

Mats were cut into small cross-sections with ease and were manipulated with a pair of fine forceps. The final formation of the hollow conduit sheath required wrapping the cut sections of mat around Tygon tubing. The electrostatic nature of the PCL mats kept the wrapped mats secured around the segment of Tygon tubing. Once slipped off from the Tygon tubing, the mats retained their shape to yield a stable hollow sheath. Since the sides of the hollow sheath were susceptible to unraveling, the ends of the sheath were secured with sutures. In terms of mechanical stability, the electro-spun PCL mats were sufficient in strength to support 9-0 nylon sutures.

Despite the stability of the hollow conduit, it was prone to collapse without the presence of a filler material within the lumen. Hence, a collagen hydrogel was incorporated as a filler matrix to provide a 3-D space for growing axons and to make the conduit more stable. Previous data collected in the lab indicate that neurite outgrowth of

embryonic DRGs was optimal in collagen gels with 0.8 mg/ml concentration. Similar conclusions were also drawn from studies using collagen and laminin-filled tubes compared to control tubes [12, 226, 243, 244]. For example, one previous study reported that dilute collagen at 1.28 mg/ml and laminin at 4 mg/ml both enhanced nerve regeneration significantly better than their more concentration counterparts [5, 226, 244]. Hence, 0.8 mg/ml collagen gels were allowed to self-assemble within the lumen of the conduit outer sheath by incubation at 37^{o}C. The collagen mixture was given at least 30 minutes to self-assembly into semi-solid hydrogels. The constituency of the hydrogels was sufficiently stable within the conduit to manipulate without collapsing. Collagen hydrogels were successfully loaded into the lumen of conduits containing collagen fiber bundles. The collagen mixture adequately filled the empty voids of the volume surrounding the fiber bundle. A volume of 40 μL was determined to be sufficient for filling the lumen of conduits measuring 1.5 cm in length, 1.75 mm inner diameter and 2.25 mm outer diameter.

The multi-filament structures for the conduit consisted of collagen fiber bundles, which were constructed by 1.0% genipin cross-linking for 24 hr. The duration of cross-linking was determined based on the enhanced mechanical results for collagen fibers undergoing genipin cross-linking as previously mentioned in earlier chapters.

CHAPTER 5

CONCLUSION

Engineering and characterizing a miniaturized wet spinning device has helped us gain a better understanding of the key parameters and/or limitations that must be taken into account to improve the fiber manufacturing process of continuous collagen fibers *in vitro*. In the process, an optimal weight percentage for the collage dispersion was determined to be suitable for future neuronal cell studies on these wet-spun collagen scaffolds. Collagen dispersions of smaller weight percentages between 0.75 and 1.0% wt have proven to show improved fiber uniformity, mechanical stability and thermal behavior. We are currently experimenting with more cross-linking and surface modification methods to immobilize extra-cellular matrix proteins on the surface for enhanced axon outgrowth and Schwann cell migration response to the wet-spun collagen fibers. While these new additions to the study will improve the application of wet-spun collagen fibers in tissue engineering, this miniaturized wet spinning device has expanded upon currently used wet spinning apparatuses in industry by providing compactness, cost-effectiveness in use of reagents and portability into sterile working environments.

The wet spinning technique and device in this study can be used for other tissue engineering applications such as cartilage and bone repair. Furthermore, wet spinning has been previously used to fabricate chitosan and silk fiber scaffolds [178, 245, 246]. Interestingly, wet-spun chitosan and silk may have potential use as suturing materials for wound healing.

This study successfully validates the concept of a fiber-hydrogel nerve tissue construct consisting of either PLLA or wet-spun collagen fibers within a collagen hydrogel. Importantly, the addition of bulk fibers (<100 μm in diameter) within a 3-D hydrogel has shown a significant improvement of axon outgrowth in 3-D space. While PLLA also was shown to be a favorable substrate for growth in 3-D gel matrices, the presence of collagen significantly enhances the neurite outgrowth response as seen in both embryonic and adult DRGs. Furthermore, embryonic and adult DRGs responded favorably to wet-spun collagen fibers. The surface modification of PLLA and collagen fibers with ECM proteins successfully demonstrated the feasibility of using ECM constituents to enhance the axon growth response on scaffold materials. Among the ECM proteins evaluated, only matrigel exhibited a notable improvement in the outgrowth response of adult DRG axons. The ability of wet-spun collagen fibers to support oriented growth and elongation by neurons warrants further investigation into the possibility of using such structures for the basis of three-dimensional guidance scaffolds intended to enhance nerve regeneration and repair.

In developing a proof-of-concept collagen-based fiber-gel guidance conduit, it was observed that adult rat DRG neurons survived at least 21 days in culture and grew preferentially along the longitudinal axis of collagen fibers. Schwann cell migration and orientation along the collagen fiber bundles were observed growing in tandem with axonal processes from DRGs. The findings in this study signify an early step towards the development of semisynthetic, tailor-made collagen-based scaffolds for the treatment of neuronal injury.

CHAPTER 6

FUTURE WORK

The results from adult sensory neuronal and Schwann cell growth *in vitro* have given a solid indication that the collagen fiber-gel constructs in the form of a conduit will provide guidance cues for cell orientation and migration *in vivo*. Mechanical stability assessed from conduit assembly, handling and surgical manipulation in animal cadavers suggest that the proof-of-concept conduit will be a viable material under *in vivo* conditions. Additionally, the control of swelling response of the collagen fiber component revealed that cross-linking agents such as genipin can be further used to fabricate guidance substrates with tailor-made properties for *in vivo* applications.

The primary contributing factor to a successful outcome *in vivo* will be the long-term structural integrity and chronic lifetime of the fiber and gel components involved in the fabrication of the conduit. The advantage of collagen-based biomaterials in nerve conduits is its biodegradability. The remodeling of collagen within the conduit lumen will depend on rate of resorption and degradation *in vivo*. The degradation rate of collagen is influenced by host enzymatic cleavage and the presence of fibroblasts and glia in the surrounding microenvironment of the conduit within the injury site. Since the collagen fiber component of the conduit plays a key role in contact-guided growth and orientation of neurons and Schwann cells, its residence time *in vivo* will need to be assessed. Degradation studies of mass loss from the fiber component at 2, 6, 8, and 12 weeks of implantation will provide valuable information on the lifetime of these guidance substrates within the conduit.

Specifically, this collagen-based fiber-gel conduit will offer a lasting impact in the area of bioengineered conduits if it is able to promote axon outgrowth within lesions surpassing 2 cm. To date, bioengineered nerve conduits consisting of silicone or porous natural/synthetic polymers are able to bridge injured nerve stumps with lesions limited to less than 10-12 mm in rats [247]. Previous studies have demonstrated that silicone tubes filled with laminin, fibronectin, and collagen have improved regeneration over a 10 mm rat sciatic nerve gap compared to empty silicone controls [248]. Oriented mats or filaments with fibronectin have also been used to bridge 10 mm nerve defects in rats with comparable results to the nerve autograft [249].

In order to evaluate regeneration in an animal model, specimens for histological studies would need to be taken from the nerve proximal and distal to the conduit and from the center of the conduit. Specimens of 10 micron thin sections would be collected to evaluate total number of axon fibers and axon density (fibers/mm^2). If the collagen-based fiber-gel conduit is transplanted into an animal model, the hypothesis is that there will be more axon fibers traversing the conduit compared to control groups consisting of conduit filled with collagen hydrogel alone or conduit filled with DMEM medium or saline. The presence of the collagen fiber bundle within the gel matrix will provide physical cues to mediate axon growth cone extension via contact-guided growth as seen with neurite extension on the fiber-gel constructs *in vitro*.

A final conduit would be designed for transplantation into a 2 cm rat sciatic nerve lesion to demonstrate efficacy. The hypothesis is that conduits containing genipin-treated collagen fibers in a gel will facilitate improved axon growth and axon density across the 2 cm nerve gap compared to un-treated collagen fibers in a gel. Based on the increased

stiffness of genipin-treated collagen fibers, axon fibers will likely extend further on the fibers cross-linked with genipin in relation to un-treated fibers and the control group consisting of conduit with gel only. A nerve autograft from the animal will also be evaluated as a positive control group in the study.

Although the collagen fiber-gel conduit is hypothesized to improve nerve regeneration within a 2 cm nerve gap in a rat sciatic nerve model, a combinatorial approach is needed in order to achieve sustained axonal regeneration for nerve lesions longer than 2 cm. Previous studies have reported that the incorporation of nerve segments or minced sensory and motor nerves into a conduit has a beneficial effect on regenerating axons and the length of regeneration [117, 250]. Hence, the collagen fiber-gel conduit with the addition minced motor and sensory nerves onto the collagen fibers would further improve guided growth and long distance regeneration. If the minced nerve segments were applied topically over the collagen fibers, the hypothesis is that they will expedite nerve regeneration by providing a source of trophic factors and nerve architecture. Another approach to consider is incorporating drug delivery within the conduit to release cAMP, which is an intrinsic factor previously known to facilitate axonal regrowth and functional recovery after injury [251, 252].

Overall, this collagen-based nerve guidance conduit has demonstrated initial promising results in promoting viability and directed growth of adult sensory neurons and Schwann cells. With the addition of further *in vivo* studies to test the efficacy of the conduit in a rat model, this conduit may have potential clinical implications in treating peripheral nerve trauma in humans. Specifically, nerve injuries to small diameter sural

nerves in the feet or median nerves from the hand would be a suitable first translational model, in which this conduit may have an immediate impact on functional recovery.

APPENDIX A

EMBRYONIC DORSAL ROOT GANGLIA ISOLATION

The following protocol, adapted from Dr. Bryan Pfister, outlines the procedure for isolation of embryonic DRGs from pregnant rats.

Surgical Tools:

1. Micro-knife
2. Dumont #4 forceps
3. Dumont #5 forceps
4. Dumont #5/45 forceps
5. Dumont #5 Curved forceps

Tissue Isolation:

- Under dissection hood, remove E15-E17 embryos from the uterus and place in Lebovitz L-15 or other non-CO_2 sensitive balanced medium.

- Cut the head off the embryo between the skull and the first vertebra. Using a micro knife, cut on the caudal side of the pronounced bump on the back of the head (between the two pronounced bumps) and under the snout. Leaving some brain stem to handle and pull out the cord.

- With the embryo on its side, remove the anterior portion of the abdomen and limbs with a micro-knife. Place embryo on its back and remove remaining viscera with fine forceps (Dumont #4) until you have a clear view of the vertebral column.

- Beginning at the rostal end, pinch through the vertebral column with fine forceps (Dumont #4).

- Using the #5/45 forceps, grasp the brainstem/ménages and **pull straight up** and place in dish with balanced medium.

- With a fresh pair of #5 Dumont forceps, pluck off the DRGs from the isolated spinal cords and place in a 1.5mL microcentrifuge tube containing L-15 medium and keep on ice or at 4^{o}C up to an hour prior to plating.

Growth Medium Preparation	(For 50mL aliquots)
B-27	1 mL
L-glutamine	100µL
20% glucose	500µL
1% fetal bovine serum (FBS)	500µL
Penicillin/Streptomycin (P/S)	500µL
Mitotic Inhibitors (20µM FdU, 20µM Uridine)	100µL
10 ng/mL NGF	100µL
Neuralbasal medium	47.2mL
Total	**50mL**

APPENDIX B

ADULT DORSAL ROOT GANGLIA ISOLATION

The following protocol, adapted and modified from Dr. Bryan Pfister, outlines the procedure for isolation and dissociation of adult sensory neurons from DRGs.

DRG Dissection:

1. Euthanize rat by exposing to CO_2 for 5 minutes.
2. Place the rat on its abdomen and douse the dorsal surface with 70% alcohol.
3. Using a No. 15 or 10 Blade, make a single dorsal-midline incision along the length of the body.
4. Expose vertebral column by pulling the skin aside.
5. Remove vertebral column by:
    a. Cutting the column at the tail.
    b. Carefully cutting through the tissue and rib bones along each side of the column.
    c. Cut as close to the brainstem as possible to capture the large cervical ganglia.
6. Once removed place in a sterile dish.
7. Using scissors, clean all viscera away from the column so that the centerline can be followed.
8. Starting at thoracic region, cut vertebral column in half, making sure to stay centered.
9. Gently pull spinal cord away from vertebral column to expose the DRGs.
10. Using forceps, peel away the membrane along the inner spinal column.
11. Grab the DRG gently and pull out of the hole.
12. Using small spring scissors, cut the nerves on both sides of the DRG.
13. Place ganglia into eppendorf tube containing L-15 medium.

Cell Dissociation:

1. Treat ganglia with 4mL 0.25% collagenase for 1 hour at 37^0C in a small dish. Gently swirl dish every 15 minutes.
2. Centrifuge cells at 100g (setting 3) for 5 minutes. Remove supernatant.
3. Treat ganglia with 5mL 0.25% trypsin for 1 hour.
4. Pipette up and down about 25 times to break up the DRGs.
5. Inactivate trypsin with 5mL complete media and centrifuge for 5 minutes at 100g (setting 3).
6. Remove supernatant and resuspend with 1 mL media.

Neuron Enrichment:

1. Prepare 2 two-layer BSA gradients (5% and 10%) by adding about 3 mL of a 5% BSA solution in a 15mL centrifuge tube.
2. Using a autoclaved glass pipette, add the second layer underneath the 5% BSA by slowly pipetting a 10% BSA solution with the glass pipette tip at the bottom of the tube. The 5% BSA will float atop the 10% BSA.
3. Carefully place the DRG suspension on top of the BSA gradient by slowly adding it along the side of the tube.
4. Centrifuge the cells at 100g (setting 3) for 4 minutes. Remove all except the pellet. Resuspend with 1 mL media.
5. Pass the cell suspension through the second gradient.
6. Resuspend the pellet in complete media and perform cell count.
7. Plate cells in high density to ensure viability.

(Modified protocol courtesy of Ling Lin)

APPENDIX C

COLLAGEN I EXTRACTION AND PURIFICATION

The following protocol, adapted from previous studies cited earlier, outlines the procedure for isolation and purification of collagen I from rat tail tendons.

1. Obtain rat tails from **3-month to 1 year old male** (or female).
2. Remove rat tails and store on ice.
3. Sterilize by rinsing in antiseptic soap/water solution and 80% alcohol
4. Rinse in sterile distilled water (RO water)
5. Freeze for 24h on filter paper in Petri dish
6. Sterilize in 80% alcohol immersion for 15 min and dry
7. Pick up 1-1.5 cm of tail from small end with a **hemostat**
8. Scrap away outer skin and hair dander using a scalpel 1-2 mm **distal** to point where **hemostat** is applied
9. Use **bone-cutting forceps** to fracture the vertebrate from the tip by rocking back and forth against the hemostat on the proximal end of the tail
10. Slowly pull away the cracked vertebrate fragments to separate from rest of tail.
11. Pull out attached tendons along with the detached vertebrate fragment, hanging free
12. Cut the free hanging tendons with scissors
13. Place tendons in pre-weighed dish of 50 mL **sterile** distilled water
14. Move 1.5 cm toward larger end of tail and repeat procedure from step 8 until last of tail is used
15. Extract tendons by immersing into 0.1% acetic acid **sterile** aqueous solution @ (150ml/1g tendon) for 5-8 days at 4^{o}C with daily agitation (stir bar) for proper mixing
16. Transfer mixture to sterile 50 mL polycarbonate centrifuge tubes and centrifuge at **3500 RPM** for **30 min**, keeping the supernatant (collagen), discarding the rest.
17. Re-centrifuge the supernatant collagen solution at **2500 RPM** for **10-15 min**, then collect the supernatant while discarding the rest
18. Transfer the extracted collagen solution to dialysis tubing bags (**MWCO 12,000-14,000**) with lengths of 8-9 inches
19. Dialyze the collagen extract overnight at 4 ^{o}C in pre-made dialysis buffer (Na_2HPO_4, NaH_2PO_4, pH 7.4)
20. Transfer the semi-solid gel collagen extract from the dialysis tubing into 50 mL centrifuge tubes and spin at **3500 RPM** for **30 min**
21. Discard the supernatant while saving the collagen pellet
22. Store collagen up to 3 months at 4^{o}C or indefinitely be freezing at -70^{o}C

23. Spread out semi-solid gel collagen pellets flat onto pans and lyophilize by steadily increasing temperature range: -20^{o}C to 15 ^{o}C to obtain dry collagen sponge after 48 hours.

APPENDIX D

COLLAGEN I QUANTIFICATION

The following protocol details the assays and methods for quantifying the concentration of collagen extracts and determining the purity of the final lots of collagen product.

BCA Protein Assay

*Note: Protocol is modified from the Pierce BCA Protein Assay

BD© (Becton Dickinson) Rat Tail Collagen Protein Standards:

- Prepare protein standards from BD rat tail collagen (or any other commercial collagen of known concentration) by diluting BD collagen stock (3.41 mg/ml) into following concentrations: 2.0 mg/ml, 1.0 mg/ml and 0.75 mg/ml in 0.02 M acetic acid, 100 µl each.
- BD rat tail collagen standards can be made into aliquots and stored at -20^{o}C for future studies

Rat Tail Collagen Extract Unknowns:

- Prepare a 4.0 mg/ml of rat tail collagen by dissolving dry weight lyophilized rat tail collagen extract into desired volume of 0.02 M acetic acid.
- Dilute the 4.0 mg/ml stock into 2.0 mg/ml and 1.0 mg/ml of collagen samples in 0.02 M acetic acid, 150 µl each.

Sample Loading:

- Load 25 µl of each sample into the wells of a 96-well assay plate (Table 1).
- Cover the assay plate with lid to prevent evaporation
- Prepare BCA reagent by mixing 10 mL of reagent A to 200 µL of reagent B (50 parts reagent A:1 part reagent B)
- Add 200 µL of SDS to the BCA reagent and gently vortex
- Load 200 µL of prepared BCA reagent/SDS solution into each well containing samples (standards and unknowns)
- Cover the assay plate again with lid to prevent evaporation
- Place the assay plate onto an orbital shaker set to the lowest setting for 270 min

- Load the assay plate into the plate reader
- Open the software program on the desktop computer and label the layout of wells
- Click on "Read" to collect absorption values at a wavelength of 570 nm.
- Export collected data as text files to be pasted later into Excel
- Use Excel to make a scatter plot for values of know concentration on the x-axis and corresponding calculated average absorption values on the y-axis for BD collagen standards, D.1.
- Perform a linear regression of the data points on the graph to obtain equation (y= ax + b) of the best-fit line
- Use the equation to calculate experimental values of concentration for BD collagen standards and concentrations for your unknown rat tail collagen samples

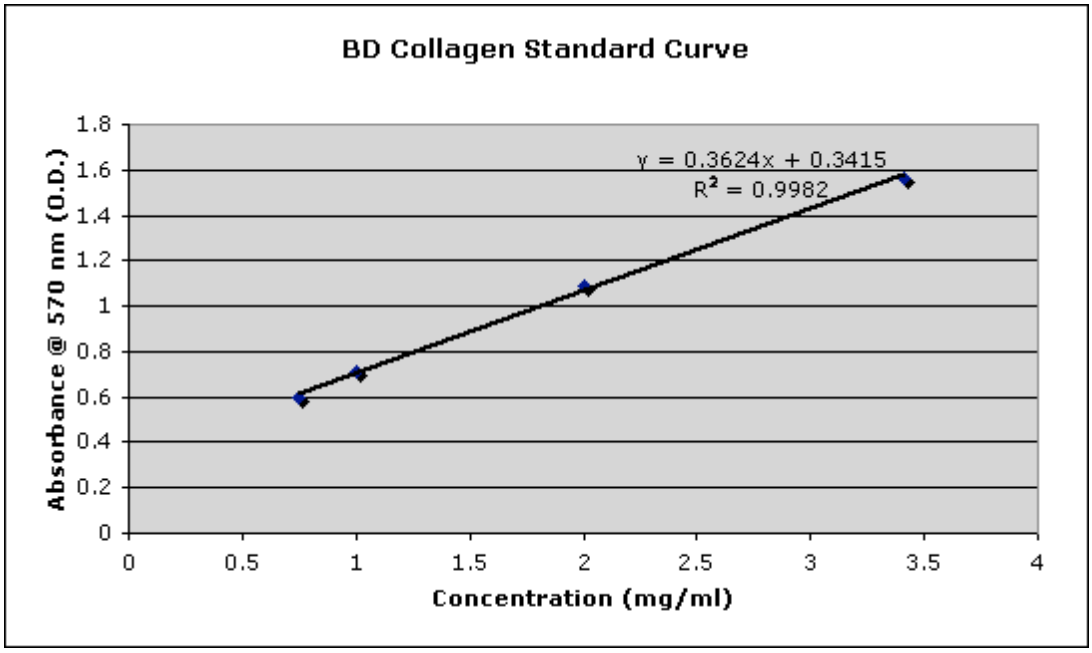

D.1 Example of a typical standard curve of BD collagen standards

Previous experiments conducted in the lab have shown that heating/shaking (orbital shaker) your 96-well plate for discrete time points (30, 60, or 90 min) may improve the unfolding of protein and provide more efficient BCA binding, which could result in more accurate absorbance values. However, this step is optional.

Purity Analysis of Collagen: SDS PAGE

Purpose:

SDS PAGE was run as an attempt to quantify rat tail collagen samples with respect to BD collagen and a known protein standard.

Principle:

SDS PAGE stands for sodium dodecyl sulfate polyacrylamide gel electrophoresis. This technique separates proteins based on their size. The first step in the separation process is the denaturing of proteins so that all the proteins only retain their primary amino acid structures. This is accomplished by SDS in this process. Since SDS is a detergent with the presence of a negative charge due to sulphate, proteins are soluablized by it along with an addition of negative charges. This aids in the movement of these protein primary structures towards the positive pole when placed in an electric field. In order to achieve an environment where different sized proteins move at a different rate in an electric field, polyacrylamide gel is employed which allows the proteins to move through tunnel like structures in a mesh of fibers.

Materials and Methods:

To run SDS PAGE, two types of gels need to be prepared- Resolving gel to be placed on the bottom covering most of the volume of the electrophoresis cassette and stacking gel to be fill the top part of the cassette. However, before preparing the gels, all the samples were prepared. The protein standard used in the process was Novex Sharp Standard and collagen samples were prepared as 2.5 ug and 5ug each of BD collagen (3.41 mg/ml) and rat tail collagen (2mg/ml and 4 mg/ml).

To prepare 10 ml of 7% acrylamide resolving gel, a solution was prepared by mixing 5.1 ml deionized water, 2.3 ml of 30% Acrylamide/Bis, 2.5 ml gel buffer (1.5 M tris HCl with pH 8.8) and 0.1 ml 10% SDS. Polymerizing agent added to this solution was prepared by adding 5ul TEMED to 50 ul 10% APS solution. This gel solution was carefully added to the bottom of the cassette filling most of its volume leaving only about one fifth of the top to be filled by the stacking gel.

For this experiment, 5 ml of 7% acrylamide stacking gel was prepared by mixing 2.55 ml deionized water, 1.15 ml of 30% Acrylamide/Bis, 1.25 ml gel buffer (0.5 M tris HCl with pH 6.8) and 0.05 ml of 10% SDS. In this case, polymerizing agent was prepared by adding 5 ul of TEMED to 25 ul of 10% APS solution. After loading the stacking gel solution on the top of resolving gel, it was allowed to gel and then wells were created to add sampled using a comb. The samples were added based on the predetermined sequence shown below:

Table D.1 Sequence of the samples in PAGE

Standard 10 ul	2.5 ug BD 3.41 mg/ml 25 ul	5 ug BD 3.41mg/ml 25 ul	2.5 ug RT 2 mg/ml 25 ul	5 ug RT 2 mg/ml 25 ul	2.5 ug RT 4 mg/ml 25 ul	5 ug RT 4 mg/ml 25 ul

Electrophoresis was run at 120 volts for 90 minutes until the last band of the standard protein ladder (3.5 KDa) was visible at the bottom end of the gel.

Table D.2 Order of protein bands for the standard protein ladder

260 KDa
160 KDa
110 KDa
80 KDa
60 KDa
50 KDa
40 KDa
30 KDa
20 KDa
15 KDa
10 KDa
3.5 KDa

The gel was then stained with Coomassie blue to obtain a better vision of the protein bands and was then destained after an hour to make all the bands visible.

The following figure shows the protein bands obtained after the completion of electrophoresis and staining process.

Standard 10 ul	2.5 ug BD 3.41 mg/ml 25 ul	5 ug BD 3.41mg/ml 25 ul	2.5 ug RT 2 mg/ml 25 ul	5 ug RT 2 mg/ml 25 ul	2.5 ug RT 4 mg/ml 25 ul	5 ug RT 4 mg/ml 25 ul

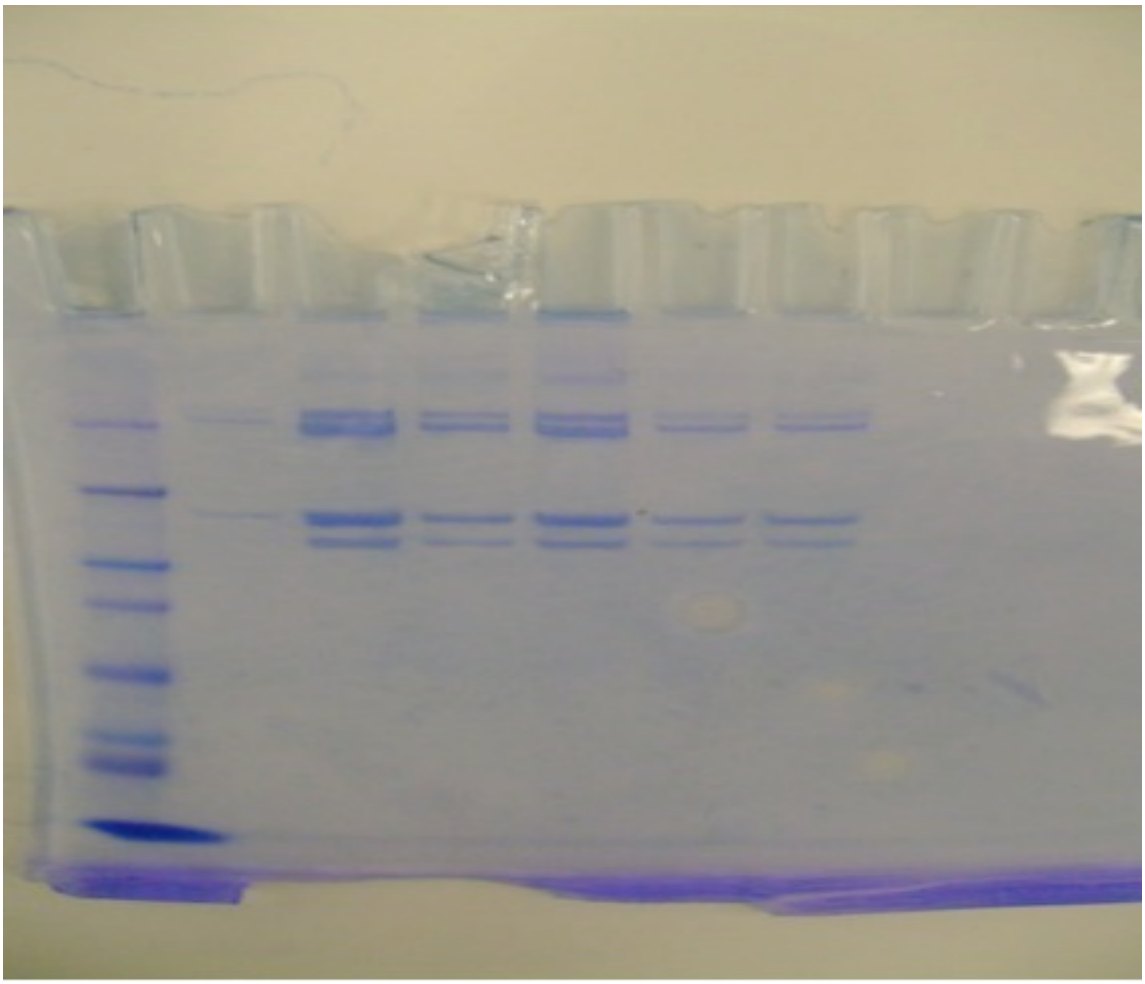

D.2 Protein Bands obtained after running SDS PAGE, (BD: Commercial Collagen, RT: extracted collagen in lab.

The protein ladder can be seen in the bottom with the other samples above it. While the bands of BD collagen are not very clear, matching of particular bands of the samples of rat tail collagen of different concentrations can be seen. The corresponding bonds of BD collagen are also present but are very light in color and thinner, which correlates the presence of the same protein in different concentration in these samples.

SDS PAGE was successfully run to obtain protein bands based on the size of protein molecules. They were matched to correlate the presence of the same protein, which was collagen I in this case, in BD collagen and the extracted rat tail collagen at different concentrations. Bands observed around 220 kDa, confirm the presence of collagen I in the in-house extracted lot. Furthermore, the banding patterns from the commercial BD collagen matched closely with the bands seen from our extracted collagen lots (D.2).

REFERENCES

1. Wood, M.D., et al., *Outcome measures of peripheral nerve regeneration.* Annals of anatomy = Anatomischer Anzeiger : official organ of the Anatomische Gesellschaft, 2011. **193**(4): p. 321-33.
2. Pfister, B.J., et al., *Biomedical engineering strategies for peripheral nerve repair: surgical applications, state of the art, and future challenges.* Critical reviews in biomedical engineering, 2011. **39**(2): p. 81-124.
3. Lundborg, G. and B. Rosen, *Hand function after nerve repair.* Acta physiologica, 2007. **189**(2): p. 207-17.
4. Noble, J., et al., *Analysis of upper and lower extremity peripheral nerve injuries in a population of patients with multiple injuries.* The Journal of trauma, 1998. **45**(1): p. 116-22.
5. Belkas, J.S., M.S. Shoichet, and R. Midha, *Peripheral nerve regeneration through guidance tubes.* Neurological research, 2004. **26**(2): p. 151-60.
6. Stang, F., et al., *Structural parameters of collagen nerve grafts influence peripheral nerve regeneration.* Biomaterials, 2005. **26**(16): p. 3083-91.
7. Scholz, T., et al., *Peripheral nerve injuries: an international survey of current treatments and future perspectives.* Journal of reconstructive microsurgery, 2009. **25**(6): p. 339-44.
8. Hubert, T., et al., *Collagens in the developing and diseased nervous system.* Cellular and molecular life sciences : CMLS, 2009. **66**(7): p. 1223-38.
9. Vandenabeele, F., J. Creemers, and I. Lambrichts, *Ultrastructure of the human spinal arachnoid mater and dura mater.* Journal of anatomy, 1996. **189 (Pt 2)**: p. 417-30.
10. Krarup, C., S.J. Archibald, and R.D. Madison, *Factors that influence peripheral nerve regeneration: an electrophysiological study of the monkey median nerve.* Annals of neurology, 2002. **51**(1): p. 69-81.
11. Liu, S., et al., *Axonal regrowth through collagen tubes bridging the spinal cord to nerve roots.* Journal of neuroscience research, 1997. **49**(4): p. 425-32.
12. Willits, R.K. and S.L. Skornia, *Effect of collagen gel stiffness on neurite extension.* Journal of biomaterials science. Polymer edition, 2004. **15**(12): p. 1521-31.
13. Schmidt, C.E. and J.B. Leach, *Neural tissue engineering: strategies for repair and regeneration.* Annual review of biomedical engineering, 2003. **5**: p. 293-347.
14. Purves, D., et al., *Neuroscience*. 3rd ed2004, Sunderland, Massachusetts: Sinauer Associates, Inc. 833.

15. Chaudhry, V., J.D. Glass, and J.W. Griffin, *Wallerian degeneration in peripheral nerve disease.* Neurologic clinics, 1992. **10**(3): p. 613-27.

16. Lundborg, G., *Nerve Injury and Repair*1988, London: Churchill-Livingstone.

17. Ribeiro-Resende, V.T., et al., *Strategies for inducing the formation of bands of Bungner in peripheral nerve regeneration.* Biomaterials, 2009. **30**(29): p. 5251-9.

18. Dubovy, P., *Schwann cells: Development, and regeneration of the nervous system.* Acta Fac Med Univ Brun Mas, 1998. **114**: p. 1-142.

19. Fu, S.Y. and T. Gordon, *The cellular and molecular basis of peripheral nerve regeneration.* Molecular neurobiology, 1997. **14**(1-2): p. 67-116.

20. Ide, C., *Peripheral nerve regeneration.* Neuroscience research, 1996. **25**(2): p. 101-21.

21. Longo, F.M., et al., *Neurite-promoting factors and extracellular matrix components accumulating in vivo within nerve regeneration chambers.* Brain research, 1984. **309**(1): p. 105-17.

22. Politis, M.J., K. Ederle, and P.S. Spencer, *Tropism in nerve regeneration in vivo. Attraction of regenerating axons by diffusible factors derived from cells in distal nerve stumps of transected peripheral nerves.* Brain research, 1982. **253**(1-2): p. 1-12.

23. Dubovy, P., *Schwann cells and endoneurial extracellular matrix molecules as potential cues for sorting of regenerated axons: a review.* Anatomical science international, 2004. **79**(4): p. 198-208.

24. Harrison, R.G., *The outgrowth of the nerve fiber as a mode of protoplasmic movement.* Journal of Experimental Zoology, 1910. **9**: p. 787-846.

25. Nguyen, Q.T., J.R. Sanes, and J.W. Lichtman, *Pre-existing pathways promote precise projection patterns.* Nature neuroscience, 2002. **5**(9): p. 861-7.

26. Lorimier, P., et al., *Ultrastructural localization of the major components of the extracellular matrix in normal rat nerve.* The journal of histochemistry and cytochemistry : official journal of the Histochemistry Society, 1992. **40**(6): p. 859-68.

27. Bignami, A., N.H. Chi, and D. Dahl, *Laminin in rat sciatic nerve undergoing Wallerian degeneration. Immunofluorescence study with laminin and neurofilament antisera.* Journal of neuropathology and experimental neurology, 1984. **43**(1): p. 94-103.

28. Salonen, V., et al., *Laminin in traumatized peripheral nerve: basement membrane changes during degeneration and regeneration.* Journal of neurocytology, 1987. **16**(5): p. 713-20.

29. Tona, A., et al., *Extracellular matrix in regenerating rat sciatic nerve: a comparative study on the localization of laminin, hyaluronic acid, and chondroitin sulfate proteoglycans, including versican.* The journal of histochemistry and cytochemistry : official journal of the Histochemistry Society, 1993. **41**(4): p. 593-9.

30. Hammarback, J.A., et al., *Growth cone guidance by substrate-bound laminin pathways is correlated with neuron-to-pathway adhesivity.* Developmental biology, 1988. **126**(1): p. 29-39.

31. Graf, J., et al., *A pentapeptide from the laminin B1 chain mediates cell adhesion and binds the 67,000 laminin receptor.* Biochemistry, 1987. **26**(22): p. 6896-900.

32. Jucker, M., H.K. Kleinman, and D.K. Ingram, *Fetal rat septal cells adhere to and extend processes on basement membrane, laminin, and a synthetic peptide from the laminin A chain sequence.* Journal of neuroscience research, 1991. **28**(4): p. 507-17.

33. Dadsetan, M., et al., *Stimulation of neurite outgrowth using positively charged hydrogels.* Biomaterials, 2009. **30**(23-24): p. 3874-81.

34. Horn, E.M., et al., *Influence of cross-linked hyaluronic acid hydrogels on neurite outgrowth and recovery from spinal cord injury.* Journal of neurosurgery. Spine, 2007. **6**(2): p. 133-40.

35. Wen, X. and P.A. Tresco, *Effect of filament diameter and extracellular matrix molecule precoating on neurite outgrowth and Schwann cell behavior on multifilament entubulation bridging device in vitro.* Journal of biomedical materials research. Part A, 2006. **76**(3): p. 626-37.

36. Mukhopadhyay, G., et al., *A novel role for myelin-associated glycoprotein as an inhibitor of axonal regeneration.* Neuron, 1994. **13**(3): p. 757-67.

37. Bedi, K.S., et al., *Adult Rat Dorsal Root Ganglion Neurons Extend Neurites on Predegenerated But Not on Normal Peripheral Nerves In Vitro.* The European journal of neuroscience, 1992. **4**(3): p. 193-200.

38. Fox, M.A., *Novel roles for collagens in wiring the vertebrate nervous system.* Current opinion in cell biology, 2008. **20**(5): p. 508-13.

39. Chernousov, M.A., et al., *Glypican-1 and alpha4(V) collagen are required for Schwann cell myelination.* The Journal of neuroscience : the official journal of the Society for Neuroscience, 2006. **26**(2): p. 508-17.

40. Duan, X. and H. Sheardown, *Crosslinking of collagen with dendrimers.* Journal of biomedical materials research. Part A, 2005. **75**(3): p. 510-8.

41. Silver, F. and D.L. Christiansen, *Biomaterials Science and Biocompatibility*1999, New York: Spring-Verlag.

42. Leclere, P.G., et al., *Impaired axonal regeneration by isolectin B4-binding dorsal root ganglion neurons in vitro.* The Journal of neuroscience : the official journal of the Society for Neuroscience, 2007. **27**(5): p. 1190-9.

43. Klapka, N. and H.W. Muller, *Collagen matrix in spinal cord injury.* Journal of neurotrauma, 2006. **23**(3-4): p. 422-35.

44. Weller, R.O., *Microscopic morphology and histology of the human meninges.* Morphologie : bulletin de l'Association des anatomistes, 2005. **89**(284): p. 22-34.

45. D'Antonio, M., et al., *Gene profiling and bioinformatic analysis of Schwann cell embryonic development and myelination.* Glia, 2006. **53**(5): p. 501-15.

46. Lui, V.C., et al., *The mRNAs for the three chains of human collagen type XI are widely distributed but not necessarily co-expressed: implications for homotrimeric, heterotrimeric and heterotypic collagen molecules.* The Biochemical journal, 1995. **311 (Pt 2)**: p. 511-6.

47. Silver, F. and A. Garg, *Collagen: characterization, processing and medical applications*, in *Handbook of Biodegradable Polymers*, A. Domb, J. Kost, and D. Wiseman, Editors. 1977, Hardwood Academic Publishers.

48. Hughes, P.M., et al., *Comparison of matrix metalloproteinase expression during Wallerian degeneration in the central and peripheral nervous systems.* Neuroscience, 2002. **113**(2): p. 273-87.

49. Zuo, J., et al., *Neuronal matrix metalloproteinase-2 degrades and inactivates a neurite-inhibiting chondroitin sulfate proteoglycan.* The Journal of neuroscience : the official journal of the Society for Neuroscience, 1998. **18**(14): p. 5203-11.

50. Nathaniel, E.J. and D.C. Pease, *Collagen and Basement Membrane Formation by Schwann Cells during Nerve Regeneration.* Journal of ultrastructure research, 1963. **52**: p. 550-60.

51. Pfister, L.A., et al., *Nerve conduits and growth factor delivery in peripheral nerve repair.* Journal of the peripheral nervous system : JPNS, 2007. **12**(2): p. 65-82.

52. Silver, F.H., J.W. Freeman, and G.P. Seehra, *Collagen self-assembly and the development of tendon mechanical properties.* Journal of biomechanics, 2003. **36**(10): p. 1529-53.

53. Lodish, H., et al., *Molecular Cell Biology*. 5th ed2004, New York: W.H. Freeman and Company.

54. Leikin, S., D.C. Rau, and V.A. Parsegian, *Temperature-favoured assembly of collagen is driven by hydrophilic not hydrophobic interactions.* Nature structural biology, 1995. **2**(3): p. 205-10.

55. De Simone, A., L. Vitagliano, and R. Berisio, *Role of hydration in collagen triple helix stabilization.* Biochemical and biophysical research communications, 2008. **372**(1): p. 121-5.

56. Bella, J., B. Brodsky, and H.M. Berman, *Hydration structure of a collagen peptide.* Structure, 1995. **3**(9): p. 893-906.

57. Sung, H.W., et al., *Crosslinking of biological tissues using genipin and/or carbodiimide.* Journal of biomedical materials research. Part A, 2003. **64**(3): p. 427-38.

58. Friess, W. and G. Lee, *Basic thermoanalytical studies of insoluble collagen matrices.* Biomaterials, 1996. **17**(23): p. 2289-94.

59. Friess, W., G. Lee, and M.J. Groves, *Insoluble collagen matrices for prolonged delivery of proteins.* Pharmaceutical development and technology, 1996. **1**(2): p. 185-93.

60. Davis, J. and G. Maffia, *Collagen dispersions for liquid-solid separations in water treatment and sludge dewatering.* Separation Technology, 1995: p. 147-152.

61. Meyer, M., H. Baltzer, and K. Schwikal, *Collagen fibers by thermoplastic and wet spinning.* Materials Science and Engineering C, 2010. **30**: p. 1266-1271.

62. Lee, C.H., A. Singla, and Y. Lee, *Biomedical applications of collagen.* International journal of pharmaceutics, 2001. **221**(1-2): p. 1-22.

63. Patino, M.G., et al., *Collagen as an implantable material in medicine and dentistry.* The Journal of oral implantology, 2002. **28**(5): p. 220-5.

64. Bunyaratavej, P. and H.L. Wang, *Collagen membranes: a review.* Journal of periodontology, 2001. **72**(2): p. 215-29.

65. Stenzel, K.H., T. Miyata, and A.L. Rubin, *Collagen as a biomaterial.* Annual review of biophysics and bioengineering, 1974. **3**(0): p. 231-53.

66. Zeugolis, D.I., et al., *Electro-spinning of pure collagen nano-fibres - just an expensive way to make gelatin?* Biomaterials, 2008. **29**(15): p. 2293-305.

67. Rajan, N., et al., *Preparation of ready-to-use, storable and reconstituted type I collagen from rat tail tendon for tissue engineering applications.* Nature protocols, 2006. **1**(6): p. 2753-8.

68. Huang, Y., et al., *Anaylsis of birefringence during wound healing and remodeling following alkali burns in rabbit cornea.* Experimental eye research, 2001. **73**(4): p. 521-32.

69. Jarvinen, T.A., et al., *Collagen fibres of the spontaneously ruptured human tendons display decreased thickness and crimp angle.* Journal of orthopaedic research : official publication of the Orthopaedic Research Society, 2004. **22**(6): p. 1303-9.

70. Rho, K.S., et al., *Electrospinning of collagen nanofibers: effects on the behavior of normal human keratinocytes and early-stage wound healing.* Biomaterials, 2006. **27**(8): p. 1452-61.

71. Telemeco, T.A., et al., *Regulation of cellular infiltration into tissue engineering scaffolds composed of submicron diameter fibrils produced by electrospinning.* Acta biomaterialia, 2005. **1**(4): p. 377-85.

72. Zhang, Y.Z., et al., *Characterization of the surface biocompatibility of the electrospun PCL-collagen nanofibers using fibroblasts.* Biomacromolecules, 2005. **6**(5): p. 2583-9.

73. Wess, T.J. and J.P. Orgel, *Changes in collagen structure drying, dehydrothermal treatment and relation to long term deterioration.* Thermochimica Acta, 2000. **365**: p. 119-128.

74. Cornwell, K.G., et al., *Crosslinking of discrete self-assembled collagen threads: Effects on mechanical strength and cell-matrix interactions.* Journal of biomedical materials research. Part A, 2007. **80**(2): p. 362-71.

75. Barnes, C.P., et al., *Cross-linking electrospun type II collagen tissue engineering scaffolds with carbodiimide in ethanol.* Tissue engineering, 2007. **13**(7): p. 1593-605.

76. Tsai, C.C., et al., *In vitro evaluation of the genotoxicity of a naturally occurring crosslinking agent (genipin) for biologic tissue fixation.* Journal of biomedical materials research, 2000. **52**(1): p. 58-65.

77. Charulatha, V. and A. Rajaram, *Influence of different crosslinking treatments on the physical properties of collagen membranes.* Biomaterials, 2003. **24**(5): p. 759-67.

78. Cheung, D.T., et al., *Mechanism of crosslinking of proteins by glutaraldehyde III. Reaction with collagen in tissues.* Connective tissue research, 1985. **13**(2): p. 109-15.

79. Wu, K.J., C.Y. Wang, and H.K. Lu, *Effect of glutaraldehyde on the humoral immunogenicity and structure of porcine dermal collagen membranes.* Archives of oral biology, 2004. **49**(4): p. 305-11.

80. Sheu, M.T., et al., *Characterization of collagen gel solutions and collagen matrices for cell culture.* Biomaterials, 2001. **22**(13): p. 1713-9.

81. Xu, B., M.J. Chow, and Y. Zhang, *Experimental and modeling study of collagen scaffolds with the effects of crosslinking and fiber alignment.* International journal of biomaterials, 2011. **2011**: p. 172389.

82. Sung, H.W., et al., *Mechanical properties of a porcine aortic valve fixed with a naturally occurring crosslinking agent.* Biomaterials, 1999. **20**(19): p. 1759-72.

83. Bedran-Russo, A.K., et al., *Application of crosslinkers to dentin collagen enhances the ultimate tensile strength.* Journal of biomedical materials research. Part B, Applied biomaterials, 2007. **80**(1): p. 268-72.

84. Liang, H.C., et al., *Effects of crosslinking degree of an acellular biological tissue on its tissue regeneration pattern.* Biomaterials, 2004. **25**(17): p. 3541-52.

85. Touyama R, et al., *Studies on the blue pigments produced from genipin and methylamine (I): Structure of brownish-red pigments, intermediates leading to blue pigments.* Chem Pharm Bull, 1994. **42**: p. 668-673.

86. Solorio, L., et al., *Gelatin microspheres crosslinked with genipin for local delivery of growth factors.* Journal of tissue engineering and regenerative medicine, 2010. **4**(7): p. 514-23.

87. Ferrara, G., *Nuova Selva di Cirurgia Divisia tre Parti Venice.* S Combi, 1608.

88. Huber, G.C., *A study of the operative treatment for loss of nerve substance in peripheral nerves.* Journal of Morphology, 1895. **11**: p. 629-735.

89. Sanders, F.K., *The repair of large gaps in the peripheral nerves.* Brain, 1942. **65**: p. 281-337.

90. Siemionow, M. and G. Brzezicki, *Chapter 8: Current techniques and concepts in peripheral nerve repair.* International review of neurobiology, 2009. **87**: p. 141-72.

91. Diao, E. and T. Vannuyen, *Techniques for primary nerve repair.* Hand clinics, 2000. **16**(1): p. 53-66, viii.

92. Townsend, P.L., *Microsurgical techniques in reconstructive surgery. In ''Operative Surgery and Management*, ed. K.a.J.R. Farndon1994, Oxford, UK: Butterworth-Heinemann.

93. Trumble, T.E., *Peripheral nerve injury: Pathophysiology and repair.* Trauma, ed. D.V. Feliciano, E.E. Moore, and K.L. Mattox1999, New York, NY: McGraw-Hill.

94. Dahlin, L.B. and G. Lundborg, *Use of tubes in peripheral nerve repair.* Neurosurgery clinics of North America, 2001. **12**(2): p. 341-52.

95. Dvali, L. and S. Mackinnon, *Nerve repair, grafting, and nerve transfers.* Clinics in plastic surgery, 2003. **30**(2): p. 203-21.

96. Harris, M.E. and S.C. Tindall, *Techniques of peripheral nerve repair.* Neurosurgery clinics of North America, 1991. **2**(1): p. 93-104.

97. Mackinnon, S.E., *New directions in peripheral nerve surgery.* Annals of plastic surgery, 1989. **22**(3): p. 257-73.

98. Maggi, S.P., J.B. Lowe, 3rd, and S.E. Mackinnon, *Pathophysiology of nerve injury.* Clinics in plastic surgery, 2003. **30**(2): p. 109-26.

99. Tetik, C., et al., *Conventional versus epineural sleeve neurorrhaphy technique: functional and histomorphometric analysis.* Annals of plastic surgery, 2002. **49**(4): p. 397-403.

100. Siemionow, M., et al., *Epineural sleeve neurorrhaphy: surgical technique and functional results--a preliminary report.* Annals of plastic surgery, 2002. **48**(3): p. 281-5.

101. Sunderland, S., *The anatomy and physiology of nerve injury.* Muscle & nerve, 1990. **13**(9): p. 771-84.

102. Martini, A. and B. Fromm, *A new operation for the prevention and treatment of amputation neuromas.* The Journal of bone and joint surgery. British volume, 1989. **71**(3): p. 379-82.

103. Birch, R. and A.R. Raji, *Repair of median and ulnar nerves. Primary suture is best.* The Journal of bone and joint surgery. British volume, 1991. **73**(1): p. 154-7.

104. Kline, D.G., et al., *Effect of mobilization on the blood supply and regeneration of injured nerves.* The Journal of surgical research, 1972. **12**(4): p. 254-66.

105. Lundborg, G. and B. Rydevik, *Effects of stretching the tibial nerve of the rabbit. A preliminary study of the intraneural circulation and the barrier function of the perineurium.* The Journal of bone and joint surgery. British volume, 1973. **55**(2): p. 390-401.

106. Matsuyama, T., M. Mackay, and R. Midha, *Peripheral nerve repair and grafting techniques: a review.* Neurologia medico-chirurgica, 2000. **40**(4): p. 187-99.

107. Philipeaux, J.M. and A. Vulpian, *Note sur des esseys de greVe d'un troncon du nerf lingual entre les deux bouts du nerf hypoglosse, apres excision d'un segment de ce derniernerf.* Arch. Physiol. Norm. Path. Paris, 1870: p. 618-620.

108. Huber, C., *Repair of peripheral nerve injuries.* Surg Gyn Obstet, 1920. **30**: p. 464-471.

109. Seddon, H.J., *The use of autogenous grafts for the repair of large gaps in peripheral nerves.* The British journal of surgery, 1947. **35**(138): p. 151-67.

110. Millesi, H., G. Meissl, and A. Berger, *The interfascicular nerve-grafting of the median and ulnar nerves.* The Journal of bone and joint surgery. American volume, 1972. **54**(4): p. 727-50.

111. Millesi, H., *Nerve grafting.* Clinics in plastic surgery, 1984. **11**(1): p. 105-13.

112. Martini, R., *Expression and functional roles of neural cell surface molecules and extracellular matrix components during development and regeneration of peripheral nerves.* Journal of neurocytology, 1994. **23**(1): p. 1-28.

113. Ortiguela, M.E., M.B. Wood, and D.R. Cahill, *Anatomy of the sural nerve complex.* The Journal of hand surgery, 1987. **12**(6): p. 1119-23.

114. Brushart, T.M., *Preferential reinnervation of motor nerves by regenerating motor axons.* The Journal of neuroscience : the official journal of the Society for Neuroscience, 1988. **8**(3): p. 1026-31.

115. Brushart, T.M., *Motor axons preferentially reinnervate motor pathways.* The Journal of neuroscience : the official journal of the Society for Neuroscience, 1993. **13**(6): p. 2730-8.

116. Brushart, T.M. and W.A.t. Seiler, *Selective reinnervation of distal motor stumps by peripheral motor axons.* Experimental neurology, 1987. **97**(2): p. 289-300.

117. Lloyd, B.M., et al., *Use of motor nerve material in peripheral nerve repair with conduits.* Microsurgery, 2007. **27**(2): p. 138-45.

118. Ghalib, N., et al., *Morphometric analysis of early regeneration of motor axons through motor and cutaneous nerve grafts.* Annals of anatomy = Anatomischer Anzeiger : official organ of the Anatomische Gesellschaft, 2001. **183**(4): p. 363-8.

119. Nichols, C.M., et al., *Effects of motor versus sensory nerve grafts on peripheral nerve regeneration.* Experimental neurology, 2004. **190**(2): p. 347-55.

120. Brenner, M.J., et al., *Repair of motor nerve gaps with sensory nerve inhibits regeneration in rats.* The Laryngoscope, 2006. **116**(9): p. 1685-92.

121. Martini, R., M. Schachner, and T.M. Brushart, *The L2/HNK-1 carbohydrate is preferentially expressed by previously motor axon-associated Schwann cells in reinnervated peripheral nerves.* The Journal of neuroscience : the official journal of the Society for Neuroscience, 1994. **14**(11 Pt 2): p. 7180-91.

122. Martini, R., et al., *The L2/HNK-1 Carbohydrate Epitope is Involved in the Preferential Outgrowth of Motor Neurons on Ventral Roots and Motor Nerves.* The European journal of neuroscience, 1992. **4**(7): p. 628-639.

123. Midha, R., et al., *Comparison of regeneration across nerve allografts with temporary or continuous cyclosporin A immunosuppression.* Journal of neurosurgery, 1993. **78**(1): p. 90-100.

124. Midha, R., S.E. Mackinnon, and L.E. Becker, *The fate of Schwann cells in peripheral nerve allografts.* Journal of neuropathology and experimental neurology, 1994. **53**(3): p. 316-22.

125. Bain, J.R., *Peripheral nerve and neuromuscular allotransplantation: current status.* Microsurgery, 2000. **20**(8): p. 384-8.

126. Gulati, A.K., *Immune response and neurotrophic factor interactions in peripheral nerve transplants.* Acta haematologica, 1998. **99**(3): p. 171-4.

127. Hettiaratchy, S., et al., *Tolerance to composite tissue allografts across a major histocompatibility barrier in miniature swine.* Transplantation, 2004. **77**(4): p. 514-21.

128. Ishida, O., et al., *Regeneration following rejection of peripheral nerve allografts of rats on withdrawal of cyclosporine.* Plastic and reconstructive surgery, 1993. **92**(5): p. 916-26.

129. Zalewski, A.A. and A.K. Gulati, *Survival of nerve and Schwann cells in allografts after cyclosporin A treatment.* Experimental neurology, 1980. **70**(2): p. 219-25.

130. Mackinnon, S.E., et al., *Clinical outcome following nerve allograft transplantation.* Plastic and reconstructive surgery, 2001. **107**(6): p. 1419-29.

131. Glasby, M.A., et al., *Degenerated muscle grafts used for peripheral nerve repair in primates.* Journal of hand surgery, 1986. **11**(3): p. 347-51.

132. Norris, R.W., et al., *Peripheral nerve repair in humans using muscle autografts. A new technique.* The Journal of bone and joint surgery. British volume, 1988. **70**(4): p. 530-3.

133. Tang, J.B., *Vein conduits with interposition of nerve tissue for peripheral nerve defects.* Journal of reconstructive microsurgery, 1995. **11**(1): p. 21-6.

134. Walton, R.L., et al., *Autogenous vein graft repair of digital nerve defects in the finger: a retrospective clinical study.* Plastic and reconstructive surgery, 1989. **84**(6): p. 944-9; discussion 950-2.

135. Doolabh, V.B., M.C. Hertl, and S.E. Mackinnon, *The role of conduits in nerve repair: a review.* Reviews in the neurosciences, 1996. **7**(1): p. 47-84.

136. Meek, M.F. and J.H. Coert, *US Food and Drug Administration /Conformit Europe- approved absorbable nerve conduits for clinical repair of peripheral and cranial nerves.* Annals of plastic surgery, 2008. **60**(4): p. 466-72.

137. Lundborg, G. and H.A. Hansson, *Nerve regeneration through preformed pseudosynovial tubes. A preliminary report of a new experimental model for studying the regeneration and reorganization capacity of peripheral nerve tissue.* The Journal of hand surgery, 1980. **5**(1): p. 35-8.

138. Seckel, B.R., et al., *Nerve regeneration through synthetic biodegradable nerve guides: regulation by the target organ.* Plastic and reconstructive surgery, 1984. **74**(2): p. 173-81.

139. Hudson, T.W., G.R. Evans, and C.E. Schmidt, *Engineering strategies for peripheral nerve repair.* Clinics in plastic surgery, 1999. **26**(4): p. 617-28, ix.

140. Molander, H., et al., *Regeneration of peripheral nerve through a polyglactin tube.* Muscle & nerve, 1982. **5**(1): p. 54-7.

141. Bryan, D.J., et al., *Enhanced peripheral nerve regeneration elicited by cell-mediated events delivered via a bioresorbable PLGA guide.* Journal of reconstructive microsurgery, 2003. **19**(2): p. 125-34.

142. Wang, S., et al., *A new nerve guide conduit material composed of a biodegradable poly(phosphoester).* Biomaterials, 2001. **22**(10): p. 1157-69.

143. Valero-Cabre, A., et al., *Superior muscle reinnervation after autologous nerve graft or poly-L-lactide-epsilon-caprolactone (PLC) tube implantation in comparison to silicone tube repair.* Journal of neuroscience research, 2001. **63**(2): p. 214-23.

144. Sundback, C., et al., *Manufacture of porous polymer nerve conduits by a novel low-pressure injection molding process.* Biomaterials, 2003. **24**(5): p. 819-30.

145. Young, R.C., M. Wiberg, and G. Terenghi, *Poly-3-hydroxybutyrate (PHB): a resorbable conduit for long-gap repair in peripheral nerves.* British journal of plastic surgery, 2002. **55**(3): p. 235-40.

146. de Ruiter, G.C.W., et al., *Designing ideal conduits for peripheral nerve repair.* Neurosurg Focus, 2009. **26**(2): p. 1-9.

147. Cohen, S., et al., *Design of synthetic polymeric structures for cell transplantation and tissue engineering.* Clin Mater, 1993. **13**(1-4): p. 3-10.

148. Langer, R. and J.P. Vacanti, *Tissue engineering.* Science, 1993. **260**(5110): p. 920-6.

149. Langer, R.S. and J.P. Vacanti, *Tissue engineering: the challenges ahead.* Sci Am, 1999. **280**(4): p. 86-9.

150. Vacanti, J.P. and R. Langer, *Tissue engineering: the design and fabrication of living replacement devices for surgical reconstruction and transplantation.* Lancet, 1999. **354 Suppl 1**: p. SI32-4.

151. Schmidt, C.E. and J.B. Leach, *Neural Tissue Engineering: Strategies for Repair and Regeneration.* Annu. Rev. Biomed. Eng, 2003. **5**: p. 293-347.

152. Sarkar, S., et al., *Vascular tissue engineering: microtextured scaffold templates to control organization of vascular smooth muscle cells and extracellular matrix.* Acta Biomater, 2005. **1**(1): p. 93-100.

153. Cooper, J.A., et al., *Fiber-based tissue-engineered scaffold for ligament replacement: design considerations and in vitro evaluation.* Biomaterials, 2005. **26**(13): p. 1523-32.

154. Khademhosseini, A., et al., *Interplay of biomaterials and micro-scale technologies for advancing biomedical applications.* Journal of biomaterials science. Polymer edition, 2006. **17**(11): p. 1221-40.

155. Khademhosseini, A., et al., *Microscale technologies for tissue engineering and biology.* Proceedings of the National Academy of Sciences of the United States of America, 2006. **103**(8): p. 2480-7.

156. Hwang, C.M., et al., *Microfluidic chip-based fabrication of PLGA microfiber scaffolds for tissue engineering.* Langmuir, 2008. **24**(13): p. 6845-51.

157. Kim, T.K., et al., *Gas foamed open porous biodegradable polymeric microspheres.* Biomaterials, 2006. **27**(2): p. 152-9.

158. Oh, S.H., S.G. Kang, and J.H. Lee, *Degradation behavior of hydrophilized PLGA scaffolds prepared by melt-molding particulate-leaching method: comparison with control hydrophobic one.* J Mater Sci Mater Med, 2006. **17**(2): p. 131-7.

159. Lee, Y.H., et al., *Electrospun dual-porosity structure and biodegradation morphology of Montmorillonite reinforced PLLA nanocomposite scaffolds.* Biomaterials, 2005. **26**(16): p. 3165-72.

160. Chevalier, E., et al., *Influence of process parameters on pellets elaborated in a Mi-pro high-shear granulator.* Pharm Dev Technol, 2007. **12**(2): p. 133-44.

161. Leong, K.F., C.M. Cheah, and C.K. Chua, *Solid freeform fabrication of three-dimensional scaffolds for engineering replacement tissues and organs.* Biomaterials, 2003. **24**(13): p. 2363-78.

162. Leong, K.F., et al., *Fabrication of porous polymeric matrix drug delivery devices using the selective laser sintering technique.* Proc Inst Mech Eng H, 2001. **215**(2): p. 191-201.

163. Fedorovich, N.E., et al., *Hydrogels as extracellular matrices for skeletal tissue engineering: state-of-the-art and novel application in organ printing.* Tissue Eng, 2007. **13**(8): p. 1905-25.

164. Kretsinger, J.K., et al., *Cytocompatibility of self-assembled beta-hairpin peptide hydrogel surfaces.* Biomaterials, 2005. **26**(25): p. 5177-86.

165. Branco, M.C., et al., *Macromolecular diffusion and release from self-assembled beta-hairpin peptide hydrogels.* Biomaterials, 2009. **30**(7): p. 1339-47.

166. Chau, Y., et al., *Incorporation of a matrix metalloproteinase-sensitive substrate into self-assembling peptides - a model for biofunctional scaffolds.* Biomaterials, 2008. **29**(11): p. 1713-9.

167. Jung, J.P., et al., *Modulating the mechanical properties of self-assembled peptide hydrogels via native chemical ligation.* Biomaterials, 2008. **29**(13): p. 2143-51.

168. Cao, X. and M.S. Shoichet, *Photoimmobilization of biomolecules within a 3-dimensional hydrogel matrix.* J Biomater Sci Polym Ed, 2002. **13**(6): p. 623-36.

169. Leipzig, N.D. and M.S. Shoichet, *The effect of substrate stiffness on adult neural stem cell behavior.* Biomaterials, 2009. **30**(36): p. 6867-78.

170. Bashur, C.A., L.A. Dahlgren, and A.S. Goldstein, *Effect of fiber diameter and orientation on fibroblast morphology and proliferation on electrospun poly(D,L-lactic-co-glycolic acid) meshes.* Biomaterials, 2006. **27**(33): p. 5681-8.

171. Fridrikh, S.V., et al., *Controlling the fiber diameter during electrospinning.* Phys Rev Lett, 2003. **90**(14): p. 144502.

172. Kim, I.A., et al., *Effects of Mechanical Stimuli and Microfiber-Based Substrate on Neurite Outgrowth and Guidance.* Journal of Bioscience and Bioengineering, 2006. **101**(2): p. 120-126.

173. Corey, J.M., Lin, D. Y. , Mycek, K. B. , Chen, Q., Samuel, S. , Feldman, E. L., and Martin, D. C., *Aligned electrospun nanofibers specify the direction of dorsal root ganglia neurite growth.* Journal of Biomedical Materials Research - Part A 2007. **83**(3): p. 636-645.

174. Smolders, C.A., et al., *Microstructures in phase-inversion membranes. Part 1. Formation of macrovoids.* Journal Membrane Science, 1992. **73**: p. 259-275.

175. Vogel, R., et al., *Melt spinning of poly(3-hydroxybutyrate) fibers for tissue engineering using alpha-cyclodextrin/polymer inclusion complexes as the nucleation agent.* Macromolecular bioscience, 2006. **6**(9): p. 730-6.

176. Nelson, K.D., et al., *Technique paper for wet-spinning poly(L-lactic acid) and poly(DL-lactide-co-glycolide) monofilament fibers.* Tissue engineering, 2003. **9**(6): p. 1323-30.

177. Marsano, E., et al., *Regenerated cellulose-silk fibroin blends fibers.* International journal of biological macromolecules, 2008. **43**(2): p. 106-14.

178. Pati, F., B. Adhikari, and S. Dhara, *Collagen Intermingled Chitosan-Tripolyphosphate Nano/Micro Fibrous Scaffolds for Tissue-Engineering Application.* Journal of biomaterials science. Polymer edition, 2011.

179. Ragetly, G., D.J. Griffon, and Y.S. Chung, *The effect of type II collagen coating of chitosan fibrous scaffolds on mesenchymal stem cell adhesion and chondrogenesis.* Acta biomaterialia, 2010. **6**(10): p. 3988-97.

180. Shao, X. and C.J. Hunter, *Developing an alginate/chitosan hybrid fiber scaffold for annulus fibrosus cells.* Journal of biomedical materials research. Part A, 2007. **82**(3): p. 701-10.

181. Shim, I.K., et al., *Homogeneous chitosan-PLGA composite fibrous scaffolds for tissue regeneration.* Journal of biomedical materials research. Part A, 2008. **84**(1): p. 247-55.

182. Mano, J.F., et al., *Natural origin biodegradable systems in tissue engineering and regenerative medicine: present status and some moving trends.* Journal of the Royal Society, Interface / the Royal Society, 2007. **4**(17): p. 999-1030.

183. Vunjak-Novakovic, G., et al., *Tissue engineering of ligaments.* Annu Rev Biomed Eng, 2004. **6**: p. 131-56.

184. Kim, J., et al., *Bone regeneration using hyaluronic acid-based hydrogel with bone morphogenic protein-2 and human mesenchymal stem cells.* Biomaterials, 2007. **28**(10): p. 1830-7.

185. Shin, S.J., et al., *"On the fly" continuous generation of alginate fibers using a microfluidic device.* Langmuir, 2007. **23**(17): p. 9104-8.

186. Tian, F., et al., *Quantitative analysis of cell adhesion on aligned micro- and nanofibers.* J Biomed Mater Res A, 2008. **84**(2): p. 291-9.

187. Vasilev, M.P., et al., *The spinning of collagen fibers.* Fibre Chemistry, 1972. **4**(1): p. 48-50.

188. Meyer, M., H. Baltzer, and K. Schwikal, *Collagen fibres by thermoplastic and wet spinning.* Materials Science and Engineering C, 2010. **30**: p. 1266-1271.

189. Rupprecht, A., *Preparation of oriented DNA by wet spinning.* Acta chemica Scandinavica, 1966. **20**(2): p. 494-504.

190. Rajan, N., et al., *Preparation of ready-to-use, storable and reconstituted type I collagen from rat tail tendon for tissue engineering applications.* Nat Protoc, 2006. **1**(6): p. 2753-8.

191. Lopez, J.M., et al., *An improved Bradford protein assay for collagen proteins.* Clinica chimica acta; international journal of clinical chemistry, 1993. **220**(1): p. 91-100.

192. Flory, P.J. and R.R. Garrett, *Phase transitions in collagen and gelatin systems.* Journal of the American Chemical Society, 1958. **80**(18): p. 4836-4845.

193. Luescher, M., M. Ruegg, and P. Schindler, *Effect of hydration upon the thermal stability of tropocollagen and its dependence on the presence of neutral salts.* Biopolymers, 1974. **13**(12): p. 2489-2503.

194. Sionkowska, A. and A. Kaminska, *Thermal helix-coil transition in UV irradiated collagen from rat tail tendon.* International journal of biological macromolecules, 1999. **24**(4): p. 337-40.

195. Usha, R. and T. Ramasami, *The effects of urea and n-propanol on collagen denaturation: using DSC, circular dichroism and viscosity.* Termochimica Acta, 2004. **409**: p. 2001-2206.

196. Zeugolis, D.I., R.G. Paul, and G. Attenburrow, *Engineering Extruded Collagen Fibers for Biomedical Applications.* J Appl Polym Sci, 2008. **108**: p. 2886–2894.

197. Laude, D., et al., *A novel injectable collagen matrix: in vitro characterization and in vivo evaluation.* Journal of biomechanical engineering, 2000. **122**(3): p. 231-5.

198. Zeugolis, D.I., R.G. Paul, and G. Attenburrow, *Extruded collagen fibres for tissue-engineering applications: influence of collagen concentration and NaCl amount.* J Biomater Sci Polym Ed, 2009. **20**(2): p. 219-34.

199. Saito, Y., et al., *New tubular bioabsorbable knitted airway stent: biocompatibility and mechanical strength.* The Journal of thoracic and cardiovascular surgery, 2002. **123**(1): p. 161-7.

200. Pins, G.D., et al., *Self-assembly of collagen fibers. Influence of fibrillar alignment and decorin on mechanical properties.* Biophys J, 1997. **73**(4): p. 2164-72.

201. Pins, G.D. and F.H. Silver, *A self-assembled collagen scaffold suitable for use in soft and hard tissue replacement.* Materials Science and Engineering C, 1995. **3**: p. 101-107.

202. Dunn, M.G., P.N. Avasarala, and J.P. Zawadsky, *Optimization of extruded collagen fibers for ACL reconstruction.* Journal of biomedical materials research, 1993. **27**(12): p. 1545-52.

203. Gentleman, E., et al., *Mechanical characterization of collagen fibers and scaffolds for tissue engineering.* Biomaterials, 2003. **24**(21): p. 3805-13.

204. Sundararaghavan, H.G., et al., *Genipin-induced changes in collagen gels: correlation of mechanical properties to fluorescence.* Journal of biomedical materials research. Part A, 2008. **87**(2): p. 308-20.

205. Flanagan, L.A., et al., *Neurite branching on deformable substrates.* Neuroreport, 2002. **13**(18): p. 2411-5.

206. Leach, J.B., et al., *Neurite outgrowth and branching of PC12 cells on very soft substrates sharply decreases below a threshold of substrate rigidity.* Journal of neural engineering, 2007. **4**(2): p. 26-34.

207. Nomura, H., Baladie, B., Katayama, Y., Morshead, C.M., Shoichet, M.S., and Tator, C.H., *Delayed Implantation of Intramedullary Chitosan Channels Containing Nerve Grafts Promotes Extensive Axonal Regeneration After Spinal Cord Injury.* Neurosurgery, 2008. **63**: p. 127-143.

208. Burdick, J.A., Ward, M., Liang E., Young, M.J., and Langer, R., *Stimulation of neurite outgrowth by neurotrophins delivered from degradable hydrogels.* Biomaterials, 2006. **27**(3): p. 452-459.

209. Gupta, D., Tator, C.H., and Shoichet, M.S., *Fast-gelling injectable blend of hyaluronan and methylcellulose for intrathecal, localized delivery to the injury spinal cord.* Biomaterials, 2006. **27**: p. 2370-2379.

210. Jain, A., Kim, Y., McKeon, R. J. , and Bellamkonda, R. V. , *In situ gelling hydrogels for conformal repair of spinal cord defects, and local delivery of BDNF after spinal cord injury* Biomaterials, 2006. **27**: p. 497-504.

211. Piantino, J., Burdick, J. A., Goldberg, D., Langer, R., & Benowitz, L. I. , *An injectable, biodegradable hydrogel for trophic factor delivery enhances axonal rewiring and improves performance after spinal cord injury.* Experimental Neurology, 2006. **201**(2): p. 359-367.

212. Balgude, A.P., Yu, X. , Szymanski, A. , Bellamkonda, R.V., *Agarose gel stiffness determines rate of DRG neurite extension in 3D cultures.* Biomaterials, 2001. **22**: p. 1077-1084.

213. Willits, R.K.a.S., S.L. , *Effect of collagen gel stiffness on neurite extension.* J. Biomater. Sci. Polymer Edn, 2004. **15**(12): p. 1521-1531.

214. Iwata, A.e.a., *Long-term survival and outgrowth of mechanically engineered nervous tissue constructs implanted into spinal cord lesions.* Tissue Engineering, 2006. **12**(1): p. 101-110.

215. Yu, T.T.a.S., M. S., *Guided cell adhesion and outgrowth in peptide-modified channels for neural tissue engineering.* Biomaterials, 2005. **26**: p. 1507-1514.

216. Bellamkonda, R.V., *Peripheral nerve regeneration: An opinion on channels, scaffolds, and anisotropy.* Biomaterials, 2006. **27**: p. 3515-3518.

217. Zheng, J., Lamoureux, P., Santiago, V., Dennerll, T., Buxbaum, R.E., and Heidemann, S.R., *Tensile regulation of axonal elongation and initiation.* Journal of Neuroscience, 1991. **11**: p. 1117-1125.

218. Lamoureux, P., Zheng, J., Buxbaum, R.E., and Heidemann, S.E., *A cytomechanical investigation of neurite growth on different culture surfaces.* Journal of Cell Biology, 1992. **118**: p. 655-661.

219. Gomez, T.M., and Letourneau, P.C., *Filopodia initiate choices made by sensory neuron growth cones at laminin/fibronectin borders in vitro.* J Neurosci, 1994. **14**(10): p. 5959-5972.

220. Rajan, N., Habermehl, J., Cote´, M., Doillon, C.J., and Mantovani, D., *Preparation of ready-to-use, storable and reconstituted type I collagen from rat tail tendon for tissue engineering applications.* Nature Protocols, 2007. **1**(6): p. 2753-2758.

221. Smeal, R.M. and P.A. Tresco, *The influence of substrate curvature on neurite outgrowth is cell type dependent.* Experimental neurology, 2008. **213**(2): p. 281-92.

222. Spencer, T. and M.T. Filbin, *A role for cAMP in regeneration of the adult mammalian CNS.* Journal of anatomy, 2004. **204**(1): p. 49-55.

223. Campbell, G., et al., *Regeneration of adult rat CNS axons into peripheral nerve autografts: ultrastructural studies of the early stages of axonal sprouting and regenerative axonal growth.* Journal of neurocytology, 1992. **21**(11): p. 755-87.

224. Hall, S.M., *Regeneration in cellular and acellular autografts in the peripheral nervous system.* Neuropathology and applied neurobiology, 1986. **12**(1): p. 27-46.

225. Clark, P., S. Britland, and P. Connolly, *Growth cone guidance and neuron morphology on micropatterned laminin surfaces.* Journal of cell science, 1993. **105 (Pt 1)**: p. 203-12.

226. Labrador, R.O., M. Buti, and X. Navarro, *Influence of collagen and laminin gels concentration on nerve regeneration after resection and tube repair.* Experimental neurology, 1998. **149**(1): p. 243-52.

227. Lander, A.D., D.K. Fujii, and L.F. Reichardt, *Laminin is associated with the "neurite outgrowth-promoting factors" found in conditioned media.* Proceedings of the National Academy of Sciences of the United States of America, 1985. **82**(7): p. 2183-7.

228. Woolley, A.L., J.P. Hollowell, and K.M. Rich, *First place--Resident Basic Science Award 1990. Fibronectin-laminin combination enhances peripheral nerve regeneration across long gaps.* Otolaryngology--head and neck surgery : official journal of American Academy of Otolaryngology-Head and Neck Surgery, 1990. **103**(4): p. 509-18.

229. Gutmann, E. and L. Guttmann, *Factors Affecting Recovery of Sensory Function after Nerve Lesions.* Journal of neurology and psychiatry, 1942. **5**(3-4): p. 117-29.

230. Gutmann, E., *Factors Affecting Recovery of Motor Function after Nerve Lesions.* Journal of neurology and psychiatry, 1942. **5**(3-4): p. 81-95.

231. Sunderland, S., *Rate of regeneration in human peripheral nerves; analysis of the interval between injury and onset of recovery.* Archives of neurology and psychiatry, 1947. **58**(3): p. 251-95.

232. Holmquist, B., et al., *A mathematical model for regeneration rate and initial delay following surgical repair of peripheral nerves.* Journal of neuroscience methods, 1993. **48**(1-2): p. 27-33.

233. Mackinnon, S.E. and A.R. Hudson, *Clinical application of peripheral nerve transplantation.* Plastic and reconstructive surgery, 1992. **90**(4): p. 695-9.

234. Samardzic, M.M., L.G. Rasulic, and D.M. Grujicic, *Results of cable graft technique in repair of large nerve trunk lesions.* Acta neurochirurgica, 1998. **140**(11): p. 1177-82.

235. Wu, J. and D.T. Chiu, *Painful neuromas: a review of treatment modalities.* Annals of plastic surgery, 1999. **43**(6): p. 661-7.

236. Recknor, J.B. and S.K. Mallapragada, *Nerve Regeneration: Tissue Engineering Strategies*, in *The Biomedical Engineering Handbook: Tissue Engineering and Artificial Organs.*, T. Francis, Editor 2006: New York.

237. Seckel, B.R., *Enhancement of peripheral nerve regeneration.* Muscle & nerve, 1990. **13**(9): p. 785-800.

238. Davies, S.J., et al., *Regeneration of adult axons in white matter tracts of the central nervous system.* Nature, 1997. **390**(6661): p. 680-3.

239. Minor, K., et al., *Decorin promotes robust axon growth on inhibitory CSPGs and myelin via a direct effect on neurons.* Neurobiology of disease, 2008. **32**(1): p. 88-95.

240. Kim, Y.P., et al., *Phosphate glass fibres promote neurite outgrowth and early regeneration in a peripheral nerve injury model.* Journal of tissue engineering and regenerative medicine, 2012.

241. Meek, M.F., et al., *Long-term evaluation of functional nerve recovery after reconstruction with a thin-walled biodegradable poly (DL-lactide-epsilon-caprolactone) nerve guide, using walking track analysis and electrostimulation tests.* Microsurgery, 1999. **19**(5): p. 247-53.

242. Flynn, L., P.D. Dalton, and M.S. Shoichet, *Fiber templating of poly(2-hydroxyethyl methacrylate) for neural tissue engineering.* Biomaterials, 2003. **24**(23): p. 4265-72.

243. Madison, R., et al., *Increased rate of peripheral nerve regeneration using bioresorbable nerve guides and a laminin-containing gel.* Experimental neurology, 1985. **88**(3): p. 767-72.

244. Midha, R., et al., *Tissue engineered alternatives to nerve transplantation for repair of peripheral nervous system injuries.* Transplantation proceedings, 2001. **33**(1-2): p. 612-5.

245. Pati, F., B. Adhikari, and S. Dhara, *Development of chitosan-tripolyphosphate non-woven fibrous scaffolds for tissue engineering application.* Journal of materials science. Materials in medicine, 2012. **23**(4): p. 1085-96.

246. Yan, J., et al., *Wet-spinning of regenerated silk fiber from aqueous silk fibroin solution: discussion of spinning parameters.* Biomacromolecules, 2010. **11**(1): p. 1-5.

247. Kim, Y.T., et al., *The role of aligned polymer fiber-based constructs in the bridging of long peripheral nerve gaps.* Biomaterials, 2008. **29**(21): p. 3117-27.

248. Chen, Y.S., et al., *Peripheral nerve regeneration using silicone rubber chambers filled with collagen, laminin and fibronectin.* Biomaterials, 2000. **21**(15): p. 1541-7.

249. Whitworth, I.H., et al., *Orientated mats of fibronectin as a conduit material for use in peripheral nerve repair.* Journal of hand surgery, 1995. **20**(4): p. 429-36.

250. Maeda, T., et al., *Regeneration across 'stepping-stone' nerve grafts.* Brain research, 1993. **618**(2): p. 196-202.

251. Lu, P., et al., *Combinatorial therapy with neurotrophins and cAMP promotes axonal regeneration beyond sites of spinal cord injury.* The Journal of neuroscience : the official journal of the Society for Neuroscience, 2004. **24**(28): p. 6402-9.

252. Pearse, D.D., et al., *cAMP and Schwann cells promote axonal growth and functional recovery after spinal cord injury.* Nature medicine, 2004. **10**(6): p. 610-6.